Institute of Sound and Vibration Research

Analytical Formulation and Finite Element Modelling of Beams with Arbitrary Active Constrained Layer Damping Treatments

C.M.A. Vasques, B.R. Mace, P. Gardonio and J. Dias Rodrigues

ISVR Technical Memorandum No 934

May 2004

University of Southampton

SCIENTIFIC PUBLICATIONS BY THE ISVR

Technical Reports are published to promote timely dissemination of research results by ISVR personnel. This medium permits more detailed presentation than is usually acceptable for scientific journals. Responsibility for both the content and any opinions expressed rests entirely with the author(s).

Technical Memoranda are produced to enable the early or preliminary release of information by ISVR personnel where such release is deemed to the appropriate. Information contained in these memoranda may be incomplete, or form part of a continuing programme; this should be borne in mind when using or quoting from these documents.

Contract Reports are produced to record the results of scientific work carried out for sponsors, under contract. The ISVR treats these reports as confidential to sponsors and does not make them available for general circulation. Individual sponsors may, however, authorize subsequent release of the material.

UNIVERSITY OF SOUTHAMPTON

INSTITUTE OF SOUND AND VIBRATION RESEARCH

DYNAMICS GROUP

Analytical Formulation and Finite Element Modelling of Beams with Arbitrary Active Constrained Layer Damping Treatments

by

C.M.A. Vasques, B.R. Mace, P. Gardonio and J. Dias Rodrigues

ISVR Technical Memorandum No: 934

May 2004

Authorised for issue by
Professor M.J. Brennan
Group Chairman

Abstract

This work concerns arbitrary active constrained layer damping (ACLD) treatments applied to beams. In order to suppress vibration, hybrid active-passive treatments composed of piezoelectric and viscoelastic layers are mounted on the substrate beam structure. These treatments combine the high capacity of passive viscoelastic materials to dissipate vibrational energy at high frequencies with the active control effects of piezoelectric materials at low frequencies.

The aim of this research is the development of a generic analytical formulation that can describe these hybrid couplings in an accurate and consistent way. The analytical formulation considers a partial layerwise theory, with an arbitrary number of layers, both viscoelastic and piezoelectric, attached to both surfaces of the beam. A fully coupled electro-mechanical theory for modelling the piezoelectric layers is considered. Both the weak and strong forms of the problem are presented.

From the strong forms, the equations of motion and electric charge equilibrium and the electro-mechanical boundary conditions are derived and presented for the composite beam with an arbitrary number of layers. Based on the weak forms, a one-dimensional finite element (FE) model is developed, with the nodal mechanical degrees of freedom being the axial displacement, transverse displacement and the rotation of the mid-plane of the host beam and the rotations of the individual layers, and the electrical elemental degrees of freedom being the electrical potential difference of each piezoelectric layer. The damping behavior of the viscoelastic layers is modeled with the complex modulus approach.

Three frequency response functions were measured experimentally and evaluated numerically for a clamped aluminium beam with a partial ACLD treatment (viscoelastic layer sandwiched between the beam and piezoelectric patch): acceleration per unit force, acceleration per unit voltage into the piezoelectric actuator and induced voltage per unit force. The numerical results are presented and compared with experimental results to validate the FE model.

Contents

Nomenclature

Abbreviations

ACLD	active constrained layer damping
ADF	anelastic displacement fields
CMA	complex modulus approach
DoF	degree of freedom
FE	finite element
GHM	Gholla-Hughes-McTavish
PCLD	passive constrained layer damping
PLD	passive layer damping

Indices

c	indice denoting the core layer ($c = 0$)
k	indice denoting a generic layer ($k = \bar{m}, \ldots, -1, 0, 1, \ldots, \bar{n}$)
$\bar{m}$	indice denoting the last bottom layer ($\bar{m} < 0$)
$\hat{m}$	indice denoting the sandwiched bottom layers ($\hat{m} = \bar{m} + 1, \ldots, -1; \hat{m} < 0$)
m	indice denoting a generic bottom layer ($m = \bar{m}, \ldots, -1; m < 0$)
$\bar{n}$	indice denoting the last top layer ($\bar{n} > 0$)
$\hat{n}$	indice denoting the sandwiched top layers ($\hat{n} = 1, \ldots, \bar{n} - 1; \hat{n} > 0$)
n	indice denoting a generic top layer ($n = 1, \ldots, \bar{n}; n > 0$)
p	indice denoting a generic piezoelectric layer ($p = n, m$)

Greek Symbols

δ	variation
ε^S	dielectric constants matrix at constant strain
ε_{11}^p	axial dielectric constant of the p-th layer
ε_{33}^{*p}	transverse dielectric constant of the p-th layer
η	loss factor
θ_k	rotation of the k-th layer
ν	Poisson's ratio
ρ_k	mass density of the material into layer k
τ	electric charge density vector
τ_p	electric charge density of the p-th layer

$\bar{\phi}$	global electric degrees of freedom vector
$\bar{\phi}^e$	elemental electric degrees of freedom vector
$\bar{\mathbf{\Phi}}_a$	actuating electric potential difference amplitudes vector
$\bar{\phi}_a$	actuating electric degrees of freedom vector
$\bar{\mathbf{\Phi}}_s$	sensing electric potential difference amplitudes vector
$\bar{\phi}_s$	sensing electric degrees of freedom vector
ϕ	global generalized electric potential difference vector
ϕ^e	elemental generalized electric potential difference vector
ϕ_p	electric potential difference of the p-th layer
φ_p	electric potential of the p-th layer
ω	frequency

Roman Symbols

A_k	zero-order moment of area of the k-th layer
A_p^e	electrode area of the p-th layer
$\mathbf{B}_{xx}$	extensional deformation matrix
$\mathbf{B}_{xz}$	shear deformation matrix
b	width of the beam
$\bar{c}_{11}^{p(\phi)}$	bending effective stiffness parameter of the p-th layer
$\bar{c}_{55}^{p(\phi)}$	shear effective stiffness parameter of the p-th layer
$\mathbf{C}$	capacitance matrix
$\mathbf{c}^E$	elasticity matrix at constant electric field
c_{11}^{*k}	Young's modulus of the k-th layer
c_{55}^k	shear modulus of the k-th layer
$\mathbf{D}$	electric displacement vector
D_x^p	axial electric displacement of the p-th layer
D_z^p	transverse electric displacement of the p-th layer
$\bar{E}_x^p$	induced axial electric field of the p-th layer
$\bar{E}_z^p$	induced transverse electric field of the p-th layer
$\mathbf{E}$	electric field vector
$\mathbf{e}$	piezoelectric stress constants matrix
E^*	complex Young's modulus
e_{15}^p	piezoelectric stress constant of the p-th layer
e_{31}^{*p}	piezoelectric stress constant of the p-th layer
E_x^p	axial electric field of the p-th layer
E_z^p	transverse electric field of the p-th layer
$\bar{F}_i$	amplitude of the i-th degree of freedom of the mechanical force input
$\bar{\mathbf{F}}$	applied mechanical forces amplitudes vector
$\mathbf{F}$	applied mechanical forces global vector
$\mathbf{f}$	applied mechanical forces vector
F_x^k	axial volume force of the k-th layer

F_z^k	transverse volume force of the k-th layer
$\mathbf{G}$	shear stiffness matrix
G^*	complex shear modulus
G''	shear loss modulus
G'	shear storage modulus
H	electro-mechanical enthalpy
$H_{\phi\phi}^p$	dielectric enthalpy term of the p-th layer
$H_{\phi u}^p$	direct piezoelectric enthalpy term of the p-th layer
h_k	half thickness of the k-th layer
$H_{u\phi}^p$	converse piezoelectric enthalpy term of the p-th layer
H_{uu}^p	mechanical enthalpy term of the p-th layer
$\bar{I}_p$	first-order moment of area of the p-th layer
I_k	second-order moment of area of the k-th layer
$\mathbf{J}$	inertia matrix
$\bar{k}$	total number of generalized mechanical displacements
$\mathbf{K}_{\phi\phi}$	capacitance stiffness matrix
$\mathbf{K}_{\phi u}$	direct piezoelectric stiffness matrix
$\mathbf{K}_{u\phi}$	converse piezoelectric stiffness matrix
$\mathbf{K}_{uu}$	mechanical stiffness matrix
$\mathbf{K}_{uu}^E$	stiffness matrix of the elastic layers
$\mathbf{K}_{uu}^{P*}$	stiffness matrix of the piezoelectric layers
$\mathbf{K}_{uu}^V$	complex stiffness matrix of the viscoelastic layers
k_s	shear correction factor
$\mathbf{L}_{xx}$	extensional differential operator matrix
$\mathbf{L}_{zx}$	shear differential operator matrix
L	length of the beam
L_e	elemental length
$\mathbf{M}_{uu}$	mass matrix
$\mathbf{N}_\phi$	electrical interpolation matrix
$\mathbf{N}_u$	mechanical interpolation matrix
$\bar{p}$	total number of piezoelectric layers
$\mathbf{P}$	piezoelectric equivalent stiffness matrix
$\mathbf{R}_\phi^e$	electrical connectivity matrix
$\mathbf{R}_u^e$	mechanical connectivity matrix
$\mathbf{S}$	strain vector
S_{xx}^k	extensional strain of the k-th layer
S_{xz}^k	shear strain of the k-th layer
$\mathbf{T}$	stress vector
T	kinetic energy
t	time
T^k	kinetic energy of the k-th layer

$T_{oi}^{\phi u}$	induced voltage per unit force frequency response
$T_{oi}^{\phi\phi}$	induced voltage per unit voltage frequency response
$T_{oi}^{u\phi}$	displacement per unit voltage frequency response
T_{oi}^{uu}	displacement per unit force frequency response
T_{xx}^{k}	extensional stress of the k-th layer
T_{zx}^{k}	shear stress of the k-th layer
$\bar{U}_o$	displacement amplitude extracted from the o-th degree of freedom
$\bar{\mathbf{U}}$	complex mechanical amplitudes vector
$\bar{\mathbf{u}}$	global mechanical degrees of freedom vector
$\bar{\mathbf{u}}^e$	elemental mechanical degrees of freedom vector
$\mathbf{u}$	global generalized mechanical displacements vector
$\mathbf{u}^e$	elemental generalized mechanical displacements vector
$\tilde{u}_k$	axial displacement of the beam
u_0	axial displacement of the beam's mid-plane
$\tilde{w}_k$	transverse displacement of the beam
W	work of the applied mechanical forces and electrical charge density
w_0	transverse displacement of the beam's mid-plane
W_{ϕ}^{p}	work of the applied electric charge density of the p-th layer
W_{u}^{k}	work of the applied mechanical forces of the k-th layer
x	longitudinal axis of the beam
$\mathbf{Y}$	extensional stiffness matrix
y	transverse axis in the width direction of the beam
z_k	transverse axis in the thickness direction of the k-th layer

Chapter 1

Introduction

1.1 Damping Treatments

Passive damping treatments have been extensively used in engineering to reduce vibration and noise radiation [1]. The simplest form of passive damping is the one where single layers of viscoelastic materials are attached to the host structure. This is known as *passive layer damping* (PLD). When the structure vibrates, energy is dissipated in the viscoelastic layer. Increasing the thickness and length of the viscoelastic treatment would increase the energy dissipation and consequently the damping [2]. However, in applications where the weight is of critical importance, a more efficient treatment is required, and other alternatives to increase damping must be found.

It is well known that the inclusion of elastic constraining layers covering the viscoelastic layer can enhance the energy dissipation through an increase in shear deformations (Figure 1.1). This type of treatment is known as *passive constrained layer damping* (PCLD). Some examples can be found in references [3–5]. However, while passive damping treatments can greatly improve damping of the system, there are limitations. Viscoelastic materials have frequency and temperature dependent mechanical properties which can vary the damping properties, bringing limitations to the effective temperature and frequency range of the treatment. In order to provide adequate damping over a broad frequency band, different viscoelastic materials must be chosen which often complicates the analysis and design of the system. Therefore, while viscoelastic treatments are easy to apply, the damping is often of limited bandwidth.

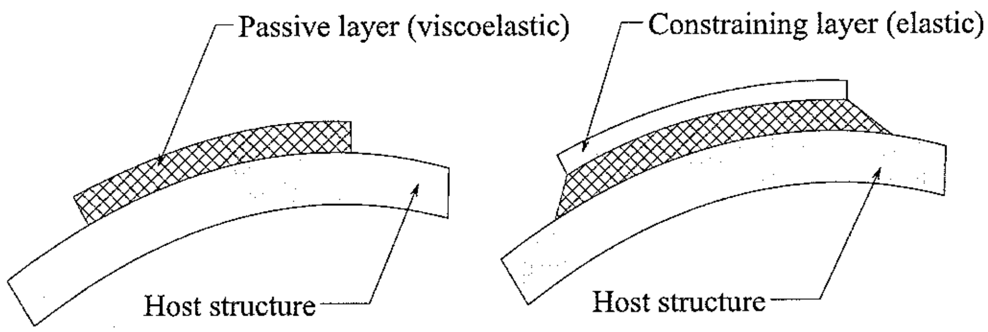

Figure 1.1: Viscoelastic (PLD) and passive constrained layer damping (PCLD) treatments .

From the early 90's the so-called *active constrained layer damping* (ACLD) approach has been developed and applied to structures [6–9]. Those are hybrid treatments with constraining layers made of piezoelectric materials (Figure 1.2). One of the unique features of piezoelectric materials is that they can serve both as sensors and actuators [10]. If utilized as actuators, and actuated according to an appropriate control law, the active constraining layer can increase the shear deformation of the viscoelastic layer and overcome some of the PCLD limitations. The ACLD treatments combine the high capacity of passive viscoelastic materials to dissipate vibrational energy at high frequencies with the active capacity of piezoelectric materials at low frequencies. Therefore, in the same damping treatment, a broader band control is achieved benefiting from the advantages of both passive (simplicity, stability, fail-safe, low-cost) and active (adaptability, high-performance) systems. Some examples can be found in references [11–13].

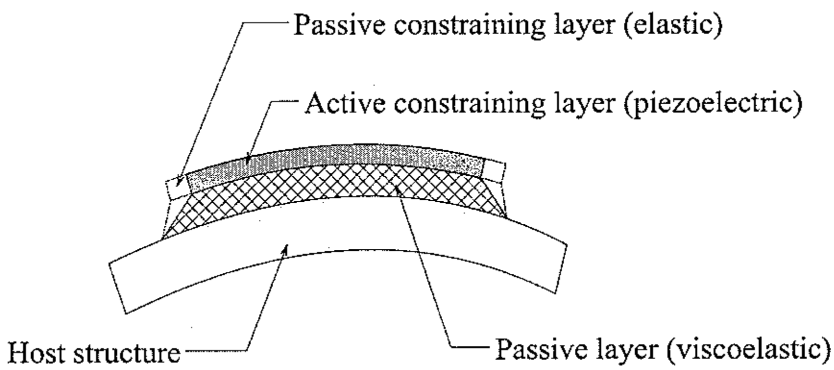

Figure 1.2: Active constrained layer damping (ACLD) treatment .

Various configurations of active and passive layers have been proposed in an attempt to improve performance. In general the so-called hybrid active-passive (or arbitrary ACLD) treatments involving arbitrary arrangements of constraining and passive layers, integrating piezoelectric sensors and actuators, might be utilized [14–18]. A survey of advances in hybrid active-passive vibrations and noise control via piezoelectric and viscoelastic constrained layer treatments can be found in references [19,20].

1.2 Modelling Considerations

Modeling this kind of structural system often requires a coupled model of the structure, which comprises piezoelectric, viscoelastic and elastic layers. These treatments are applied to beams, plates and shells. They can be modeled as either lumped or distributed parameter systems, and usually have complicated geometries that make the analytical solution of the equations of motion difficult, if not impossible. Alternatively, various discretization techniques, such as finite element (FE) modelling, modal analysis, and lumped parameters models, allow the approximation of the partial differential equations by a finite set of ordinary differential equations.

The temperature and frequency dependent material properties of the viscoelastic materials complicate the mathematical model. Usually the temperature is assumed constant and only models concerning frequency dependence are utilized. The simplest way of modelling those materials is achieved by a *complex modulus approach* (CMA) where the material properties are assumed frequency independent [21]. The complex modulus approach is a frequency domain method that is limited to steady state vibrations and single-frequency harmonic excitations. Time domain models such as the *Golla-Hughes-McTavish* (GHM) model [22], the *anelastic displacement fields*

(ADF) approach [23] or the *fractional calculus approach* [24], have been developed in the last few years and represent good alternatives to the complex modulus approach when the study of transient response is of interest.

In the development of FE models with piezoelectric actuators or sensors, different assumptions can be taken into account in the theoretical model when considering the electro-mechanical coupling. A survey on the advances in FE modelling of piezoelectric adaptive structures is presented by Benjeddou [25]. These assumptions regard mainly the use (or not) of electric degrees of freedom (DoFs) and the approximations of the through-the-thickness variation of the electric potential. Therefore, they lead to decoupled, partial and fully coupled electro-mechanical theories, which in turn can lead to different modifications of the structure's stiffness and different approximations of the physics of the system. Furthermore, these electro-mechanical coupling theories can be considered by the use of *effective stiffness parameters*, defined according to the electric boundary condition considered, as shown in [26, 27] for a smart beam.

1.3 Objectives and Structure of the Work

The objective of this work is the development of a generic analytical model that can account for the hybrid couplings in an accurate and consistent way. It can therefore be seen as an initial step from which different analytical and discretization methods can be used for the solution of arbitrary hybrid active-passive treatments on beams.

When designing hybrid active-passive treatments it is important to know the configuration of the structure and treatment that gives optimal damping. The designer needs a model of the system in order to define the optimal locations, thicknesses, configurations, control law, etc. Thus, there are numerous options at design stage.

We start by presenting the structural analytical model of a composite beam with an arbitrary number of layers of elastic, piezoelectric and viscoelastic materials, attached to both surfaces of the beam. The kinematic assumptions, based in a partial layerwise theory, are first presented. Then, the constitutive equations and electric model assumptions for the piezoelectric materials, which account for a fully coupled electro-mechanical theory, are described. Moreover, the frequency and temperature dependent constitutive behavior of the viscoelastic layers is discussed.

Hamilton's principle is utilized to derive the weak and strong forms governing the motion and electric charge equilibrium of the beam with arbitrary ACLD treatments. The strong forms of the general analytical model are then presented by a set of partial differential equations, namely, the equations of motion and electric charge equilibrium, and the electro-mechanical boundary conditions.

Based on the weak forms of the analytical model a FE solution is presented and a composite beam FE is developed. The spatial model and piezoelectric sensors and actuators equations are then presented. The damping behavior of the viscoelastic layers stiffness matrix is modeled by the complex modulus approach and the frequency response generation algorithm of the FE model is presented.

Finally, a case study concerning a clamped aluminium beam with a partial ACLD treatment (viscoelastic layer sandwiched between the beam and piezoelectric patch) is analyzed. The developed FE is used in the prediction of three frequency response functions: acceleration per unit force and voltage into the piezoelectric actuator and induced voltage per unit force. Numerical results are presented and compared with experimental results to validate the FE numerical tool.

Chapter 2

Analytical Model

2.1 Introduction

In this chapter the analytical model for a beam with arbitrary ACLD treatments is developed. For the sake of brevity the development of the weak and strong forms, governing the motion and electric charge equilibrium, is presented in Appendix A and the reader will be referred to it when convenient. The resultant set of partial differential equations, namely, the equations of motion and electric charge equilibrium and electro-mechanical boundary conditions, are obtained from the strong forms. Concerning the weak forms, they will be used in the next chapter as the basis for the development of a one-dimensional FE model.

2.2 Displacements and Strains

Consider the layered beam illustrated in Figure 2.1. The composite beam consists of a host beam, layer 0, of thickness $2h_0$, to which other layers (treatments) are attached. In order to be able to model several configurations of the treatments, the composite beam theory allows an arbitrary number of layers of elastic, piezoelectric and viscoelastic materials, in arbitrary positions. There are $\bar{n}$ layers on the top surface and $-\bar{m}$ layers on the bottom surface. The displacement field is defined according to a partial layerwise theory where the axial and transverse displacements, $\tilde{u}_k(x, z_k, t)$ and $\tilde{w}_k(x, t)$, of the top ($n = 1, \ldots, \bar{n}$), core ($c = 0$) and bottom ($m = \bar{m}, \ldots, -1$) layers are given by

$$\tilde{u}_n(x, z_n, t) = u_0(x,t) + h_0\theta_0(x,t) + \sum_{i=1}^{n-1} 2h_i\theta_i(x,t) + (z_n + h_n)\theta_n(x,t), \tag{2.1a}$$

$$\tilde{u}_c(x, z_c, t) = u_0(x,t) + z_0\theta_0(x,t), \tag{2.1b}$$

$$\tilde{u}_m(x, z_m, t) = u_0(x,t) - h_0\theta_0(x,t) - \sum_{i=m+1}^{-1} 2h_i\theta_i(x,t) + (z_m - h_m)\theta_m(x,t), \tag{2.1c}$$

$$\tilde{w}_k(x,t) = \tilde{w}_n(x,t) = \tilde{w}_c(x,t) = \tilde{w}_m(x,t) = w_0(x,t), \tag{2.1d}$$

where $2h_k$ is the thickness of layers k ($k = \bar{m}, \ldots, -1, 0, 1, \ldots, \bar{n}$), $u_0(x,t)$, $w_0(x,t)$ and $\theta_0(x,t)$ are, respectively, the generalized axial and transverse displacements and the rotation of the beam's mid-plane, and $\theta_n(x,t)$ and $\theta_m(x,t)$ are the rotation of each n-th top and m-th bottom layer. It is worth noting that positive indices are used to denote the top layers and negative indices are used to the bottom ones, i.e., $n > 0$ and $m < 0$. The z-coordinates in Equations (2.1a) and (2.1c) are measured from the interface between layers n and $n-1$ and m and $m+1$ through the terms $z_n + h_n$ and $z_m - h_m$. They represent a translation of the rotation axis of each top and bottom layer from the layer mid-plane to the interface of the adjacent layer. Furthermore, note that axial displacement continuity at the interfaces of the layers is assured, leading to coupling terms in the axial displacements of the layers, and that a constant through-the-thickness transverse displacement $w_0(x,t)$ is assumed.

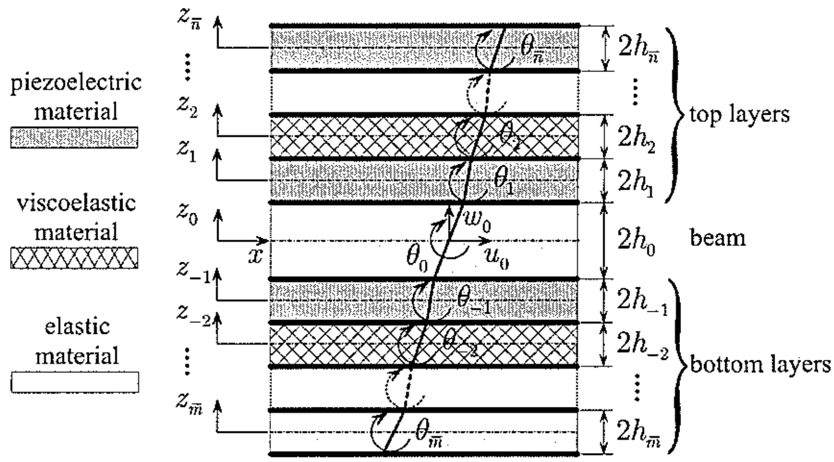

Figure 2.1: Layerwise displacement field of the beam with arbitrary ACLD treatments.

According to the displacement field (2.1) the extensional and shear strains of the layers are determined by the usual linear strain-displacement relations, to be

$$S_{xx}^n = \frac{\partial \tilde{u}_n}{\partial x} = u_0' + h_0\theta_0' + \sum_{i=1}^{n-1} 2h_i\theta_i' + (z_n + h_n)\theta_n', \tag{2.2a}$$

$$S_{xx}^c = \frac{\partial \tilde{u}_c}{\partial x} = u_0' + z_0\theta_0', \tag{2.2b}$$

$$S_{xx}^m = \frac{\partial \tilde{u}_m}{\partial x} = u_0' - h_0\theta_0' - \sum_{i=m+1}^{-1} 2h_i\theta_i' + (z_m - h_m)\theta_m', \tag{2.2c}$$

$$S_{zx}^k = \frac{\partial \tilde{w}_k}{\partial x} - \frac{\partial \tilde{u}_k}{\partial z_k} = w_0' - \theta_k, \tag{2.2d}$$

where the notation $(\cdot)'$ is used to denote the spatial derivative in the x-direction. The kinematic hypotheses considered previously lead to null transverse strains and a first-order shear deformation theory (FSDT) for each layer.

2.3 Constitutive Equations

The linear piezoelectric constitutive equations in compact matrix notation [28] are given by

$$\mathrm{T} = \mathrm{c}^E\mathrm{S} - \mathrm{e}^\mathrm{T}\mathrm{E}, \tag{2.3a}$$

$$\mathrm{D} = \mathrm{eS} + \varepsilon^S\mathrm{E}, \tag{2.3b}$$

where T, S, E and D are, respectively, the stress, strain, electric field and electric displacement vectors, and $\mathbf{c}^E$, $\mathbf{e}^\mathrm{T}$ and $\boldsymbol{\varepsilon}^S$ are, respectively, the elasticity (at constant electric field), transpose piezoelectric and dielectric (at constant strain) matrices appropriate for the material.

The material of the piezoelectric layers is assumed to be orthotropic, with the axes of orthotropy parallel to the axes of the beam, x, y, z_k, and polarized in the transverse direction z_p. They have the behavior of normal piezoelectric materials, with the symmetry properties of an orthorhombic crystal of the class $mm2$ [28, 29]. Representing Equations (2.3), with their full matrix and vector terms, for a generic piezoelectric layer p, yields

$$\begin{Bmatrix} T^p_{xx} \\ T^p_{yy} \\ T^p_{zz} \\ T^p_{yz} \\ T^p_{zx} \\ T^p_{xy} \end{Bmatrix} = \begin{bmatrix} c^p_{11} & c^p_{12} & c^p_{13} & 0 & 0 & 0 \\ c^p_{12} & c^p_{22} & c^p_{23} & 0 & 0 & 0 \\ c^p_{13} & c^p_{23} & c^p_{33} & 0 & 0 & 0 \\ 0 & 0 & 0 & c^p_{44} & 0 & 0 \\ 0 & 0 & 0 & 0 & c^p_{55} & 0 \\ 0 & 0 & 0 & 0 & 0 & c^p_{66} \end{bmatrix} \begin{Bmatrix} S^p_{xx} \\ S^p_{yy} \\ S^p_{zz} \\ S^p_{yz} \\ S^p_{zx} \\ S^p_{xy} \end{Bmatrix} - \begin{bmatrix} 0 & 0 & e^p_{31} \\ 0 & 0 & e^p_{32} \\ 0 & 0 & e^p_{33} \\ 0 & e^p_{24} & 0 \\ e^p_{15} & 0 & 0 \\ 0 & 0 & 0 \end{bmatrix} \begin{Bmatrix} E^p_x \\ E^p_y \\ E^p_z \end{Bmatrix}, \tag{2.4a}$$

$$\begin{Bmatrix} D^p_x \\ D^p_y \\ D^p_z \end{Bmatrix} = \begin{bmatrix} 0 & 0 & 0 & 0 & e^p_{15} & 0 \\ 0 & 0 & 0 & e^p_{24} & 0 & 0 \\ e^p_{31} & e^p_{32} & e^p_{33} & 0 & 0 & 0 \end{bmatrix} \begin{Bmatrix} S^p_{xx} \\ S^p_{yy} \\ S^p_{zz} \\ S^p_{yz} \\ S^p_{zx} \\ S^p_{xy} \end{Bmatrix} + \begin{bmatrix} \varepsilon^p_{11} & 0 & 0 \\ 0 & \varepsilon^p_{22} & 0 \\ 0 & 0 & \varepsilon^p_{33} \end{bmatrix} \begin{Bmatrix} E^p_x \\ E^p_y \\ E^p_z \end{Bmatrix}. \tag{2.4b}$$

The displacement field considered in (2.1) is independent of the y-axis and null along that direction. As consequence,

$$S^p_{yy} = S^p_{yz} = 0. \tag{2.5}$$

Moreover, assuming $T^p_{zz} \approx 0$ as a priority choice to the one of $S^p_{zz} = 0$, which results from the kinematic assumptions, yields

$$S^p_{zz} = \frac{1}{c^p_{33}}\left(e^p_{33}E^p_z - c^p_{13}S^p_{xx}\right). \tag{2.6}$$

Thus, considering (2.5) and substituting (2.6) in (2.4), the constitutive equations of a generic top or bottom piezoelectric layer p can be written in the following reduced form,

$$\begin{Bmatrix} T^p_{xx} \\ T^p_{zx} \end{Bmatrix} = \begin{bmatrix} c^{*p}_{11} & 0 \\ 0 & c^p_{55} \end{bmatrix} \begin{Bmatrix} S^p_{xx} \\ S^p_{zx} \end{Bmatrix} - \begin{bmatrix} 0 & e^{*p}_{31} \\ e^p_{15} & 0 \end{bmatrix} \begin{Bmatrix} E^p_x \\ E^p_z \end{Bmatrix}, \tag{2.7a}$$

$$\begin{Bmatrix} D^p_x \\ D^p_z \end{Bmatrix} = \begin{bmatrix} 0 & e^p_{15} \\ e^{*p}_{31} & 0 \end{bmatrix} \begin{Bmatrix} S^p_{xx} \\ S^p_{zx} \end{Bmatrix} + \begin{bmatrix} \varepsilon^p_{11} & 0 \\ 0 & \varepsilon^{*p}_{33} \end{bmatrix} \begin{Bmatrix} E^p_x \\ E^p_z \end{Bmatrix}, \tag{2.7b}$$

where

$$c^{*p}_{11} = c^p_{11} - \frac{{c^p_{13}}^2}{c^p_{33}},\; e^{*p}_{31} = e^p_{31} - e^p_{33}\frac{c^p_{13}}{c^p_{33}},\; \varepsilon^{*p}_{33} = \varepsilon^p_{33} + \frac{{e^p_{33}}^2}{c^p_{33}}. \tag{2.8a-c}$$

The modification of constants c^p_{11}, e^p_{31} and ε^p_{33} is due to the transverse stress assumption, $T^p_{zz} \approx 0$, and to the fact that the components T^p_{yz}, T^p_{xy}, S^p_{yz} and S^p_{xy}, and the y-component of the electric field E^p_y and electric displacement D^p_y, are considered negligible to the electro-mechanical energy.

Equations (2.7) are the reduced constitutive equations of a generic piezoelectric layer, tipically utilized when considering FSDT. As can be seen, the electro-mechanical coupling takes place between the extensional strain and the transverse electric field, and the shear strain and axial electric field components. Furthermore, for the characterization of the core layer or any other top or bottom viscoelastic or elastic layers, Equation (2.7a) can also be used by setting the piezoelectric contants e_{31}^{*p} and e_{15}^{p} to zero and by using the appropriate values of the Young's and shear modulus c_{11}^{*p} and c_{55}^{p} in the elasticity matrix.

2.4 Electric Field and Potential Assumptions

In the present work, a fully coupled electro-mechanical theory which takes into account the direct piezoelectric effect with a non-linear distribution of the electric potential is utilized. The electric displacement vector in Equation (2.7b) can be written as

$$\begin{Bmatrix} D_x^p \\ D_z^p \end{Bmatrix} = \begin{bmatrix} \varepsilon_{11}^p & 0 \\ 0 & \varepsilon_{33}^{*p} \end{bmatrix} \begin{Bmatrix} E_x^p - \bar{E}_x^p \\ E_z^p - \bar{E}_z^p \end{Bmatrix}, \tag{2.9}$$

with

$$\bar{E}_x^p = -\frac{e_{15}^p}{\varepsilon_{11}^p} S_{zx}^p, \quad \bar{E}_z^p = -\frac{e_{31}^{*p}}{\varepsilon_{33}^{*p}} S_{xx}^p, \tag{2.10a,b}$$

where $\bar{E}_x^p$ and $\bar{E}_z^p$ are the electric fields induced by the mechanical strains.

According to reference [26], for electroded layers with the electric potential being prescribed and with the assumption of zero electric displacement in the x-direction, the axial and transverse electric fields, E_x^p and E_z^p, and the electric potential φ_p, are given by

$$E_x^p = \bar{E}_x^p, \quad E_z^p = -\frac{\phi_p}{2h_p} + \bar{E}_z^p - \frac{1}{2h_p}\int_{-h_p}^{h_p} \bar{E}_z^p \mathrm{d}z_p, \tag{2.11a,b}$$

$$\varphi_p = \frac{\phi_p}{2h_p}(z_p + h_p) - \int_{-h_p}^{z_p} \bar{E}_z^p \mathrm{d}z_p + \frac{(z_p + h_p)}{2h_p}\int_{-h_p}^{h_p} \bar{E}_z^p \mathrm{d}z_p, \tag{2.12}$$

where ϕ_p denotes the electrical potential difference between the electrodes of each piezoelectric layer. Substituting into Equations (2.11) and (2.12) the induced electric fields in (2.10) and considering the strain definitions in (2.2), the electric field and potential become [27]

$$E_x^p = -\frac{e_{15}^p}{\varepsilon_{11}^p}\left(w_0' - \theta_p\right), \quad E_z^p = -\frac{\phi_p}{2h_p} - \frac{e_{31}^{*p}}{\varepsilon_{33}^{*p}} z_p \theta_p', \tag{2.13a,b}$$

$$\varphi_p = \frac{\phi_p}{2h_p}\left(z_p + h_p\right) + \frac{1}{2}\frac{e_{31}^{*p}}{\varepsilon_{33}^{*p}}\left({z_p}^2 - {h_p}^2\right)\theta_p'. \tag{2.14}$$

It is worth noting that the first part of Equation (2.14) is a linear through-the-thickness electric potential term concerning the applied electric potential difference and that the second part is a parabolic term concerning the electric potential induced by the mechanical strains.

2.5 Complex Modulus of Viscoelastic Materials

Viscoelastic materials are a class of materials which exhibit a strong temperature and frequency dependent constitutive behavior. Assuming a fixed temperature, they can be characterized in the frequency domain by a complex shear or extensional modulus, $G^*(\omega)$ or $E^*(\omega)$, and a loss factor $\eta(\omega)$ which accounts for energy dissipation effects. Considering simple harmonic excitation and a fixed temperature, it is possible to use the complex modulus approach to describe the viscoelastic behavior by putting

$$G^*(\omega) = G'(\omega) + jG''(\omega), \tag{2.15}$$

where $G'(\omega)$ is the shear storage modulus, $G''(\omega)$ is the shear loss modulus, ω is the frequency and $j = \sqrt{-1}$. The loss factor of the viscoelastic materials is defined as

$$\eta(\omega) = \frac{G''(\omega)}{G'(\omega)}, \tag{2.16}$$

and hence equation (2.15) becomes

$$G^*(\omega) = G'(\omega)\left[1 + j\eta(\omega)\right]. \tag{2.17}$$

If we consider a linear, homogeneous and isotropic viscoelastic material, the Young's storage modulus $E'(\omega)$ and shear storage modulus $G'(\omega)$ are related by

$$G'(\omega) = \frac{E'(\omega)}{2\left[1 + \nu(\omega)\right]}, \tag{2.18}$$

where $\nu(\omega)$ is the Poisson's ratio. In general, the complex moduli $E^*(\omega)$ and $G^*(\omega)$ are not proportional because the Poisson's ratio is also frequency dependent and the loss factors $\eta_E(\omega)$ and $\eta_G(\omega)$ are not equal. However, for simplicity, one can relax that condition and put $\eta_E(\omega) = \eta_G(\omega) = \eta(\omega)$ and $\nu(\omega) = \nu$.

2.6 Variational Formulation

In order to derive the weak and strong forms, governing the motion and electric charge equilibrium of the composite beam with ACLD treatments, Hamilton's principle is used. The Lagrangian and the work of the applied forces are adapted for the electrical and mechanical contributions [30], so that

$$\delta \int_{t_0}^{t_1} (T - H + W)\, \mathrm{d}t = 0, \tag{2.19}$$

where t_0 and t_1 define the time interval, δ denotes the variation, T is the kinetic energy, H is the electro-mechanical enthalpy (energy stored in the piezoelectric and non-piezoelectric layers) and W denotes the work done by the applied mechanical forces and electrical charges. In the following, it will be assumed that all the top and bottom layers are piezoelectric. However, the formulation still holds for non piezoelectric layers by considering only the mechanical virtual work terms for those layers.

2.6.1 Virtual Work of the Internal Electro-Mechanical Forces

The work of the internal electro-mechanical forces is given by the sum of the virtual work contributions of all layers. Considering a generic piezoelectric layer $p = n, m = \bar{m}, \ldots, -1, 1, \ldots, \bar{n}$, and separating the total virtual work δH^p into mechanical δH^p_{uu}, piezoelectric $\delta H^p_{u\phi}$ and $\delta H^p_{\phi u}$, and dielectric $\delta H^p_{\phi\phi}$ terms, for the piezoelectric layer of volume V_p, yields

$$\delta H^p = \delta H^p_{uu} - \delta H^p_{u\phi} - \delta H^p_{\phi u} - \delta H^p_{\phi\phi}, \tag{2.20}$$

where

$$\delta H^p_{uu} = \int_{V_p} (\delta S^p_{xx} c^{*p}_{11} S^p_{xx} + \delta S^p_{zx} c^p_{55} S^p_{zx})\, \mathrm{d}V_p, \tag{2.21}$$

$$\delta H^p_{u\phi} = \int_{V_p} (\delta S^p_{xx} e^{*p}_{31} E^p_z + \delta S^p_{zx} e^p_{15} E^p_x) \mathrm{d}V_p, \tag{2.22}$$

$$\delta H^p_{\phi u} = \int_{V_p} (\delta E^p_z e^{*p}_{31} S^p_{xx} + \delta E^p_x e^p_{15} S^p_{zx}) \mathrm{d}V_p, \tag{2.23}$$

$$\delta H^p_{\phi\phi} = \int_{V_p} (\delta E^p_x \varepsilon^p_{11} E^p_x + \delta E^p_z \varepsilon^{*p}_{33} E^p_z) \mathrm{d}V_p. \tag{2.24}$$

Furthermore, for the definition of the core's internal forces virtual work, $\delta H^c = \delta H^c_{uu}$, Equation (2.21) can also be used by considering the appropriate elastic coefficients and strain components.

Substituting the strain definitions (2.2) and the electric field components (2.13) into Equations (2.21)-(2.24) and integrating with respect to the cross section, the mechanical terms for the top, core and bottom layers, are given by

$$\begin{aligned}
\delta H^n_{uu} = \int_L \Big[& \delta u'_0 \Big(c^{*n}_{11} A_n u'_0 + c^{*n}_{11} h_0 A_n \theta'_0 + c^{*n}_{11} \sum_{i=1}^{n-1} 2h_i A_n \theta'_i + c^{*n}_{11} \bar{I}_n \theta'_n \Big) + \delta w'_0 \Big(c^n_{55} A_n w'_0 \\
& - c^n_{55} A_n \theta_n \Big) + \delta\theta'_0 \Big(c^{*n}_{11} h_0 A_n u'_0 + c^{*n}_{11} {h_0}^2 A_n \theta'_0 + c^{*n}_{11} h_0 \sum_{i=1}^{n-1} 2h_i A_n \theta'_i + c^{*n}_{11} h_0 \bar{I}_n \theta'_n \Big) \\
& + \sum_{i=1}^{n-1} \delta\theta'_i \Big(c^{*n}_{11} 2h_i A_n u'_0 + c^{*n}_{11} 2h_i h_0 A_n \theta'_0 + c^{*n}_{11} 2h_i \sum_{j=1}^{n-1} 2h_j A_n \theta'_j + c^{*n}_{11} 2h_i \bar{I}_n \theta'_n \Big) + \delta\theta'_n \Big(c^{*n}_{11} \bar{I}_n u'_0 \\
& + c^{*n}_{11} h_0 \bar{I}_n \theta'_0 + c^{*n}_{11} \sum_{i=1}^{n-1} 2h_i \bar{I}_n \theta'_i + c^{*n}_{11} I_n \theta'_n \Big) + \delta\theta_n \Big(c^n_{55} A_n \theta'_n - c^n_{55} A_n w'_0 \Big) \Big] \mathrm{d}L,
\end{aligned} \tag{2.25}$$

$$\begin{aligned}
\delta H^c_{uu} = \int_L \Big[& \delta u'_0 c^{*c}_{11} A_c u'_0 + \delta w'_0 \Big(c^c_{55} A_c w'_0 - c^c_{55} A_c \theta_0 \Big) + \delta\theta'_0 c^{*c}_{11} I_c \theta'_0 \\
& + \delta\theta_0 \Big(c^c_{55} A_c \theta_0 - c^c_{55} A_c w'_0 \Big) \Big] \mathrm{d}L,
\end{aligned} \tag{2.26}$$

$$\begin{aligned}
\delta H^m_{uu} = \int_L \Big[& \delta u'_0 \Big(c^{*m}_{11} A_m u'_0 - c^{*m}_{11} h_0 A_m \theta'_0 - c^{*m}_{11} \sum_{i=m+1}^{-1} 2h_i A_m \theta'_i + c^{*m}_{11} \bar{I}_m \theta'_m \Big) + \delta w'_0 \Big(c^m_{55} A_m w'_0 \\
& - c^m_{55} A_m \theta_m \Big) + \delta\theta'_0 \Big(- c^{*m}_{11} h_0 A_m u'_0 + c^{*m}_{11} {h_0}^2 A_m \theta'_0 + c^{*m}_{11} h_0 \sum_{i=m+1}^{-1} 2h_i A_m \theta'_i - c^{*m}_{11} h_0 \bar{I}_m \theta'_m \Big) \\
& + \sum_{i=m+1}^{-1} \delta\theta'_i \Big(- c^{*m}_{11} 2h_i A_m u'_0 + c^{*m}_{11} 2h_i h_0 A_m \theta'_0 + c^{*m}_{11} 2h_i \sum_{j=m+1}^{-1} 2h_j A_m \theta'_j - c^{*m}_{11} 2h_i \bar{I}_m \theta'_m \Big) \\
& + \delta\theta'_m \Big(c^{*m}_{11} \bar{I}_m u'_0 - c^{*m}_{11} h_0 \bar{I}_m \theta'_0 - c^{*m}_{11} \sum_{i=m+1}^{-1} 2h_i \bar{I}_m \theta'_i + c^{*m}_{11} I_m \theta'_m \Big) \\
& + \delta\theta_m \Big(c^m_{55} A_m \theta'_m - c^m_{55} A_m w'_0 \Big) \Big] \mathrm{d}L,
\end{aligned} \tag{2.27}$$

where L is the length of the beam and A_k, $\bar{I}_p$ and I_k represent the zero-, first- and second-order moments of area, respectively. They are given by

$$A_k = 2h_k b,\ \bar{I}_n = \frac{(2h_n)^2 b}{2},\ \bar{I}_m = -\frac{(2h_m)^2 b}{2},\ I_p = \frac{(2h_p)^3 b}{3},\ I_c = \frac{(2h_c)^3 b}{12}, \tag{2.28a-e}$$

where b is the width of the beam.

Similarly, the electrical terms become

$$\delta H^p_{u\phi} = -\delta H^{p(\phi)}_{u\phi} - \delta \bar{H}^{p(\phi)}_{u\phi}, \tag{2.29}$$

$$\delta H^p_{\phi u} = -\delta H^{p(\phi)}_{\phi u} - \delta \bar{H}^{p(\phi)}_{\phi u}, \tag{2.30}$$

$$\delta H^p_{\phi\phi} = \delta H^{p(\phi)}_{\phi\phi} + \delta \bar{H}^{p(\phi)}_{\phi\phi}, \tag{2.31}$$

where

$$\delta H^{n(\phi)}_{u\phi} = \int_L \frac{e^{*n}_{31}}{2h_n}\phi_n\Big(A_n\delta u_0' + h_0 A_n \delta\theta_0' + \sum_{i=1}^{n-1} 2h_i A_n \delta\theta_i' + \bar{I}_n\delta\theta_n'\Big)\mathrm{d}L, \tag{2.32}$$

$$\delta H^{m(\phi)}_{u\phi} = \int_L \frac{e^{*m}_{31}}{2h_m}\phi_m\Big(A_m\delta u_0' - h_0 A_m \delta\theta_0' - \sum_{i=m+1}^{-1} 2h_i A_m \delta\theta_i' + \bar{I}_m\delta\theta_m'\Big)\mathrm{d}L, \tag{2.33}$$

$$\delta H^{n(\phi)}_{\phi u} = \int_L \frac{e^{*n}_{31}}{2h_n}\delta\phi_n\Big(A_n u_0' + h_0 A_n \theta_0' + \sum_{i=1}^{n-1} 2h_i A_n \theta_i' + \bar{I}_n\theta_n'\Big)\mathrm{d}L, \tag{2.34}$$

$$\delta H^{m(\phi)}_{\phi u} = \int_L \frac{e^{*m}_{31}}{2h_m}\delta\phi_m\Big(A_m u_0' - h_0 A_m \theta_0' - \sum_{i=m+1}^{-1} 2h_i A_m \theta_i' + \bar{I}_m\theta_m'\Big)\mathrm{d}L, \tag{2.35}$$

$$\delta H^{p(\phi)}_{\phi\phi} = \int_L \frac{\varepsilon^{*p}_{33} A_p}{(2h_p)^2}\delta\phi_p\phi_p \mathrm{d}L, \tag{2.36}$$

$$\begin{aligned}\delta \bar{H}^{p(\phi)}_{u\phi} &= \delta \bar{H}^{p(\phi)}_{\phi u} = \delta \bar{H}^{p(\phi)}_{\phi\phi} \\ &= \int_L \Big\{ \frac{e^{*p\,2}_{31}}{\varepsilon^{*p}_{33}} I_p \delta\theta_p'\theta_p' + \frac{e^{p\,2}_{15}}{\varepsilon^{p}_{11}} A_p\Big[\delta w_0'\Big(w_0' - \theta_p\Big) + \delta\theta_p\Big(\theta_p - w_0'\Big)\Big]\Big\}\mathrm{d}L.\end{aligned} \tag{2.37}$$

The induced terms $\delta \bar{H}^{p(\phi)}_{u\phi}$, $\delta \bar{H}^{p(\phi)}_{\phi u}$ and $\delta \bar{H}^{p(\phi)}_{\phi\phi}$ in (2.37), are expressed only in terms of the mechanical strains. Therefore, those terms can be summed with the purely mechanical ones in (2.25) and (2.27),

$$\delta H^{p(\phi)}_{uu} = \delta H^p_{uu} + \delta \bar{H}^{p(\phi)}_{u\phi} + \delta \bar{H}^{p(\phi)}_{\phi u} - \delta \bar{H}^{p(\phi)}_{\phi\phi}, \tag{2.38}$$

which after some algebra yields

$$\begin{aligned}\delta H^{n(\phi)}_{uu} = \int_L &\Big[\delta u_0'\Big(c^{*n}_{11} A_n u_0' + c^{*n}_{11} h_0 A_n \theta_0' + c^{*n}_{11}\sum_{i=1}^{n-1} 2h_i A_n \theta_i' + c^{*n}_{11}\bar{I}_n\theta_n'\Big) + \delta w_0'\Big(\bar{c}^{n(\phi)}_{55} A_n w_0' \\ &- \bar{c}^{n(\phi)}_{55} A_n \theta_n\Big) + \delta\theta_0'\Big(c^{*n}_{11} h_0 A_n u_0' + c^{*n}_{11} h_0^2 A_n \theta_0' + c^{*n}_{11} h_0 \sum_{i=1}^{n-1} 2h_i A_n\theta_i' + c^{*n}_{11} h_0 \bar{I}_n \theta_n'\Big) \\ &+ \sum_{i=1}^{n-1}\delta\theta_i'\Big(c^{*n}_{11} 2h_i A_n u_0' + c^{*n}_{11} 2h_i h_0 A_n \theta_0' + c^{*n}_{11} 2h_i \sum_{j=1}^{n-1} 2h_j A_n \theta_j' + c^{*n}_{11} 2h_i \bar{I}_n \theta_n'\Big) + \delta\theta_n'\Big(c^{*n}_{11}\bar{I}_n u_0' \\ &+ c^{*n}_{11} h_0 \bar{I}_n \theta_0' + c^{*n}_{11}\sum_{i=1}^{n-1} 2h_i \bar{I}_n \theta_i' + \bar{c}^{n(\phi)}_{11} I_n \theta_n'\Big) + \delta\theta_n\Big(\bar{c}^{n(\phi)}_{55} A_n \theta_n' - \bar{c}^{n(\phi)}_{55} A_n w_0'\Big)\Big]\mathrm{d}L,\end{aligned} \tag{2.39}$$

$$
\begin{aligned}
\delta H_{uu}^{m(\phi)} = \int_L \Big[& \delta u_0' \Big(c_{11}^{*m} A_m u_0' - c_{11}^{*m} h_0 A_m \theta_0' - c_{11}^{*m} \sum_{i=m+1}^{-1} 2h_i A_m \theta_i' + c_{11}^{*m} \bar{I}_m \theta_m' \Big) \\
& + \delta w_0' \Big(\bar{c}_{55}^{m(\phi)} A_m w_0' - \bar{c}_{55}^{m(\phi)} A_m \theta_m \Big) + \delta \theta_0' \Big(- c_{11}^{*m} h_0 A_m u_0' + c_{11}^{*m} {h_0}^2 A_m \theta_0' \\
& + c_{11}^{*m} h_0 \sum_{i=m+1}^{-1} 2h_i A_m \theta_i' - c_{11}^{*m} h_0 \bar{I}_m \theta_m' \Big) + \sum_{i=m+1}^{-1} \delta \theta_i' \Big(- c_{11}^{*m} 2h_i A_m u_0' + c_{11}^{*m} 2h_i h_0 A_m \theta_0' \\
& + c_{11}^{*m} 2h_i \sum_{j=m+1}^{-1} 2h_j A_m \theta_j' - c_{11}^{*m} 2h_i \bar{I}_m \theta_m' \Big) + \delta \theta_m' \Big(c_{11}^{*m} \bar{I}_m u_0' - c_{11}^{*m} h_0 \bar{I}_m \theta_0' \\
& - c_{11}^{*m} \sum_{i=m+1}^{-1} 2h_i \bar{I}_m \theta_i' + \bar{c}_{11}^{m(\phi)} I_m \theta_m' \Big) + \delta \theta_m \Big(\bar{c}_{55}^{m(\phi)} A_m \theta_m' - \bar{c}_{55}^{m(\phi)} A_m w_0' \Big) \Big] \mathrm{d}L, \qquad (2.40)
\end{aligned}
$$

where

$$
\bar{c}_{11}^{p(\phi)} = c_{11}^{*p} + \frac{e_{31}^{*p\,2}}{4\varepsilon_{33}^{*p}}, \quad \bar{c}_{55}^{p(\phi)} = c_{55}^{p} + \frac{e_{15}^{p\ 2}}{\varepsilon_{11}^{p}}. \qquad (2.41a,b)
$$

Expressions (2.41) are the so-called *effective stiffness parameters* [27] and they represent the stiffness increase due to the direct piezoelectric effect. As can be seen in (2.39) and (2.40), the parameter $\bar{c}_{11}^{p(\phi)}$ only affects the bending stiffness and it represents the effects of the induced parabolic electric potential. Regarding $\bar{c}_{55}^{p(\phi)}$, it represents the stiffness increase due to the assumption of zero electric displacement in the axial direction and it affects only the shear stiffness.

Finally, the total virtual work of the internal electro-mechanical forces in all the layers (elastic, piezoelectric or viscoelastic layers) is given by

$$
\begin{aligned}
\delta H \;=\; & \delta H_{uu}^{c} + \sum_{n=1}^{\bar{n}} \Big(\delta H_{uu}^{n(\phi)} + \delta H_{u\phi}^{n(\phi)} + \delta H_{\phi u}^{n(\phi)} - \delta H_{\phi\phi}^{n(\phi)} \Big) \\
& + \sum_{m=\bar{m}}^{-1} \Big(\delta H_{uu}^{m(\phi)} + \delta H_{u\phi}^{m(\phi)} + \delta H_{\phi u}^{m(\phi)} - \delta H_{\phi\phi}^{m(\phi)} \Big) \qquad (2.42)
\end{aligned}
$$

2.6.2 Virtual Work of the Inertial Forces

The virtual work of the inertial forces in a generic layer k is given by

$$
\delta T^k = - \int_{V_k} \rho_k \Big(\delta \tilde{u}_k \ddot{\tilde{u}}_k + \delta \tilde{w}_k \ddot{\tilde{w}}_k \Big) \mathrm{d}V_k, \qquad (2.43)
$$

where ρ_k is the density of the material into layer. Substituting the displacement field defined in equation (2.1) into (2.43) gives, after integration, for the top, bottom and core layers,

$$
\begin{aligned}
\delta T^n = - \int_L \Big[& \delta u_0 \Big(\rho_n A_n \ddot{u}_0 + \rho_n h_0 A_n \ddot{\theta}_0 + \rho_n \sum_{i=1}^{n-1} 2h_i A_n \ddot{\theta}_i + \rho_n \bar{I}_n \ddot{\theta}_n \Big) + \delta w_0 \rho_n A_n \ddot{w}_0 \\
& + \delta \theta_0 \Big(\rho_n h_0 A_n \ddot{u}_0 + \rho_n {h_0}^2 A_n \ddot{\theta}_0 + \rho_n h_0 \sum_{i=1}^{n-1} 2h_i A_n \ddot{\theta}_i + \rho_n h_0 \bar{I}_n \ddot{\theta}_n \Big) \\
& + \sum_{i=1}^{n-1} \delta \theta_i \Big(\rho_n 2h_i A_n \ddot{u}_0 + \rho_n 2h_i h_0 A_n \ddot{\theta}_0 + \rho_n 4h_i \sum_{j=1}^{n-1} h_j A_n \ddot{\theta}_j + \rho_n 2h_i \bar{I}_n \ddot{\theta}_n \Big) \\
& + \delta \theta_n \Big(\rho_n \bar{I}_n \ddot{u}_0 + \rho_n h_0 \bar{I}_n \ddot{\theta}_0 + \rho_n \sum_{i=1}^{n-1} 2h_i \bar{I}_n \ddot{\theta}_i + \rho_n I_n \ddot{\theta}_n \Big) \Big] \mathrm{d}L, \qquad (2.44)
\end{aligned}
$$

$$\delta T^c = -\int_L \Big(\delta u_0 \rho_c A_c \ddot{u}_0 + \delta\theta_0 \rho_c I_c \ddot{\theta}_0 + \delta w_0 \rho_c A_c \ddot{w}_0\Big)\mathrm{d}L, \tag{2.45}$$

$$\begin{aligned}\delta T^m = -\int_L \Big[&\delta u_0\Big(\rho_m A_m \ddot{u}_0 - \rho_m h_0 A_m \ddot{\theta}_0 - \rho_m \sum_{i=m+1}^{-1} 2h_i A_m \ddot{\theta}_i + \rho_m \bar{I}_m \ddot{\theta}_m\Big) + \delta w_0 \rho_m A_m \ddot{w}_0 \\ &+\delta\theta_0\Big(-\rho_m h_0 A_m \ddot{u}_0 + \rho_m {h_0}^2 A_m \ddot{\theta}_0 + \rho_m h_0 \sum_{i=m+1}^{-1} 2h_i A_m \ddot{\theta}_i - \rho_m h_0 \bar{I}_m \ddot{\theta}_m\Big) \\ &+ \sum_{i=m+1}^{-1} \delta\theta_i\Big(-\rho_m 2h_i A_m \ddot{u}_0 + \rho_m 2h_i h_0 A_m \ddot{\theta}_0 + \rho_m 4h_i \sum_{j=m+1}^{-1} h_j A_m \ddot{\theta}_j - \rho_m 2h_i \bar{I}_m \ddot{\theta}_m\Big) \\ &+\delta\theta_m\Big(\rho_m \bar{I}_m \ddot{u}_0 + \rho_m h_0 \bar{I}_m \ddot{\theta}_0 - \rho_m \sum_{i=m+1}^{-1} 2h_i \bar{I}_m \ddot{\theta}_i + \rho_m I_m \ddot{\theta}_m\Big)\Big]\mathrm{d}L,\end{aligned} \tag{2.46}$$

The total virtual work of the inertial forces is then given by the sum of the virtual work of all the layers,

$$\delta T = \delta T^c + \sum_{n=1}^{\bar{n}} \delta T^n + \sum_{m=\bar{m}}^{-1} \delta T^m. \tag{2.47}$$

2.6.3 Virtual Work of the External Forces

In the determination of the virtual work of the mechanical external forces, two types of applied mechanical forces are considered, namely, axial and transverse volume forces F_x^k and F_z^k. The virtual work of those forces for the generic layer k is given by

$$\delta W_u^k = \int_{V_k} \Big(F_x^k \delta\tilde{u}_k + F_z^k \delta\tilde{w}_k\Big)\mathrm{d}V_k. \tag{2.48}$$

Substituting the displacement field (2.1) into (2.48) and integrating, yields

$$\delta W_u^n = \int_L \Big[\Big(\delta u_0 + h_0\delta\theta_0 + \sum_{i=1}^{n-1} 2h_i\delta\theta_i + h_n\delta\theta_n\Big)X_n + \delta\theta_n M_n + \delta w_0 Z_n\Big]\mathrm{d}L, \tag{2.49}$$

$$\delta W_u^c = \int_L \Big(\delta u_0 X_c + \delta\theta_0 M_c + \delta w_0 Z_c\Big)\mathrm{d}L, \tag{2.50}$$

$$\delta W_u^m = \int_L \Big[\Big(\delta u_0 - h_0\delta\theta_0 - \sum_{i=m+1}^{-1} 2h_i\delta\theta_i - h_m\delta\theta_m\Big)X_m + \delta\theta_m M_m + \delta w_0 Z_m\Big]\mathrm{d}L, \tag{2.51}$$

where

$$\Big(X_k, M_k, Z_k\Big) = \int_{A_k} \Big(F_x^k, z_k F_x^k, F_z^k\Big)\mathrm{d}A_k. \tag{2.52}$$

Thus, the total virtual work of the applied mechanical forces is given by

$$\delta W_u = \delta W_u^c + \sum_{n=1}^{\bar{n}} \delta W_u^n + \sum_{m=\bar{m}}^{-1} \delta W_u^m. \tag{2.53}$$

The virtual work of the electric charge density in each piezoelectric layer is defined by

$$\delta W_\phi^p = -\int_{A_p^e} \delta\varphi_p \tau_p \mathrm{d}A_p^e = -\int_L \delta\phi_p b\tau_p \mathrm{d}L, \tag{2.54}$$

where A_p^e is the electrode area and τ_p is the applied electric charge density at the electrode. Note that from the definition of the electric potential (2.14), and considering only the applied potential term, one finds that $\varphi_p(z_p = -h_p) = 0$ and $\varphi_p(z_p = h_p) = \phi_p$. The total virtual work of the applied electric charge density is given by

$$\delta W_\phi = \sum_{n=1}^{\bar{n}} \delta W_\phi^n + \sum_{m=\bar{m}}^{-1} \delta W_\phi^n. \tag{2.55}$$

Finally, the total virtual work δW of the applied external forces, comprising the virtual work of the applied mechanical forces δW_u and that of the applied electric charge density at the electrodes δW_ϕ, is given by

$$\delta W = \delta W_u + \delta W_\phi = \sum_{k=\bar{m}}^{\bar{n}} \delta W_u^k + \sum_{n=1}^{\bar{n}} \delta W_\phi^n + \sum_{m=\bar{m}}^{-1} \delta W_\phi^n. \tag{2.56}$$

2.7 Strong Forms

As derived in Appendix A, the equations of motion are obtained from the Hamilton's principle by substituting expressions (2.42), (2.47) and (2.56) into (2.19), integrating by parts and collecting the terms involving the variations δu_0, δw_0, $\delta\theta_0$, $\delta\theta_{\hat{n}}$ ($\hat{n} = 1, \ldots, \bar{n}-1$), $\delta\theta_{\bar{n}}$, $\delta\theta_{\bar{m}}$ and $\delta\theta_{\hat{m}}$ ($\hat{m} = \bar{m}+1, \ldots, -1$), independent and arbitrary in the interval $[0, L]$. They are given by

δu_0 :

$$\begin{aligned}
&\sum_{k=\bar{m}}^{\bar{n}} c_{11}^{*k} A_k u_0'' + \Big(\sum_{n=1}^{\bar{n}} c_{11}^{*n} h_0 A_n - \sum_{m=\bar{m}}^{-1} c_{11}^{*m} h_0 A_m \Big) \theta_0'' + \sum_{\hat{n}=1}^{\bar{n}-1} \Big(\sum_{i=\hat{n}+1}^{\bar{n}} \rho_i 2h_{\hat{n}} A_i + \rho_{\hat{n}} \bar{I}_{\hat{n}} \Big) \theta_{\hat{n}}'' \\
&\quad + c_{11}^{*\bar{n}} \bar{I}_{\bar{n}} \theta_{\bar{n}}'' + c_{11}^{*\bar{m}} \bar{I}_{\bar{m}} \theta_{\bar{m}}'' + \sum_{\hat{m}=\bar{m}+1}^{-1} \Big(- \sum_{i=\bar{m}}^{\hat{m}-1} \rho_i 2h_{\hat{m}} A_i + \rho_{\hat{m}} \bar{I}_{\hat{m}} \Big) \theta_{\hat{m}}'' + \sum_{n=1}^{\bar{n}} A_n \frac{e_{31}^{*n}}{2h_n} \phi_n' \\
&\quad + \sum_{m=\bar{m}}^{-1} A_m \frac{e_{31}^{*m}}{2h_m} \phi_m' + \sum_{k=\bar{m}}^{\bar{n}} X_k = \sum_{k=\bar{m}}^{\bar{n}} \rho_k A_k \ddot{u}_0 + \Big(\sum_{n=1}^{\bar{n}} \rho_n h_0 A_n - \sum_{m=\bar{m}}^{-1} \rho_m h_0 A_m \Big) \ddot{\theta}_{0i} \\
&\qquad + \sum_{\hat{n}=1}^{\bar{n}-1} \Big(\sum_{i=\hat{n}+1}^{\bar{n}} c_{11}^{*i} 2h_{\hat{n}} A + c_{11}^{*\hat{n}} \bar{I}_{\hat{n}} \Big) \ddot{\theta}_{\hat{n}} + \rho_{\bar{n}} \bar{I}_{\bar{n}} \ddot{\theta}_{\bar{n}} + \rho_{\bar{m}} \bar{I}_{\bar{m}} \ddot{\theta}_{\bar{m}} \\
&\qquad\quad + \sum_{\hat{m}=\bar{m}+1}^{-1} \Big(- \sum_{i=\bar{m}}^{\hat{m}-1} c_{11}^{*i} 2h_{\hat{m}} A_i + c_{11}^{*\hat{m}} \bar{I}_{\hat{m}} \Big) \ddot{\theta}_{\hat{m}},
\end{aligned} \tag{2.57}$$

δw_0 :

$$\begin{aligned}
&\Big(\sum_{n=1}^{\bar{n}} \bar{c}_{55}^{n(\phi)} A_n + c_{55}^0 A_0 + \sum_{m=\bar{m}}^{-1} \bar{c}_{55}^{m(\phi)} A_m \Big) w_0'' - c_{55}^c A_c \theta_0' - \sum_{\hat{n}=1}^{\bar{n}-1} \bar{c}_{55}^{\hat{n}(\phi)} A_{\hat{n}} \theta_{\hat{n}}' - \bar{c}_{55}^{\bar{n}(\phi)} A_{\bar{n}} \theta_{\bar{n}}' \\
&\qquad - \bar{c}_{55}^{\bar{m}(\phi)} A_{\bar{m}} \theta_{\bar{m}}' - \sum_{\hat{m}=\bar{m}+1}^{-1} \bar{c}_{55}^{\hat{m}(\phi)} A_{\hat{m}} \theta_{\hat{m}}' + \sum_{k=\bar{m}}^{\bar{n}} Z_k = \sum_{k=\bar{m}}^{\bar{n}} \rho_k A_k \ddot{w}_0,
\end{aligned} \tag{2.58}$$

$\delta\theta_0$:

$$\Big(\sum_{n=1}^{\bar n} c_{11}^{*n} h_0 A_n - \sum_{m=\bar m}^{-1} c_{11}^{*m} h_0 A_m\Big) u_0'' + \Big(\sum_{n=1}^{\bar n} c_{11}^{*n} {h_0}^2 A_n + c_{11}^{*0} I_0 + \sum_{m=\bar m}^{-1} c_{11}^{*m} {h_0}^2 A_m\Big)\theta_0''$$
$$+\sum_{\hat n=1}^{\bar n-1}\Big(2h_0 h_{\hat n}\sum_{i=\hat n+1}^{\bar n} c_{11}^{*i} A_i + c_{11}^{*\hat n} h_0 \bar I_{\hat n}\Big)\theta_{\hat n}'' + c_{11}^{*\bar n} h_0 \bar I_{\bar n}\theta_{\bar n}'' - \rho_{\bar m} h_0 \bar I_{\bar m}\theta_{\bar m}''$$
$$+\sum_{\hat m=\bar m+1}^{-1}\Big(2h_0 h_{\hat m}\sum_{i=\bar m}^{\hat m-1} c_{11}^{*i} A_i - c_{11}^{*\hat m} h_0 \bar I_{\hat m}\Big)\theta_{\hat m}'' + c_{55}^0 A_0 w_0' - c_{55}^0 A_0 \theta_0 + \sum_{n=1}^{\bar n}\frac{e_{31}^{*n}}{2h_n} h_0 A_n \phi_n'$$
$$-\sum_{m=\bar m}^{-1}\frac{e_{31}^{*m}}{2h_m} h_0 A_m \phi_m' + \sum_{n=1}^{\bar n} h_0 X_n + M_0 - \sum_{m=\bar m}^{-1} h_0 X_m = \Big(\sum_{n=1}^{\bar n}\rho_n h_0 A_n - \sum_{m=\bar m}^{-1}\rho_m h_0 A_m\Big)\ddot u_0$$
$$+\ddot\theta_0\Big(\sum_{n=1}^{\bar n}\rho_n h_0^2 A_n + \rho_0 I_0 + \sum_{m=\bar m}^{-1}\rho_m h_0^2 A_m\Big) + \sum_{\hat n=1}^{\bar n-1}\Big(2h_0 h_{\hat n}\sum_{i=\hat n+1}^{\bar n}\rho_i A_i + \rho_{\hat n} h_0 \bar I_{\hat n}\Big)\ddot\theta_{\hat n}$$
$$+\rho_{\bar n} h_0 \bar I_{\bar n}\ddot\theta_{\bar n} - c_{11}^{*\bar m} h_0 \bar I_{\bar m}\ddot\theta_{\bar m} + \sum_{\hat m=\bar m+1}^{-1}\Big(2h_0 h_{\hat m}\sum_{i=\bar m}^{\hat m-1}\rho_i A_i - \rho_{\hat m} h_0 \bar I_{\hat m}\Big)\ddot\theta_{\hat m} \tag{2.59}$$

$\delta\theta_{\hat n}$:

$$\Big(\sum_{i=\hat n+1}^{\bar n} c_{11}^{*i} 2h_{\hat n} A_i + c_{11}^{*\hat n}\bar I_{\hat n}\Big)u_0'' + \Big(2h_0 h_{\hat n}\sum_{i=\hat n+1}^{\bar n} c_{11}^{*i} A_i + c_{11}^{*\hat n} h_0 \bar I_{\hat n}\Big)\theta_0'' + \sum_{i=1}^{\hat n-1}\Big(\sum_{j=\hat n+1}^{\bar n}\rho_j 4h_{\hat n} h_i A_j$$
$$+\rho_{\hat n} 2h_i \bar I_{\hat n}\Big)\theta_i'' + \Big(\sum_{i=\hat n+1}^{\bar n} c_{11}^{*i} 4{h_{\hat n}}^2 A_i + \bar c_{11}^{\hat n(\phi)} I_{\hat n}\Big)\theta_{\hat n}'' + \sum_{j=\hat n+1}^{\bar n-1}\Big(\sum_{i=j+1}^{\bar n} c_{11}^{*i} 4h_{\hat n} h_j A_i + c_{11}^{*j} 2h_{\hat n}\bar I_j\Big)\theta_j''$$
$$+c_{11}^{*\bar n} 2h_{\hat n}\bar I_{\bar n}\theta_{\bar n}'' + \bar c_{55}^{\hat n(\phi)} A_{\hat n} w_0' - \bar c_{55}^{\hat n(\phi)} A_{\hat n}\theta_{\hat n} + \frac{e_{31}^{*\hat n}}{2h_{\hat n}}\bar I_{\hat n}\phi_{\hat n}' + \sum_{i=\hat n+1}^{\bar n} 2h_{\hat n} A_i \frac{e_{31}^{*i}}{2h_i}\phi_i' + h_{\hat n} X_{\hat n}$$
$$+\sum_{i=\hat n+1}^{\bar n} 2h_{\hat n} X_i + M_{\hat n} = \Big(\sum_{i=\hat n+1}^{\bar n}\rho_i 2h_{\hat n} A_i + \rho_{\hat n}\bar I_{\hat n}\Big)\ddot u_0 + \Big(2h_0 h_{\hat n}\sum_{i=\hat n+1}^{\bar n}\rho_i A_i + \rho_{\hat n} h_0 \bar I_{\hat n}\Big)\ddot\theta_0$$
$$+\sum_{i=1}^{\hat n-1}\Big(\sum_{j=\hat n+1}^{\bar n}\rho_j 4h_{\hat n} h_i A_j + \rho_{\hat n} 2h_i \bar I_{\hat n}\Big)\ddot\theta_i + \Big(\sum_{i=\hat n+1}^{\bar n}\rho_i 4{h_{\hat n}}^2 A_i + \rho_{\hat n} I_{\hat n}\Big)\ddot\theta_{\hat n}$$
$$+\sum_{j=\hat n+1}^{\bar n-1}\Big(\sum_{i=j+1}^{\bar n}\rho_i 4h_{\hat n} h_j A_i + \rho_j 2h_{\hat n}\bar I_j\Big)\ddot\theta_j + \rho_{\bar n} 2h_{\hat n}\bar I_{\bar n}\ddot\theta_{\bar n}, \tag{2.60}$$

$\delta\theta_{\bar n}$:

$$c_{11}^{*\bar n}\bar I_{\bar n} u_0'' + c_{11}^{*\bar n} h_0 \bar I_{\bar n}\theta_0'' + \sum_{\hat n=1}^{\bar n-1} c_{11}^{*\bar n} 2h_{\hat n}\bar I_{\bar n}\theta_{\hat n}'' + \bar c_{11}^{\bar n(\phi)} I_{\bar n}\theta_{\bar n}'' + \bar c_{55}^{\bar n(\phi)} A_{\bar n} w_0' - \bar c_{55}^{\bar n(\phi)} A_{\bar n}\theta_{\bar n}$$
$$+\frac{e_{31}^{*\bar n}}{2h_{\bar n}}\bar I_{\bar n}\phi_{\bar n}' + h_{\bar n} X_{\bar n} + M_{\bar n} = \rho_{\bar n}\bar I_{\bar n}\ddot u_0 + \rho_{\bar n} h_0 \bar I_{\bar n}\ddot\theta_0 + \sum_{\hat n=1}^{\bar n-1}\rho_{\bar n} 2h_{\hat n}\bar I_{\bar n}\ddot\theta_{\hat n} + \rho_{\bar n} I_{\bar n}\ddot\theta_{\bar n}, \tag{2.61}$$

$\delta\theta_{\bar m}$:

$$c_{11}^{*\bar m}\bar I_{\bar m} u_0'' - c_{11}^{*\bar m} h_0 \bar I_{\bar m}\theta_0'' + \bar c_{11}^{\bar m(\phi)} I_{\bar m}\theta_{\bar m}'' - \sum_{\hat m=\bar m+1}^{-1} c_{11}^{*\bar m} 2h_{\bar m}\bar I_{\bar m}\theta_{\hat m}'' + \bar c_{55}^{\bar m(\phi)} A_{\bar m} w_0' - \bar c_{55}^{\bar m(\phi)} A_{\bar m}\theta_{\bar m}$$
$$+\frac{e_{31}^{*\bar m}}{2h_{\bar m}}\bar I_{\bar m}\phi_{\bar m}' - h_{\bar m} X_{\bar m} + M_{\bar m} = \rho_{\bar m}\bar I_{\bar m}\ddot u_0 - \rho_{\bar m} h_0 \bar I_{\bar m}\ddot\theta_0 - \sum_{\hat m=\bar m+1}^{-1}\rho_{\bar m} 2h_{\hat m}\bar I_{\bar m}\ddot\theta_{\hat m} + \rho_{\bar m} I_{\bar m}\ddot\theta_{\bar m}, \tag{2.62}$$

$\delta\theta_{\hat{m}}$:

$$\begin{aligned}
&\Big(-\sum_{i=\bar{m}}^{\hat{m}-1} c_{11}^{*i} 2h_{\hat{m}} A_i + c_{11}^{*\hat{m}} \bar{I}_{\hat{m}} \Big) u_0'' + \Big(2h_0 h_{\hat{m}} \sum_{i=\bar{m}}^{\hat{m}-1} c_{11}^{*i} A_i - c_{11}^{*\hat{m}} h_0 \bar{I}_{\hat{m}} \Big) \theta_0'' + \sum_{j=\bar{m}+1}^{\hat{m}-1} \Big(\sum_{i=\bar{m}}^{j-1} c_{11}^{*i} 4h_{\hat{m}} h_j A_i \\
&-c_{11}^{*j} 2h_{\hat{m}} \bar{I}_j \Big) \theta_j'' + \Big(\sum_{i=\bar{m}}^{\hat{m}-1} c_{11}^{*i} 4{h_{\hat{m}}}^2 A_i + \bar{c}_{11}^{\hat{m}(\phi)} I_{\hat{m}} \Big) \theta_{\hat{m}}'' + \sum_{i=\hat{m}+1}^{-1} \Big(\sum_{j=\bar{m}}^{\hat{m}-1} \rho_j 4h_{\hat{m}} h_i A_j - \rho_{\hat{m}} 2h_i \bar{I}_{\hat{m}} \Big) \theta_i'' \\
&-c_{11}^{*\bar{m}} 2h_{\hat{m}} \bar{I}_{\bar{m}} \theta_{\bar{m}}'' + \bar{c}_{55}^{\hat{m}(\phi)} A_{\hat{m}} w_0' - \bar{c}_{55}^{\hat{m}(\phi)} A_{\hat{m}} \theta_{\hat{m}} + \frac{e_{31}^{*\hat{m}}}{2h_{\hat{m}}} \bar{I}_{\hat{m}} \phi_{\hat{m}}' - \sum_{i=\bar{m}}^{\hat{m}-1} 2h_{\hat{m}} A_i \frac{e_{31}^{*i}}{2h_i} \phi_i' - h_{\hat{m}} X_{\hat{m}} \\
&-\sum_{i=\bar{m}}^{\hat{m}-1} 2h_{\hat{m}} X_i + M_{\hat{m}} = \Big(-\sum_{i=\bar{m}}^{\hat{m}-1} \rho_i 2h_{\hat{m}} A_i + \rho_{\hat{m}} \bar{I}_{\hat{m}} \Big) \ddot{u}_0 + \Big(2h_0 h_{\hat{m}} \sum_{i=\bar{m}}^{\hat{m}-1} \rho_i A_i - \rho_{\hat{m}} h_0 \bar{I}_{\hat{m}} \Big) \ddot{\theta}_0 \\
&\qquad \sum_{j=\bar{m}+1}^{\hat{m}-1} \Big(\sum_{i=\bar{m}}^{j-1} \rho_i 4h_{\hat{m}} h_j A_i - \rho_j 2h_{\hat{m}} \bar{I}_j \Big) \ddot{\theta}_j + \Big(\sum_{i=\bar{m}}^{\hat{m}-1} \rho_i 4{h_{\hat{m}}}^2 A_i + \rho_{\hat{m}} I_{\hat{m}} \Big) \ddot{\theta}_{\hat{m}} \\
&\qquad + \sum_{i=\hat{m}+1}^{-1} \Big(\sum_{j=\bar{m}}^{\hat{m}-1} \rho_j 4h_{\hat{m}} h_i A_j - \rho_{\hat{m}} 2h_i \bar{I}_{\hat{m}} \Big) \ddot{\theta}_i + \rho_{\bar{n}} 2h_{\hat{n}} \bar{I}_{\bar{n}} \ddot{\theta}_{\bar{n}},
\end{aligned} \tag{2.63}$$

In a similar way (see Appendix A), the electric charge equilibrium equations are obtained by collecting the terms related to the variations $\delta\phi_n$ ($n = 1, ..., \bar{n}$) and $\delta\phi_m$ ($m = -1, ..., \bar{m}$), yielding

$\delta\phi_n$:

$$\frac{e_{31}^{*n}}{2h_n} A_n u_0' + \frac{e_{31}^{*n}}{2h_n} h_0 A_n \theta_0' + \sum_{i=1}^{n-1} \frac{e_{31}^{*n}}{2h_n} 2h_i A_n \theta_i' + \frac{e_{31}^{*n}}{2h_n} \bar{I}_n \theta_n' - \frac{\varepsilon_{33}^{*n} A_n}{4{h_n}^2} \phi_n = -b\tau_n, \tag{2.64}$$

$\delta\phi_m$:

$$\frac{e_{31}^{*m}}{2h_m} A_m u_0' - \frac{e_{31}^{*m}}{2h_m} h_0 A_m \theta_0' + \frac{e_{31}^{*m}}{2h_m} \bar{I}_m \theta_m' - \sum_{i=m+1}^{-1} \frac{e_{31}^{*m}}{2h_m} 2h_i A_m \theta_i' + -\frac{\varepsilon_{33}^{*m} A_m}{4{h_m}^2} \phi_m = -b\tau_m. \tag{2.65}$$

Finally, as derived in Appendix A, the electro-mechanical boundary conditions at $x = 0, L$ are expressed as

$$\begin{aligned}
\delta u_0 \Big[&\sum_{k=\bar{m}}^{\bar{n}} c_{11}^{*k} A_k u_0' + \Big(\sum_{n=1}^{\bar{n}} c_{11}^{*n} h_0 A_n - \sum_{m=\bar{m}}^{-1} c_{11}^{*m} h_0 A_m \Big) \theta_0' + \sum_{\hat{n}=1}^{\bar{n}-1} \Big(\sum_{i=\hat{n}+1}^{\bar{n}} \rho_i 2h_{\hat{n}} A_i + \rho_{\hat{n}} \bar{I}_{\hat{n}} \Big) \theta_{\hat{n}}' \\
&+c_{11}^{*\bar{n}} \bar{I}_{\bar{n}} \theta_{\bar{n}}' + c_{11}^{*\bar{m}} \bar{I}_{\bar{m}} \theta_{\bar{m}}' + \sum_{\hat{m}=\bar{m}+1}^{-1} \Big(-\sum_{i=\bar{m}}^{\hat{m}-1} \rho_i 2h_{\hat{m}} A_i + \rho_{\hat{m}} \bar{I}_{\hat{m}} \Big) \theta_{\hat{m}}' \\
&+\sum_{n=1}^{\bar{n}} A_n \frac{e_{31}^{*n}}{2h_n} \phi_n + \sum_{m=\bar{m}}^{-1} A_m \frac{e_{31}^{*m}}{2h_m} \phi_m \Big] = 0,
\end{aligned} \tag{2.66}$$

$$\begin{aligned}
\delta w_0 \Big[&\Big(\sum_{n=1}^{\bar{n}} \bar{c}_{55}^{n(\phi)} A_n + c_{55}^{0} A_0 + \sum_{m=\bar{m}}^{-1} \bar{c}_{55}^{m(\phi)} A_m \Big) w_0' + c_{55}^{c} A_c \theta_0 + \sum_{\hat{n}=1}^{\bar{n}-1} \bar{c}_{55}^{\hat{n}(\phi)} A_{\hat{n}} \theta_{\hat{n}} + \bar{c}_{55}^{\bar{n}(\phi)} A_{\bar{n}} \theta_{\bar{n}} \\
&+\bar{c}_{55}^{\bar{m}(\phi)} A_{\bar{m}} \theta_{\bar{m}} + \sum_{\hat{m}=\bar{m}+1}^{-1} \bar{c}_{55}^{\hat{m}(\phi)} A_{\hat{m}} \theta_{\hat{m}} \Big] = 0,
\end{aligned} \tag{2.67}$$

$$\begin{aligned}\delta\theta_0\Big[&\Big(\sum_{n=1}^{\bar{n}} c_{11}^{*n} h_0 A_n - \sum_{m=\bar{m}}^{-1} c_{11}^{*m} h_0 A_m\Big)u_0' + \Big(\sum_{n=1}^{\bar{n}} c_{11}^{*n} {h_0}^2 A_n + c_{11}^{*0} I_0 + \sum_{m=\bar{m}}^{-1} c_{11}^{*m} {h_0}^2 A_m\Big)\theta_0' \\ &+\sum_{\hat{n}=1}^{\bar{n}-1}\Big(2h_0 h_{\hat{n}} \sum_{i=\hat{n}+1}^{\bar{n}} c_{11}^{*i} A_i + c_{11}^{*\hat{n}} h_0 \bar{I}_{\hat{n}}\Big)\theta_{\hat{n}}' + c_{11}^{*\bar{n}} h_0 \bar{I}_{\bar{n}} \theta_{\bar{n}}' - \rho_{\bar{m}} h_0 \bar{I}_{\bar{m}} \theta_{\bar{m}}' + \sum_{\hat{m}=\bar{m}+1}^{-1}\Big(2h_0 h_{\hat{m}} \sum_{i=\bar{m}}^{\hat{m}-1} c_{11}^{*i} A_i \\ &-c_{11}^{*\hat{m}} h_0 \bar{I}_{\hat{m}}\Big)\theta_{\hat{m}}' + \sum_{n=1}^{\bar{n}} \frac{e_{31}^{*n}}{2h_n} h_0 A_n \phi_n - \sum_{m=\bar{m}}^{-1} \frac{e_{31}^{*m}}{2h_m} h_0 A_m \phi_m\Big] = 0,\end{aligned} \tag{2.68}$$

$$\begin{aligned}\delta\theta_{\hat{n}}\Big[&\Big(\sum_{i=\hat{n}+1}^{\bar{n}} c_{11}^{*i} 2h_{\hat{n}} A_i + c_{11}^{*\hat{n}} \bar{I}_{\hat{n}}\Big)u_0' + \Big(2h_0 h_{\hat{n}} \sum_{i=\hat{n}+1}^{\bar{n}} c_{11}^{*i} A_i + c_{11}^{*\hat{n}} h_0 \bar{I}_{\hat{n}}\Big)\theta_0' \\ &+\sum_{i=1}^{\hat{n}-1}\Big(\sum_{j=\hat{n}+1}^{\bar{n}} \rho_j 4h_{\hat{n}} h_i A_j + \rho_{\hat{n}} 2h_i \bar{I}_{\hat{n}}\Big)\theta_i' + \Big(\sum_{i=\hat{n}+1}^{\bar{n}} c_{11}^{*i} 4{h_{\hat{n}}}^2 A_i + \bar{c}_{11}^{\hat{n}(\phi)} I_{\hat{n}}\Big)\theta_{\hat{n}}' \\ +\sum_{j=\hat{n}+1}^{\bar{n}-1}&\Big(\sum_{i=j+1}^{\bar{n}} c_{11}^{*i} 4h_{\hat{n}} h_j A_i + c_{11}^{*j} 2h_{\hat{n}} \bar{I}_j\Big)\theta_j' + c_{11}^{*\bar{n}} 2h_{\hat{n}} \bar{I}_{\bar{n}} \theta_{\bar{n}}' + \frac{e_{31}^{*\hat{n}}}{2h_{\hat{n}}} \bar{I}_{\hat{n}} \phi_{\hat{n}} + \sum_{i=\hat{n}+1}^{\bar{n}} 2h_{\hat{n}} A_i \frac{e_{31}^{*i}}{2h_i} \phi_i\Big] = 0,\end{aligned} \tag{2.69}$$

$$\delta\theta_{\bar{n}}\Big(c_{11}^{*\bar{n}} \bar{I}_{\bar{n}} u_0' + c_{11}^{*\bar{n}} h_0 \bar{I}_{\bar{n}} \theta_0' + \sum_{\hat{n}=1}^{\bar{n}-1} c_{11}^{*\bar{n}} 2h_{\hat{n}} \bar{I}_{\bar{n}} \theta_{\hat{n}}' + \bar{c}_{11}^{\bar{n}(\phi)} I_{\bar{n}} \theta_{\bar{n}}' + \frac{e_{31}^{*\bar{n}}}{2h_{\bar{n}}} \bar{I}_{\bar{n}} \phi_{\bar{n}}\Big) = 0, \tag{2.70}$$

$$\delta\theta_{\bar{m}}\Big(c_{11}^{*\bar{m}} \bar{I}_{\bar{m}} u_0' - c_{11}^{*\bar{m}} h_0 \bar{I}_{\bar{m}} \theta_0' + \bar{c}_{11}^{\bar{m}(\phi)} I_{\bar{m}} \theta_{\bar{m}}' - \sum_{\hat{m}=\bar{m}+1}^{-1} c_{11}^{*\bar{m}} 2h_{\bar{m}} \bar{I}_{\bar{m}} \theta_{\hat{m}}' + \frac{e_{31}^{*\bar{m}}}{2h_{\bar{m}}} \bar{I}_{\bar{m}} \phi_{\bar{m}}\Big) = 0, \tag{2.71}$$

$$\begin{aligned}\delta\theta_{\hat{m}}\Big(&-\sum_{i=\bar{m}}^{\hat{m}-1} c_{11}^{*i} 2h_{\hat{m}} A_i + c_{11}^{*\hat{m}} \bar{I}_{\hat{m}}\Big)u_0' + \sum_{j=\bar{m}+1}^{\hat{m}-1}\Big(2h_0 h_{\hat{m}} \sum_{i=\bar{m}}^{\hat{m}-1} c_{11}^{*i} A_i - c_{11}^{*\hat{m}} h_0 \bar{I}_{\hat{m}}\Big)\theta_0' \\ -c_{11}^{*\bar{m}} 2h_{\hat{m}} \bar{I}_{\bar{m}} \theta_{\bar{m}}' &+ \sum_{j=\bar{m}+1}^{\hat{m}-1}\Big(\sum_{i=\bar{m}}^{j-1} c_{11}^{*i} 4h_{\hat{m}} h_j A_i - c_{11}^{*j} 2h_{\hat{m}} \bar{I}_j\Big)\theta_j' + \Big(\sum_{i=\bar{m}}^{\hat{m}-1} c_{11}^{*i} 4{h_{\hat{m}}}^2 A_i + \bar{c}_{11}^{\hat{m}(\phi)} I_{\hat{m}}\Big)\theta_{\hat{m}}' \\ &+\sum_{i=\hat{m}+1}^{-1}\Big(\sum_{j=\bar{m}}^{\hat{m}-1} \rho_j 4h_{\hat{m}} h_i A_j - \rho_{\hat{m}} 2h_i \bar{I}_{\hat{m}}\Big)\theta_i' + \frac{e_{31}^{*\hat{m}}}{2h_{\hat{m}}} \bar{I}_{\hat{m}} \phi_{\hat{m}} - \sum_{i=\bar{m}}^{\hat{m}-1} 2h_{\hat{m}} A_i \frac{e_{31}^{*i}}{2h_i} \phi_i\Big] = 0.\end{aligned} \tag{2.72}$$

Equations (2.57)-(2.72) represent the analytical electro-mechanical model of the layered beam with arbitrary ACLD treatments, where the electric potential differences and the generalized mechanical displacements are the unknown independent variables.

Chapter 3

Finite Element Model

3.1 Introduction

In this chapter a FE model based on the weak forms of the analytical model presented in Chapter 2 is developed. The weak forms are derived in the Appendix A and the reader is referred to it for further details. First, the FE spatial model governing the motion and electric charge equilibrium of the layered beam with piezoelectric and viscoelastic layers is presented. Then, the FE piezoelectric sensor and actuator equations are described and the viscoelastic complex stiffness matrix is presented. Moreover, the frequency response model is discussed and an algorithm for the solution is shown.

3.2 Spatial Model

The weak forms of the analytical model presented in Chapter 2, governing the motion and electric charge equilibrium of the layered beam with piezoelectric and viscoelastic layers, are derived in the Appendix A. For convenience, the generalized mechanical displacements and electric potential differences are grouped in the generalized vectors of displacements and potential differences,

$$\mathrm{u}(x,t) = \{u_0(x,t), w_0(x,t), \theta_0(x,t), \theta_1(x,t), \ldots, \theta_{\bar{n}}(x,t), \theta_{\bar{m}}(x,t), \ldots, \theta_{-1}(x,t)\}^{\mathrm{T}}, \tag{3.1}$$

$$\phi(x,t) = \{\phi_1(x,t), \ldots, \phi_{\bar{n}}(x,t), \phi_{\bar{m}}(x,t), \ldots, \phi_{-1}(x,t)\}^{\mathrm{T}}. \tag{3.2}$$

The weak forms given in equations (A.26) and (A.27) are

$$\int_L [\delta\mathrm{u}^{\mathrm{T}}\mathrm{J}\ddot{\mathrm{u}} + \delta\mathrm{u}^{\mathrm{T}}(\mathrm{L}_{xx}^{\mathrm{T}}\mathrm{Y}\mathrm{L}_{xx} + \mathrm{L}_{zx}^{\mathrm{T}}\mathrm{G}\mathrm{L}_{zx})\mathrm{u} + \delta\mathrm{u}^{\mathrm{T}}\mathrm{L}_{xx}^{\mathrm{T}}\mathrm{P}^{\mathrm{T}}\phi]\, \mathrm{d}L = \int_L \delta\mathrm{u}^{\mathrm{T}}\mathrm{f}\, \mathrm{d}L, \tag{3.3}$$

$$\int_L (\delta\phi^{\mathrm{T}}\mathrm{P}\mathrm{L}_{xx}\mathrm{u} + \delta\phi^{\mathrm{T}}\mathrm{C}\phi)\mathrm{d}L = \int_L \delta\phi^{\mathrm{T}}\tau\, \mathrm{d}L. \tag{3.4}$$

The non-zero terms of the symmetric positive definite inertia matrix J and of the symmetric semi-positive definite extensional and shear stiffness matrices Y and G, of size $[(\bar{k}-1)\times(\bar{k}-1)]$, are defined in (A.19), (A.20) and (A.21), respectively. The piezoelectric equivalent stiffness and capacitance matrices P and C, of size $[\bar{p}\times(\bar{k}-1)]$ and $(\bar{p}\times\bar{p})$, have non-zero terms defined by (A.22) and (A.23). The applied mechanical forces and electric charge density vectors f and τ, of size $[(\bar{k}-1)\times 1]$ and $(\bar{p}\times 1)$, have elements defined by (A.24) and (A.25). Here, $\bar{p} = \bar{n} - \bar{m}$

is the number of piezoelectric layers and $\bar{k}-1$, with $\bar{k}=\bar{p}+4$, is the number of generalized displacements. Furthermore, the differential operators

$$\mathbf{L}_{xx} = diag\left(\frac{\partial}{\partial x}, 0, \frac{\partial}{\partial x}, \ldots, \frac{\partial}{\partial x}\right), \mathbf{L}_{zx} = diag\left(0, \frac{\partial}{\partial x}, 1, \ldots, 1\right), \tag{3.5a,b}$$

of size $[(\bar{k}-1)\times(\bar{k}-1)]$, are used for the definition of the generalized extensional and shear strains.

The FE method is utilized here with the purpose of obtaining an approximated solution of Equations (3.3) and (3.4). That involves a transformation of the global integral forms to a representation composed of the sum of the elemental integral forms, leading to the definition of the local (elemental) matrices and vectors. Thus, the beam's total length L is divided and the domain of integration is discretized into q finite elements of length L_e. With the sum taken over all q elements, the global weak forms become

$$\sum_{e=1}^{q}\int_{L_e} \delta\mathbf{u}^{e\mathrm{T}}\left[\mathbf{J}\ddot{\mathbf{u}}^e + \left(\mathbf{L}_{xx}^{\mathrm{T}}\mathbf{Y}\mathbf{L}_{xx} + \mathbf{L}_{zx}^{\mathrm{T}}\mathbf{G}\mathbf{L}_{zx}\right)\mathbf{u}^e + \mathbf{L}_{xx}^{\mathrm{T}}\mathbf{P}^{\mathrm{T}}\phi^e - \mathbf{f}\right]\mathrm{d}L_e = 0, \tag{3.6}$$

$$\sum_{e=1}^{q}\int_{L_e} \delta\phi^{e\mathrm{T}}(\mathbf{P}\mathbf{L}_{xx}\mathbf{u}^e + \mathbf{C}\phi^e - \tau^e)\,\mathrm{d}L_e = 0. \tag{3.7}$$

The mechanical (and its second time derivative) and electrical variables of (3.6) and (3.7), $\mathbf{u}^e(x,t)$ and $\phi^e(x,t)$, are restricted to the domain of integration and an approximation is considered at a local level in each sub-domain, where only the nodal values of the variables at the element boundaries contribute to the approximation. The FE mesh is then composed of $q+1$ nodal points and the global mechanical degree of freedom (DoF) vectors, $\bar{\mathbf{u}}(t)$ and $\bar{\phi}(t)$, of size $[(q+1)(\bar{p}+4)\times 1]$ and $(q\bar{p}\times 1)$, are defined as

$$\bar{\mathbf{u}}(t) = \left\{\ldots, \bar{u}_0^r(t), \bar{w}_0^r(t), \bar{\theta}_0^r(t), \bar{\theta}_1^r(t), \cdots, \bar{\theta}_{\bar{n}}^r(t), \bar{\theta}_{\bar{m}}^r(t), \cdots, \bar{\theta}_{-1}^r(t), \ldots\right\}^{\mathrm{T}}, \tag{3.8}$$

$$\bar{\phi}(t) = \left\{\ldots, \phi_1^s(t), \cdots, \phi_{\bar{n}}^s(t), \phi_{\bar{m}}^s(t), \cdots, \phi_{-1}^s(t), \ldots\right\}^{\mathrm{T}}, \tag{3.9}$$

where $r = 1, \ldots, q+1$ and $s = 1, \ldots, q$.

For the definition of the local approximation of the generalized mechanical and electrical DoFs in each sub-domain, a generic element with two nodes (1 and 2) is isolated from the FE mesh (Figure 3.1). The correspondence between each node of the element and the global node enumeration is established through the mechanical and electrical connectivity matrices $\mathbf{R}_u^e$ and $\mathbf{R}_\phi^e$, of size $[\bar{k}(q+1)\times\bar{k}(q+1)]$ and $(\bar{p}q\times\bar{p}q)$, expressed as

$$\bar{\mathbf{u}}^e = \mathbf{R}_u^e\bar{\mathbf{u}}, \ \bar{\phi}^e = \mathbf{R}_\phi^e\bar{\phi}, \tag{3.10a,b}$$

where the mechanical and electrical elemental DoFs vectors $\bar{\mathbf{u}}^e(t)$ and $\bar{\phi}^e(t)$ are defined as

$$\begin{aligned}\bar{\mathbf{u}}^e(t) = \{&\bar{u}_0^1(t), \bar{w}_0^1(t), \bar{\theta}_0^1(t), \bar{\theta}_1^1(t), \cdots, \bar{\theta}_{\bar{n}}^1(t), \bar{\theta}_{\bar{m}}^1(t), \cdots, \bar{\theta}_{-1}^1(t), \bar{u}_0^2(t),\\ &\bar{w}_0^2(t), \bar{\theta}_0^2(t), \bar{\theta}_1^2(t), \cdots, \bar{\theta}_{\bar{n}}^2(t), \bar{\theta}_{\bar{m}}^2(t), \cdots, \bar{\theta}_{-1}^2(t)\}^{\mathrm{T}},\end{aligned} \tag{3.11}$$

$$\bar{\phi}^e(t) = \left\{\bar{\phi}_1(t), \cdots, \bar{\phi}_{\bar{n}}(t), \bar{\phi}_{\bar{m}}(t), \cdots, \bar{\phi}_{-1}(t)\right\}^{\mathrm{T}}. \tag{3.12}$$

The superscripts 1 and 2 denote the node at which the DoF is defined, while the subscript identifies the layer to which the DoF refers. As usual, a variable from the mechanical DoFs global vector

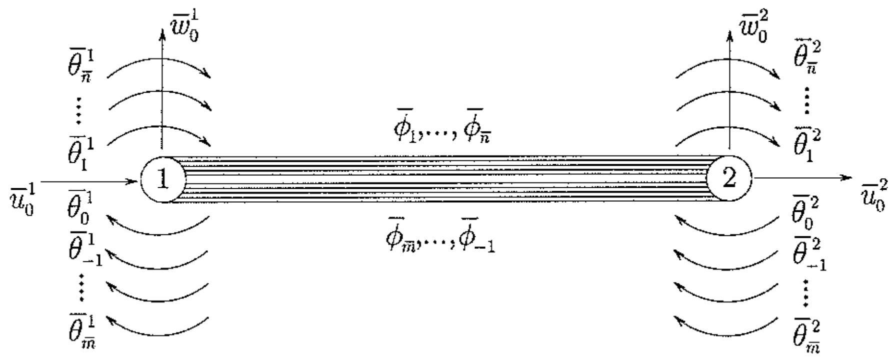

Figure 3.1: One-dimensional FE of the beam with arbitrary ACLD treatments.

appears on two elemental DoFs vectors, except for the boundary nodes of the global domain. However, for the electrical DoFs global vector that won't be the case because continuity of the electric potential difference between adjacent FEs won't be assured.

From the differential operators (3.5) it is possible to see that the variational Equations (3.3) and (3.4) contain at most first order derivatives of the generalized displacements and zero order derivatives of the electric potential differences. Thus, the displacement variables within each element domain must be, at least, approximated by linear interpolation functions. For the electric potential differences, constant functions are utilized and the electric potential difference becomes constant in each element. The interpolation functions are grouped in the mechanical and electrical interpolation matrices $\mathbf{N}_u(x)$ and $\mathbf{N}_\phi$. Therefore, the generalized displacement and electric potential vectors in each sub-domain are approximated by

$$\mathbf{u}^e(x,t) = \mathbf{N}_u(x)\bar{\mathbf{u}}^e(t), \;\; \boldsymbol{\phi}^e(t) = \mathbf{N}_\phi\bar{\boldsymbol{\phi}}^e(t). \tag{3.13a,b}$$

Substituting Equations (3.13) into (3.6) and (3.7) yields

$$\sum_{e=1}^{q} \delta\bar{\mathbf{u}}^{e\mathrm{T}}\left(\mathbf{M}_{uu}^e\ddot{\bar{\mathbf{u}}}^e + \mathbf{K}_{uu}^e\bar{\mathbf{u}}^e + \mathbf{K}_{u\phi}^e\bar{\boldsymbol{\phi}}^e - \mathbf{F}^e\right) = 0, \tag{3.14}$$

$$\sum_{e=1}^{q} \delta\bar{\boldsymbol{\phi}}^{e\mathrm{T}}\left(\mathbf{K}_{\phi u}^e\bar{\mathbf{u}}^e + \mathbf{K}_{\phi\phi}^e\bar{\boldsymbol{\phi}}^e - \mathbf{Q}^e\right) = 0, \tag{3.15}$$

where the elemental matrices and vectors are defined as

$$\mathbf{M}_{uu}^e = \int_{L_e} \mathbf{N}_u^\mathrm{T}\mathbf{J}\mathbf{N}_u \,\mathrm{d}L_e, \;\; \mathbf{K}_{uu}^e = \int_{L_e} (\mathbf{B}_{xx}^\mathrm{T}\mathbf{Y}\mathbf{B}_{xx} + k_s\mathbf{B}_{zx}^\mathrm{T}\mathbf{G}\mathbf{B}_{zx})\,\mathrm{d}L_e, \tag{3.16a,b}$$

$$\mathbf{K}_{u\phi}^e = \mathbf{K}_{\phi u}^{e\mathrm{T}} = \int_{L_e} \mathbf{B}_{xx}^\mathrm{T}\mathbf{P}^\mathrm{T}\,\mathrm{d}L_e, \;\; \mathbf{K}_{\phi\phi}^e = \int_{L_e} \mathbf{N}_\phi^\mathrm{T}\mathbf{C}\mathbf{N}_\phi\,\mathrm{d}L_e, \tag{3.17a,b}$$

$$\mathbf{F}^e = \int_{L_e} \mathbf{N}_u^\mathrm{T}\mathbf{f}\,\mathrm{d}L_e, \;\; \mathbf{Q}^e = \int_{L_e} \mathbf{N}_\phi^\mathrm{T}\boldsymbol{\tau}\,\mathrm{d}L_e, \tag{3.18a,b}$$

and the extensional and shear deformation matrices utilized are given by

$$\mathbf{B}_{xx} = \mathbf{L}_{xx}\mathbf{N}_u, \, \mathbf{B}_{xz} = \mathbf{L}_{xz}\mathbf{N}_u. \tag{3.19a,b}$$

Furthermore, a shear correction factor k_s was introduced in Equation (3.16b) in order to approximate the effects of the non-linear shear deformation distribution [31]. Moreover, reduced integration of the higher order terms of the shear stiffness matrix should be used in order to overcome the over-stiffening of the element at low thickness (shear locking).

Considering Equations (3.10) and substituting them into (3.14) and (3.15), yields

$$\forall \delta\bar{\mathrm{u}}: \quad \delta\bar{\mathrm{u}}^{\mathrm{T}}\left(\mathbf{M}_{uu}\ddot{\bar{\mathrm{u}}} + \mathbf{K}_{uu}\bar{\mathrm{u}} + \mathbf{K}_{u\phi}\bar{\phi} - \mathbf{F}\right) = 0, \tag{3.20}$$

$$\forall \delta\bar{\phi}: \quad \delta\bar{\phi}^{\mathrm{T}}\left(\mathbf{K}_{\phi u}\bar{\mathrm{u}} + \mathbf{K}_{\phi\phi}\bar{\phi} - \mathbf{Q}\right) = 0, \tag{3.21}$$

where the global matrices and vectors are given by

$$\mathbf{M}_{uu} = \sum_{e=1}^{q} \mathbf{R}_u^{e\mathrm{T}}\mathbf{M}_{uu}^e\mathbf{R}_u^e, \; \mathbf{K}_{uu} = \sum_{e=1}^{q} \mathbf{R}_u^{e\mathrm{T}}\mathbf{K}_{uu}^e\mathbf{R}_u^e, \tag{3.22a,b}$$

$$\mathbf{K}_{u\phi} = \mathbf{K}_{\phi u}^{\mathrm{T}} = \sum_{e=1}^{q} \mathbf{R}_u^{e\mathrm{T}}\mathbf{K}_{u\phi}^e\mathbf{R}_\phi^e, \; \mathbf{K}_{\phi\phi} = \sum_{e=1}^{q} \mathbf{R}_\phi^{e\mathrm{T}}\mathbf{K}_{\phi\phi}^e\mathbf{R}_\phi^e, \tag{3.23a,b}$$

$$\mathbf{F} = \sum_{e=1}^{q} \mathbf{R}_u^{e\mathrm{T}}\mathbf{F}^e, \; \mathbf{Q} = \sum_{e=1}^{q} \mathbf{R}_\phi^{e\mathrm{T}}\mathbf{Q}^e. \tag{3.24a,b}$$

Finally, the global equations of motion and charge equilibrium of the discrete system are given by the non-trivial solution of Equations (3.20) and (3.21), yielding

$$\mathbf{M}_{uu}\ddot{\bar{\mathrm{u}}}(t) + \mathbf{K}_{uu}\bar{\mathrm{u}}(t) + \mathbf{K}_{u\phi}\bar{\phi}(t) = \mathbf{F}(t), \tag{3.25}$$

$$\mathbf{K}_{\phi u}\bar{\mathrm{u}}(t) + \mathbf{K}_{\phi\phi}\bar{\phi}(t) = \mathbf{Q}(t). \tag{3.26}$$

Therefore, the FE model of the beam with arbitrary ACLD treatments is described by the elemental matrices and vectors in Equations (3.16)-(3.18) and by the global FE equations of motion and charge equilibrium in Equations (3.25)-(3.26).

3.3 Sensors and Actuators Equations

The electrical DoFs vector in Equations (3.20) and (3.21) can be partitioned into the actuating and sensing DoFs, $\bar{\phi}(t) = \{\bar{\phi}_{\mathrm{a}}(t), \bar{\phi}_{\mathrm{s}}(t)\}^{\mathrm{T}}$, where the subscripts 'a' and 's' denote the actuating and sensing capabilities. Furthermore, the stiffness matrix can be written as the sum of the elastic and piezoelectric layers stiffness matrices $\mathbf{K}_{uu}^E$ and $\mathbf{K}_{uu}^P$. Hence, considering open-circuit electrodes, and in that case $\mathbf{Q}(t) = 0$, the non specified potential differences in (3.21) can be statically condensed in (3.20), and the equations of motion and charge equilibrium become

$$\mathbf{M}_{uu}\ddot{\bar{\mathrm{u}}}(t) + (\mathbf{K}_{uu}^E + \mathbf{K}_{uu}^{P*})\bar{\mathrm{u}}(t) = -\mathbf{K}_{u\phi\mathrm{a}}\bar{\phi}_{\mathrm{a}}(t) + \mathbf{F}(t), \tag{3.27}$$

$$\bar{\phi}_{\mathrm{s}}(t) = -\mathbf{K}_{\phi\phi\mathrm{s}}^{-1}\mathbf{K}_{\phi u\mathrm{s}}\bar{\mathrm{u}}(t), \tag{3.28}$$

where

$$\mathbf{K}_{uu}^{P*} = \mathbf{K}_{uu}^{P} - \mathbf{K}_{u\phi\mathrm{s}}\mathbf{K}_{\phi\phi\mathrm{s}}^{-1}\mathbf{K}_{\phi u\mathrm{s}}. \tag{3.29}$$

It's worth to note that a non-null parabolic through-the-thickness distribution of the electric potential within the piezoelectric layers was already considered in the variational formulation through the use of effective stiffness parameters. Moreover, the static consensation in Equation (3.29) only considers the linear term of the electrical potential distribution, which is the one that in fact contributes to the sensor voltage.

3.4 Frequency Response Model

Considering the frequency dependent physical properties of the viscoelastic materials presented in Section 2.5 and assuming a fixed temperature, the FE equation of motion in (3.27) can be written as

$$\mathbf{M}_{uu}\ddot{\bar{\mathbf{u}}}(t) + [\mathbf{K}_{uu}^{E} + \mathbf{K}_{uu}^{P*} + \mathbf{K}_{uu}^{V}(\omega)]\bar{\mathbf{u}}(t) = -\mathbf{K}_{u\phi\mathrm{a}}\bar{\phi}_{\mathrm{a}}(t) + \mathbf{F}(t), \tag{3.30}$$

where $\mathbf{K}_{uu}^{V}(\omega)$ is a complex global stiffness matrix of the viscoelastic layers, whose terms are frequency dependent.

Considering simple harmonic mechanical or electric excitation,

$$\mathbf{F}(t) = \bar{\mathbf{F}}e^{j\omega t}, \;\; \bar{\phi}_{\mathrm{a}}(t) = \bar{\mathbf{\Phi}}_{\mathrm{a}}e^{j\omega t}, \tag{3.31a,b}$$

where $\bar{\mathbf{F}}$ and $\bar{\mathbf{\Phi}}_{\mathrm{a}}$ are the applied mechanical forces and electrical potential difference amplitude vectors, the steady state mechanical and electrical harmonic responses of the system can be written as

$$\bar{\mathbf{u}}(t) = \bar{\mathbf{U}}e^{j\omega t}, \;\; \bar{\phi}_{\mathrm{s}}(t) = \bar{\mathbf{\Phi}}_{\mathrm{s}}e^{j\omega t}, \tag{3.32a,b}$$

where $\bar{\mathbf{U}}$ and $\bar{\mathbf{\Phi}}_{\mathrm{s}}$ are the complex response vectors of mechanical and electrical amplitudes (displacements and sensors voltages). Substituting (3.31) and (3.32) into (3.30) and (3.28) yields

$$[\mathbf{K}_{uu}(\omega) - \omega^2\mathbf{M}_{uu}]\bar{\mathbf{U}} = -\mathbf{K}_{u\phi\mathrm{a}}\bar{\mathbf{\Phi}}_{\mathrm{a}} + \bar{\mathbf{F}}, \tag{3.33}$$

$$\bar{\mathbf{\Phi}}_{\mathrm{s}} = -\mathbf{K}_{\phi\phi\mathrm{s}}^{-1}\mathbf{K}_{\phi u\mathrm{s}}\bar{\mathbf{U}}, \tag{3.34}$$

where $\mathbf{K}_{uu}(\omega) = \mathbf{K}_{uu}^{E} + \mathbf{K}_{uu}^{P*} + \mathbf{K}_{uu}^{V}(\omega)$, from which the complex solution vectors $\bar{\mathbf{U}}$ and $\bar{\mathbf{\Phi}}_{\mathrm{s}}$ can be obtained.

The frequency response function (FRF) for a mechanical force DoF input i and mechanical displacement DoF output o, can be obtained by solving (3.33) for different values of frequency,

$$[\mathbf{K}_{uu}(\omega_l) - \omega_l^2\mathbf{M}_{uu}]\bar{\mathbf{U}}^l = \bar{\mathbf{F}}^i, \tag{3.35}$$

where $\bar{\mathbf{F}}^i$ denotes a force vector with a unit force in the i-th DoF and all other elements equal to zero, and $\bar{\mathbf{U}}^l$ is the resulting response vector (displacements) solution at frequency ω_l. Moreover, the resultant sensor voltage vector $\bar{\mathbf{\Phi}}_{\mathrm{s}}^l$ is obtained by substituting the displacement response vector $\bar{\mathbf{U}}^l$ in (3.34), yielding

$$\bar{\mathbf{\Phi}}_{\mathrm{s}}^l = -\mathbf{K}_{\phi\phi\mathrm{s}}^{-1}\mathbf{K}_{\phi u\mathrm{s}}\bar{\mathbf{U}}^l. \tag{3.36}$$

Thus, the displacement and induced voltage per unit force frequency response at frequency ω_l, T_{oi}^{uu} and $T_{oi}^{\phi u}$, are given by

$$T_{oi}^{uu} = \frac{\bar{U}_o}{\bar{F}_i} = \frac{\bar{\mathbf{U}}_o^l}{\bar{F}_i}, \tag{3.37}$$

$$T_{oi}^{\phi u} = \frac{\bar{\mathbf{\Phi}}_{\mathrm{s}}^o}{\bar{F}_i} = \frac{avg[-\mathbf{K}_{\phi\phi\mathrm{s}}^{-1}\mathbf{K}_{\phi u\mathrm{s}}\bar{\mathbf{U}}^l]}{\bar{F}_i}, \tag{3.38}$$

where $\bar{F}_i$ is the amplitude of the mechanical force input, $\bar{U}_o = \bar{\mathbf{U}}_o^l$ is the displacement amplitude extracted from the o-th DoF of the vector $\bar{\mathbf{U}}^l$, and $\bar{\mathbf{\Phi}}_{\mathrm{s}}^o$ is the o-th sensor averaged voltage output determined with the electrical DoFs of the o-th sensor. The notation $avg[\cdot]$ is utilized to denote that the sensors voltages are calculated from an average of the electrical DoFs where an electrical FE separation of the electrodes was performed.

Similarly, for a piezoelectric i-th actuator voltage input vector $\bar{\Phi}_{\mathrm{a}}^{i}$, where a unit voltage is considered only in the electrical DoFs which correspond to the i-th actuator, the mechanical displacements amplitude vector is given by solving

$$[\mathbf{K}_{uu}(\omega_l) - \omega_l^2 \mathbf{M}_{uu}]\bar{\mathbf{U}}^l = -\mathbf{K}_{u\phi \mathrm{a}}\bar{\Phi}_{\mathrm{a}}^{i}, \tag{3.39}$$

and the o-th sensor output voltage vector is given by substituting $\bar{\mathbf{U}}^l$ into (3.36). Thus, the displacement and induced voltage per unit voltage applied into the actuator frequency response at frequency w_l, $T_{oi}^{u\phi}$ and $T_{oi}^{\phi\phi}$, are given by

$$T_{oi}^{u\phi} = \frac{\bar{U}_o}{\bar{\Phi}_{\mathrm{a}}^{i}} = \frac{\bar{\mathbf{U}}_o^l}{\bar{\Phi}_{\mathrm{a}}^{i}}, \tag{3.40}$$

$$T_{oi}^{\phi\phi} = \frac{\bar{\Phi}_{\mathrm{s}}^{o}}{\bar{\Phi}_{\mathrm{a}}^{i}} = \frac{avg[-\mathbf{K}_{\phi\phi \mathrm{s}}^{-1}\mathbf{K}_{\phi u \mathrm{s}}\bar{\mathbf{U}}^l]}{\bar{\Phi}_{\mathrm{a}}^{i}}, \tag{3.41}$$

where $\bar{\Phi}_{\mathrm{a}}^{i}$ is the amplitude of the voltage applied to the i-th actuator.

Finally, the frequency response model (FRFs) can be generated from the results of many discrete frequency calculations of Equations (3.35), (3.36) and (3.39), in which the complex stiffness matrix of the viscoelastic layers is recalculated at each frequency value of the discrete frequency range $\omega = \omega_0, \ldots, \omega_l, \ldots, \omega_f$, as shown in Figure 3.2.

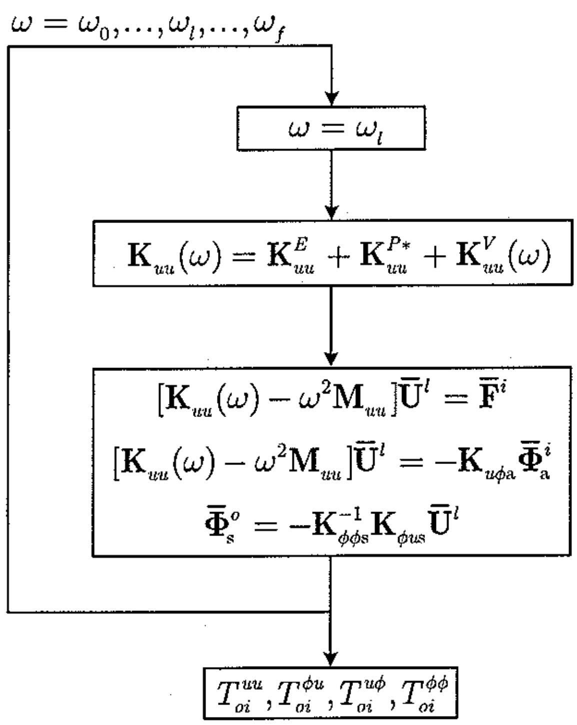

Figure 3.2: Frequency response model generation diagram.

Chapter 4

Experimental Validation

4.1 Introduction

In order to validate the FE model some measurements were taken on an aluminium beam with a partial ACLD treatment (viscoelastic layer sandwiched between the piezoelectric patch and the base beam). The aims were the validation of both the dynamics of the system and the actuating and sensing capabilities of the piezoelectric patches. Thus, three FRFs were measured experimentally and evaluated numerically: acceleration per unit force (accelerance), acceleration per unit voltage into the piezoelectric patch and induced voltage per unit force. The FE model implementation was realized in MATLAB®.

4.2 Test Rig and Experimental Setup

The test rig comprised a beam that was 400 mm long, 2.92 mm thick and 30 mm wide, and a partial ACLD treatment that was 50 mm long and 30 mm wide, with viscoelastic and piezoelectric layers of thickness 0.127 mm and 0.5 mm, respectively. Taking one end of the beam to be $x = 0$, the ACLD treatment was positioned slightly off-center on the beam, starting at $x = 202$ mm, and was realized with a passive viscoelastic layer of a material manufactured by 3M (ISD112) and a piezoelectric constraining patch manufactured by PI (PIC 255).

The mechanical and electrical material properties of the aluminium beam, viscoelastic layer and piezoelectric patch are presented in Table 4.1. The shear storage modulus and loss factor

Aluminium		3M ISD112	PIC 255			
c_{11}^*	69 GPa	—	c_{11}^*	62.11 GPa	e_{31}^*	-11.18 C/m^2
c_{55}	26.54 GPa	—	c_{55}	23.89 GPa	e_{15}	11.94 C/m^2
ρ	2700 Kg/m^3	1130 Kg/m^3	ρ	7800 Kg/m^3	ε_{11}	12.6 $\times 10^{-9}$ F/m
					ε_{33}^*	9.96 $\times$ 10^{-9} F/m

Table 4.1: Properties of the aluminium, viscoelastic layer and piezoelectric patch.

of the viscoelastic material at the ambient temperature (22 °C) were extracted from the manufacturer's nomogram [32] and are presented in Figure 4.1. The Young's storage modulus was obtained assuming a frequency independent Poisson's ratio equal to 0.45. Moreover, an hysteretic damping model with a loss factor equal to 2×10^{-3} was considered in the numerical evaluations.

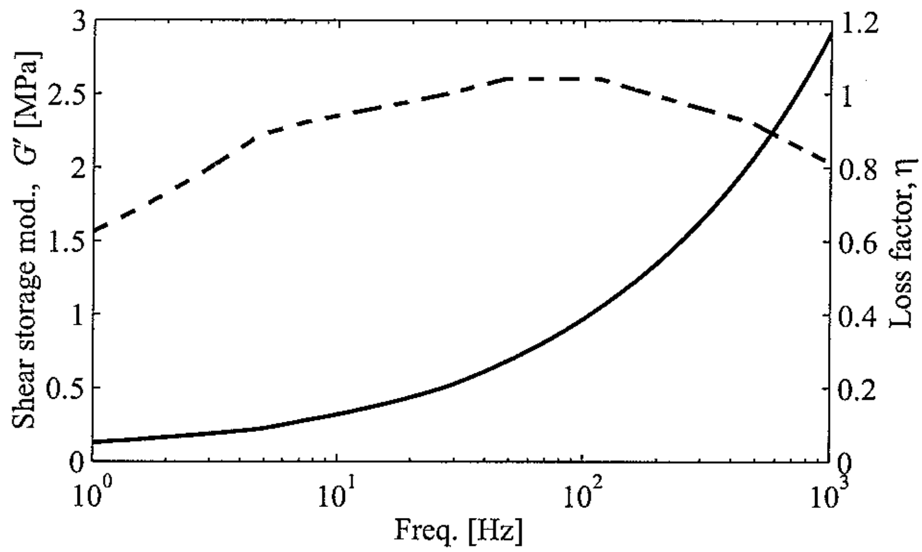

Figure 4.1: Frequency dependent properties of 3M ISD112 at 22 °C: _ _ _ , loss factor; ______ , shear storage modulus.

The analysis concerned free-free boundary conditions. The beam was suspended on two wires attached to the beam approximately at 22.4% and 77.6% of the total length of the beam as schematically presented in Figure 4.2. The placement of the wires was chosen at the locations of the nodes of the first flexural mode which minimizes the interference of the attached wires in the system. The beam was excited by an impact hammer from PCB Piezotronics (model 086C03) with a hard tip (model 084B03) mounted on it. The impulsive force was applied at $x = 275$ mm and measured by the hammer's force sensor. The response (acceleration) was measured with a PCB Piezotronics accelerometer (model 352C22), with a frequency range up to 10 kHz and a weight equal to 0.5 g, placed on the other side of the beam at the same location of the excitation force. The location of the impact was chosen in order to excite only one of the rigid body modes, swinging back and forth, and the excitation of the torsional modes was avoided.

In the measurements both the impact hammer and accelerometer were used in ICP mode and an 8-channel dynamic signal analyser HP 35650 with a signal generator module was utilized for the data acquisition, signal generation and computations of the FRFs. Furthermore, in the analysis the frequency span was set to 1.6 kHz and a frequency resolution of 0.5 Hz was defined. The impact excitation was utilized for the measurement of the acceleration and induced voltage per unit force FRFs and 10 averages were considered in that procedure. For the acquisition of the piezoelectric patch (sensor) induced voltage a Bruel & Kjaer charge amplifier (type 2635) was utilized. Concerning the measurement of the acceleration per unit voltage into the actuator, the beam was excited with a stepped sine voltage into the piezoelectric actuator which was previously amplified by a PCB Piezotronics single channel power amplifier (AVC instrumentation, series 790) with a output voltage range equal to 200 V. The acceleration was measured by the accelerometer which was kept at the same location referred to above.

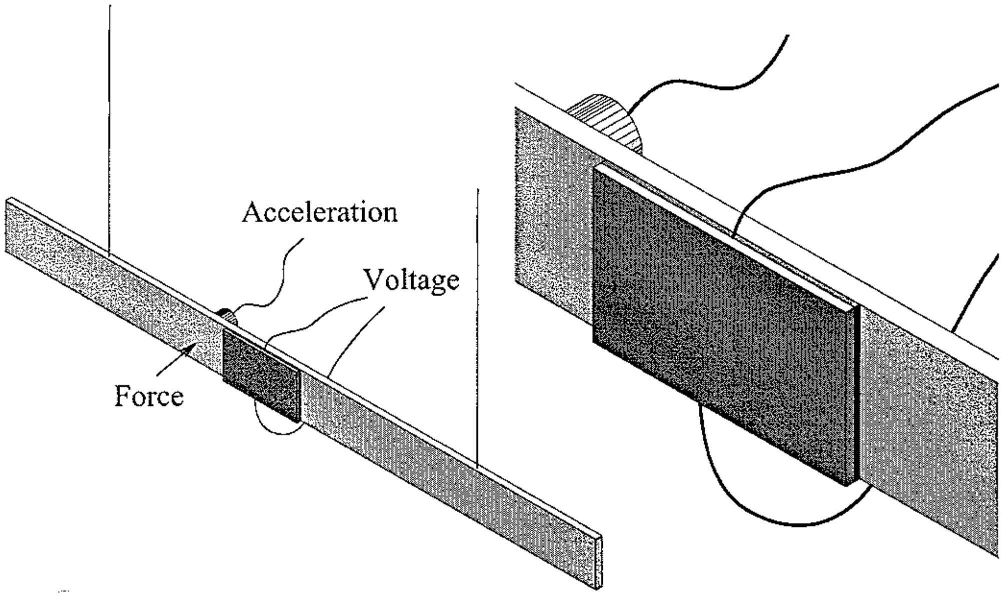

Figure 4.2: Test rig and ACLD patch.

4.3 Results and Discussion

The three measured and predicted FRFs, namely, acceleration per unit force (accelerance), acceleration per unit voltage into the piezoelectric patch and induced voltage per unit force, are shown in Figures 4.3 to 4.5.

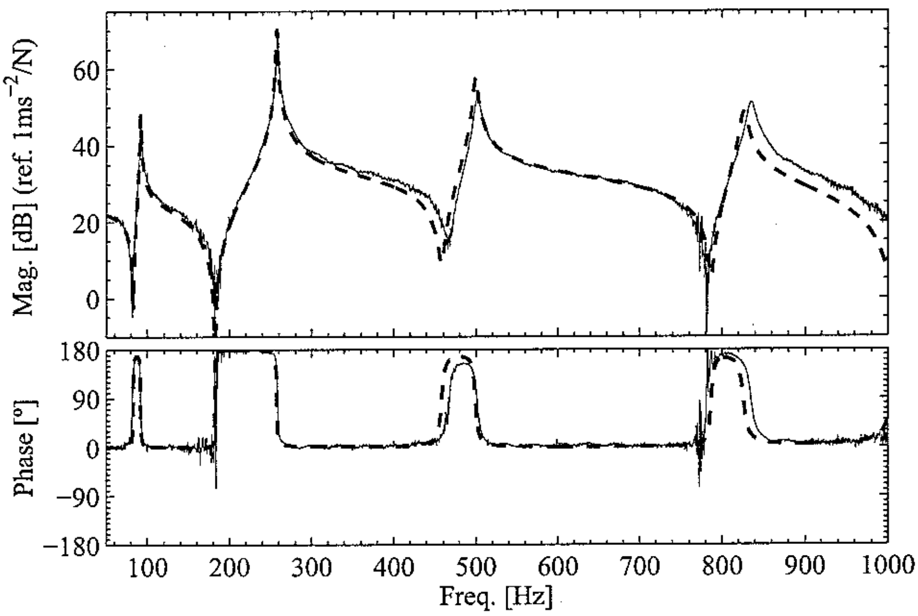

Figure 4.3: Frequency response function (acceleration per unit force) of the beam with ACLD treatment: _ _ _ , predicted; ______, measured.

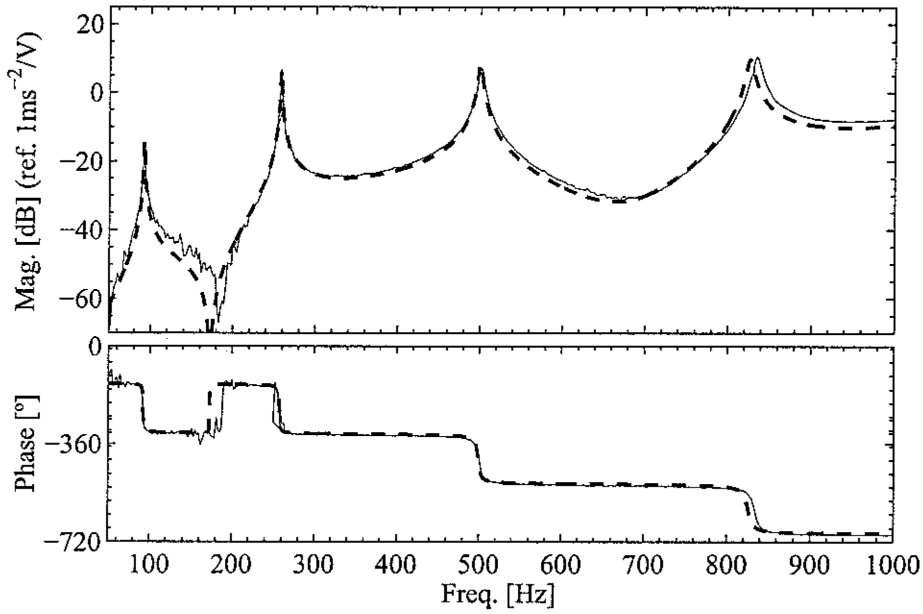

Figure 4.4: Frequency response function (acceleration per unit voltage) of the beam with ACLD treatment: _ _ _ , predicted; ______ , measured.

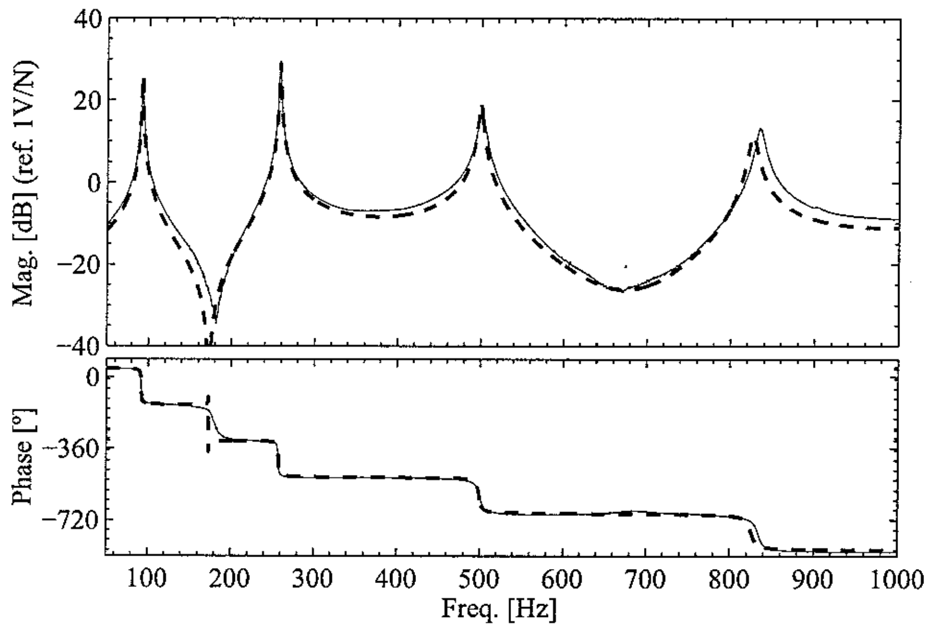

Figure 4.5: Frequency response function (voltage per unit force) of the beam with ACLD treatment: _ _ _ , predicted; ______ , measured.

As can be seen, there is a very good agreement between the predicted and measured FRFs. Small differences are found around the fourth natural frequency in all the FRFs. The reason for that discrepancy might be related to uncertainties concerning the viscoelastic material properties and with the fact that the wavelength at the fourth natural frequency is closer to the ACLD patch length than at the lower natural frequencies. Furthermore, the ACLD patch is located between consecutive nodes of the fourth mode, where the modal strains are higher, and as a consequence the influence of the uncertainties of the viscoelastic material properties becomes more pronounced. Moreover, the accelerometer adds a little mass, the wires have some effect, the FE involves assumptions and approximations, etc. However, the agreement in general is very good and both the dynamics of the system, beam and ACLD patch, and the actuating and sensing capabilities of the piezoelectric patch are validated.

Chapter 5

Conclusion

In this work a generic analytical formulation for the study of beams with arbitrary active constrained layer damping (ACLD) treatments was presented. The hybrid behavior of the elastic, viscoelastic and piezoelectric materials was considered in an accurate and consistent way.

A partial layerwise theory was considered for the definition of the displacement field leading to a first shear deformation theory (FSDT) for each layer. For thick laminates this allows a more accurate representation of the intra- and inter-laminar effects and the strain and stress distributions become better approximations to the three-dimensional elasticity theory. Moreover, the rotatory inertia is considered in a more accurate way, which might be of importance at high frequencies.

For modelling the electric field and potential of the piezoelectric layers a fully coupled electromechanical theory was utilized. The use of effective stiffness parameters allowed a representation of the system similar to the pure mechanical one to be obtained merely by modifying the elastic constitutive parameters.

A complex modulus approach was utilized to model the damping behavior of the viscoelastic materials. While the material properties and damping are modeled in a precise way, the solution model algorithm requires the re-calculation of the stiffness matrix of the viscoelastic layers, which, for a relatively large number of degrees of freedom can be very time consuming, requiring a high computational effort.

The developed strong forms, comprising the electro-mechanical equations of motion, electric charge equilibrium and electro-mechanical boundary conditions, can be used for analytical solutions. However, in some situations the solution of the partial differential equations can be difficult or even impossible to obtain. The presented finite element (FE) model solution has the well known advantages of the FE method and allows the study of partial ACLD treatments where the solution by analytical methods might be difficult to obtain.

The FE model was validated against experimental results. A very good agreement was obtained validating both the dynamics of the system and the actuator and sensor capabilities of the piezoelectric layers. The results demonstrate the capacity and robustness of the proposed theory. Thus, the presented analytical formulation and FE model solution can be utilized for the study of arbitrary ACLD treatments on beams with various configurations and arrangements of the layers and with different control strategies.

References

[1] C. D. Johnson. Design of passive damping systems. *Journal of Vibration and Acoustics*, 117B:171–176, 1995.

[2] A. Nashif, D. Jones and J. Henderson. *Vibration damping*. John Wiley & Sons, New York, 1985.

[3] M. Macé. Damping of beam vibrations by means of a thin constrained viscoelastic layer: Evaluation of a new theory. *Journal of Sound and Vibration*, 172(5):557–591, 1994.

[4] A. Bhimaraddi. Sandwich beam theory and the analysis of constrained layer damping. *Journal of Sound and Vibration*, 179(4):591–602, 1995.

[5] P. Cupial and J. Niziol. Vibration and damping analysis of a three-layered composite plate with a viscoelastic mid-layer. *Journal of Sound and Vibration*, 183(1):99–114, 1995.

[6] G. Agnes and K. Napolitano. Active constrained layer viscoelastic damping. In *Proceedings of the 34th AIAA/ASME/ASCE/AHS/ASC Structures, Structural Dynamics, and Materials Conference*, pages 3499–3506, Reston, VA, 1993.

[7] A. Baz. Active constrained layer damping. In *Proceedings of Damping 93*. Wright Patterson AFB, OH, WL-TR-93-3105, 3, IBB1-23, 1993.

[8] I. Y. Shen. Bending-vibration control of composite and isotropic plates through intelligent constrained-layer treatments. *Smart Materials and Structures*, 3(1):59–70, 1994.

[9] K. Suzuki, K. Kageyama, I. Kimpara, S. Hotta, T. Ozawa and T. Ozaki. Vibration and damping prediction of laminates with constrained viscoelastic layers - numerical analysis by a multilayer higher-order-deformable finite element and experimental observations. *Mechanics of Advanced Materials and Structures*, 10:43–75, 2003.

[10] W. G. Cady. *Piezoelectricity: An Introduction to the Theory and Applications of Electromechanical Phenomena in Crystals*. Dover Publications, New York, 1964.

[11] M. C. Ray and A. Baz. Optimization of energy dissipation of active constrained layer damping treatments of plates. *Journal of Sound and Vibration*, 208(3):391–406, 1997.

[12] C. H. Park and A. Baz. Vibration control of bending modes of plates using active constrained layer damping. *Journal of Sound and Vibration*, 227(4):711–734, 1999.

[13] A. Baz. Active constrained layer damping of thin cylindrical shells. *Journal of Sound and Vibration*, 240(5):921–935, 2001.

[14] B. Azvine, G. R. Tomlinson and R. J. Wynne. Use of active constrained-layer damping for controlling resonant vibration. *Smart Materials and Structures*, 4(1):1–6, 1995.

[15] J. Ro, A. El-Ali and A. Baz. Control of sound radiation from a fluid-loaded plate using active constrained layer damping. In *Proceedings of the Sixth International Conference on Recent Advances in Structural Dynamics*, pages 1252–1273, Southampton, UK, 1997.

[16] A. Baz. Robust control of active constrained layer damping. *Journal of Sound and Vibration*, 211(3):467–480, 1998.

[17] C. H. Park and A. Baz. Comparison between finite element formulations of active constrained layer damping using classical and layer-wise laminate theory. *Finite Elements in Analysis and Design*, 37:35–56, 2001.

[18] M. A. Trindade and A. Benjeddou. Hybrid active-passive damping treatments using viscoelastic and piezoelectric materials: Review and assessment. *Journal of Vibration and Control*, 8:699–745, 2002.

[19] A. Benjeddou. Advances in hybrid active-passive vibration and noise control via piezoelectric and viscoelastic constrained layer treatments. *Journal of Vibration and Control*, 7(4):565–602, 2001.

[20] C. H. Park and A. Baz. Vibration damping and control using active constrained layer damping: A survey. *The Shock and Vibration Digest*, 31(5):355–364, 1999.

[21] R. A. Moreira and J. D. Rodrigues. The modelisation of constrained damping layer treatment using the finite element method: Spatial and viscoelastic behavior. In *Proceedings of the International Conference on Structural Dynamics Modelling: Test, Analysis Correlation and Validation*, Madeira, 2002.

[22] D. J. McTavish and P. C. Hughes. Modeling of linear viscoelastic space structures. *Journal of Vibration and Acoustics*, 115(1):103–110, 1993.

[23] G. A. Lesieutre and E. Bianchini. Time domain modeling of linear viscoelasticity using anelastic displacement fields. *Journal of Vibration and Acoustics*, 117(4):424–430, 1995.

[24] R. L. Bagley and P. J. Torvik. Fractional calculus in the transient analysis of viscoelastically damped structures. *AIAA Journal*, 23(6):918–925, 1985.

[25] A. Benjeddou. Advances in piezoelectric finite element modelling of adaptive structural elements: A survey. *Computers and Structures*, 76(1-3):347–363, 2000.

[26] M. Krommer and H. Irschik. On the influence of the electric field on free transverse vibrations of smart beams. *Smart Materials and Structures*, 8(3):401–410, 1999.

[27] C. M. A. Vasques and J. D. Rodrigues. Coupled three-layered analysis of smart piezoelectric beams with different electric boundary conditions. *International Journal for Numerical Methods in Engineering*, in revision.

[28] The Institute of Electrical and Inc Electronics Engineers. *IEEE Standard on Piezoelectricity*. ANSI/IEEE Std 176-1987, 1988.

[29] J. F. Nye. *Physical Properties of Crystals: Their Representation by Tensors and Matrices*. Clarendon Press, Oxford, 1957.

[30] H. F. Tiersten. *Linear Piezoelectric Plate Vibrations*. Plenum Press, New York, 1969.

[31] V. Birman and C. W. Bert. On the choice of shear correction factor in sandwich structures. *Journal of Sandwich Structures and Materials*, 4:83–95, 2002.

[32] 3M. *Scotchdamp Vibration Control Systems: Product Information and Performance Data*. 3M Industrial Tape and Specialties Division, St.Paul, 1993.

Appendix A

Weak and Strong Forms

A.1 Hamilton's Principle

From Hamilton's principle in Equation (2.19) we have

$$\delta \int_{t_0}^{t_1} (T - H + W)\, \mathrm{d}t = 0. \tag{A.1}$$

Substituting the virtual works of the total internal electro-mechanical, inertial and external forces and electric charge density, presented in Chapter 2 in Equations (2.42), (2.47), (2.53) and (2.55), into (A.1), and considering the contributions of all the layers, yields

$$\int_{t_0}^{t_1} \Big\{ \sum_{n=1}^{\bar{n}} \Big[-\delta T^n + \delta H_{uu}^{n(\phi)} + \delta H_{u\phi}^{n(\phi)} + \delta H_{\phi u}^{n(\phi)} - \delta H_{\phi\phi}^{n(\phi)} - \delta W_u^n - \delta W_\phi^n \Big] - \delta T^c + \delta H_{uu}^c$$
$$-\delta W_u^c + \sum_{m=\bar{m}}^{-1} \Big[-\delta T^m + \delta H_{uu}^{m(\phi)} + \delta H_{u\phi}^{m(\phi)} + \delta H_{\phi u}^{m(\phi)} - \delta H_{\phi\phi}^{m(\phi)} - \delta W_u^m - \delta W_\phi^m \Big] \Big\} \mathrm{d}L\mathrm{d}t. \tag{A.2}$$

For convenience the signs in the previous equation were reversed and it will be used in the following for the definition of the weak and strong forms of the analytical model.

A.2 Weak Forms

Substituting the virtual work terms defined in Chapter 2 into Equation (A.2) and collecting the terms relative to the variations of the generalized displacements and electric potential differences, yields

$$\int_{t_0}^{t_1} \int_L \Big\{ \sum_{n=1}^{\bar{n}} \Big[\delta u_0 \Big(\rho_n A_n \ddot{u}_0 + \rho_n h_0 A_n \ddot{\theta}_0 + \rho_n \sum_{i=1}^{n-1} 2h_i A_n \ddot{\theta}_i + \rho_n \bar{I}_n \ddot{\theta}_n \Big) + \delta w_0 \rho_n A_n \ddot{w}_0$$
$$+\delta\theta_0 \Big(\rho_n h_0 A_n \ddot{u}_0 + \rho_n {h_0}^2 A_n \ddot{\theta}_0 + \rho_n h_0 \sum_{i=1}^{n-1} 2h_i A_n \ddot{\theta}_i + \rho_n h_0 \bar{I}_n \ddot{\theta}_n \Big) + \sum_{i=1}^{n-1} \delta\theta_i \Big(\rho_n 2h_i A_n \ddot{u}_0$$
$$+\rho_n 2h_i h_0 A_n \ddot{\theta}_0 + \rho_n 4h_i \sum_{j=1}^{n-1} h_j A_n \ddot{\theta}_j + \rho_n 2h_i \bar{I}_n \ddot{\theta}_n \Big) + \delta\theta_n \Big(\rho_n \bar{I}_n \ddot{u}_0 + \rho_n h_0 \bar{I}_n \ddot{\theta}_0$$

$$
\begin{aligned}
&+\rho_n \sum_{i=1}^{n-1} 2h_i \bar{I}_n \ddot{\theta}_i + \rho_n I_n \ddot{\theta}_n\Big) + \delta u_0'\Big(c_{11}^{*n} A_n u_0' + c_{11}^{*n} h_0 A_n \theta_0' + c_{11}^{*n} \sum_{i=1}^{n-1} 2h_i A_n \theta_i' + c_{11}^{*n} \bar{I}_n \theta_n'\Big) \\
&+\delta w_0'\Big(\bar{c}_{55}^{n(\phi)} A_n w_0' - \bar{c}_{55}^{n(\phi)} A_n \theta_n\Big) + \delta\theta_0'\Big(c_{11}^{*n} h_0 A_n u_0' + c_{11}^{*n} {h_0}^2 A_n \theta_0' + c_{11}^{*n} h_0 \sum_{j=1}^{n-1} 2h_j A_n \theta_j' \\
&+c_{11}^{*n} h_0 \bar{I}_n \theta_n'\Big) + \sum_{i=1}^{n-1} \delta\theta_i'\Big(c_{11}^{*n} 2h_i A_n u_0' + c_{11}^{*n} 2h_i h_0 A_n \theta_0' + c_{11}^{*n} 2h_i \sum_{j=1}^{n-1} 2h_j A_n \theta_j' + c_{11}^{*n} 2h_i \bar{I}_n \theta_n'\Big) \\
&+\delta\theta_n'\Big(c_{11}^{*n} \bar{I}_n u_0' + c_{11}^{*n} h_0 \bar{I}_n \theta_0' + c_{11}^{*n} \sum_{i=1}^{n-1} 2h_i \bar{I}_n \theta_i' + \bar{c}_{11}^{n(\phi)} I_n \theta_n'\Big) + \delta\theta_n\Big(c_{55}^{n} A_n \theta_n' - c_{55}^{n} A_n w_0'\Big) \\
&+\delta u_0' A_n \frac{e_{31}^{*n}}{2h_n}\phi_n + \delta\theta_0' h_0 A_n \frac{e_{31}^{*n}}{2h_n}\phi_n + \sum_{i=1}^{n-1} \delta\theta_i' 2h_i A_n \frac{e_{31}^{*n}}{2h_n}\phi_n + \delta\theta_n' \bar{I}_n \frac{e_{31}^{*n}}{2h_n}\phi_n - \delta u_0 X_n - \delta\theta_0 h_0 X_n \\
&- \sum_{i=1}^{n-1} \delta\theta_i 2h_i X_n - \delta\theta_n h_n X_n - \delta\theta_n M_n - \delta w_0 Z_n + \delta\phi_n \frac{e_{31}^{*n}}{2h_n}\Big(A_n u_0' + h_0 A_n \theta_0' + \sum_{i=1}^{n-1} 2h_i A_n \theta_i' \\
&\quad +\bar{I}_n \theta_n'\Big) - \delta\phi_n \frac{\varepsilon_{33}^{*n} A_n}{4{h_n}^2}\phi_n + \delta\phi_n b\tau_n\Big] + \delta u_0 \rho_c A_c \ddot{u}_0 + \delta w_0 \rho_c A_c \ddot{w}_0 + \delta\theta_0 \rho_c I_c \ddot{\theta}_0 \\
&+\delta u_0' c_{11}^{*c} A_c u_0' + \delta w_0'\Big(c_{55}^{c} A_c w_0' - c_{55}^{c} A_c \theta_0\Big) + \delta\theta_0' c_{11}^{*c} I_c \theta_0' + \delta\theta_0\Big(c_{55}^{c} A_c \theta_0 - c_{55}^{c} A_c w_0'\Big) \\
&-\delta u_0 X_c - \delta\theta_0 M_c - \delta w_0 Z_c + \sum_{m=\bar{m}}^{-1} \Big[\delta u_0\Big(\rho_m A_m \ddot{u}_0 - \rho_m h_0 A_m \ddot{\theta}_0 - \rho_m \sum_{i=m+1}^{-1} 2h_i A_m \ddot{\theta}_i \\
&+\rho_m \bar{I}_m \ddot{\theta}_m\Big) + \delta w_0 \rho_m A_m \ddot{w}_0 + \delta\theta_0\Big(- \rho_m h_0 A_m \ddot{u}_0 + \rho_m {h_0}^2 A_m \ddot{\theta}_0 + \rho_m h_0 \sum_{i=m+1}^{-1} 2h_i A_m \ddot{\theta}_i \\
&-\rho_m h_0 \bar{I}_m \ddot{\theta}_m\Big) + \sum_{j=m+1}^{-1} \delta\theta_j\Big(- \rho_m 2h_j A_m \ddot{u}_0 + \rho_m 2h_j h_0 A_m \ddot{\theta}_0 + \rho_m 4h_j \sum_{i=m+1}^{-1} h_i A_m \ddot{\theta}_i \\
&-\rho_m 2h_j \bar{I}_m \ddot{\theta}_m\Big) + \delta\theta_m\Big(\rho_m \bar{I}_m \ddot{u}_0 + \rho_m h_0 \bar{I}_m \ddot{\theta}_0 - \rho_m \sum_{i=m+1}^{-1} 2h_i \bar{I}_m \ddot{\theta}_i + \rho_m I_m \ddot{\theta}_m\Big) \\
&+\delta u_0'\Big(c_{11}^{*m} A_m u_0' - c_{11}^{*m} h_0 A_m \theta_0' - c_{11}^{*m} \sum_{i=m+1}^{-1} 2h_i A_m \theta_i' + c_{11}^{*m} \bar{I}_m \theta_m'\Big) + \delta w_0'\Big(\bar{c}_{55}^{m(\phi)} A_m w_0' \\
&-\bar{c}_{55}^{m(\phi)} A_m \theta_m\Big) + \delta\theta_0'\Big(- c_{11}^{*m} h_0 A_m u_0' + c_{11}^{*m} {h_0}^2 A_m \theta_0' + c_{11}^{*m} h_0 \sum_{j=m+1}^{-1} 2h_j A_m \theta_j' \\
&-c_{11}^{*m} h_0 \bar{I}_m \theta_m'\Big) + \sum_{i=m+1}^{-1} \delta\theta_i'\Big(- c_{11}^{*m} 2h_i A_m u_0' + c_{11}^{*m} 2h_i h_0 A_m \theta_0' + c_{11}^{*m} 2h_i \sum_{j=m+1}^{-1} 2h_j A_m \theta_j' \\
&-c_{11}^{*m} 2h_i \bar{I}_m \theta_m'\Big) + \delta\theta_m'\Big(c_{11}^{*m} \bar{I}_m u_0' - c_{11}^{*m} h_0 \bar{I}_m \theta_0' - c_{11}^{*m} \sum_{i=m+1}^{-1} 2h_i \bar{I}_m \theta_i' + \bar{c}_{11}^{m(\phi)} I_m \theta_m'\Big) \\
&+\delta\theta_m\Big(\bar{c}_{55}^{m(\phi)} A_m \theta_m' - \bar{c}_{55}^{m(\phi)} A_m w_0'\Big) + \delta u_0' A_m \frac{e_{31}^{*m}}{2h_m}\phi_m - \delta\theta_0' h_0 A_m \frac{e_{31}^{*m}}{2h_m}\phi_m \\
&- \sum_{i=m+1}^{-1} \delta\theta_i' 2h_i A_m \frac{e_{31}^{*m}}{2h_m}\phi_m + \delta\theta_m' \bar{I}_m \frac{e_{31}^{*m}}{2h_m}\phi_m - \delta u_0 X_m + \delta\theta_0 h_0 X_m + \sum_{i=m+1}^{-1} \delta\theta_i 2h_i X_m \\
&+h_m \delta\theta_m X_m + \delta\theta_m M_m + \delta w_0 Z_m + \delta\phi_m \frac{e_{31}^{*m}}{2h_m}\Big(A_m u_0' - h_0 A_m \theta_0' - \sum_{i=m+1}^{-1} 2h_i A_m \theta_i' \\
&\quad +\bar{I}_m \theta_m'\Big) - \delta\phi_m \frac{\varepsilon_{33}^{*m} A_m}{4{h_m}^2}\phi_m + \delta\phi_m b\tau_m\Big]\Big\}\mathrm{d}L\mathrm{d}t = 0.
\end{aligned}
\tag{A.3}
$$

Taking the following properties of sums into consideration in the previous equation,

$$\sum_{n=1}^{\bar{n}}\sum_{i=1}^{n-1} f_n f_i \delta\theta_i = \sum_{i=1}^{\bar{n}}\Big(\sum_{n=i+1}^{\bar{n}} f_n f_i\Big)\delta\theta_i, \tag{A.4}$$

$$\sum_{m=\bar{m}}^{-1}\sum_{i=m+1}^{-1} f_m f_i \delta\theta_i = \sum_{i=\bar{m}}^{-1}\Big(\sum_{m=\bar{m}}^{i-1} f_m f_i\Big)\delta\theta_i, \tag{A.5}$$

$$\sum_{n=i+1}^{\bar{n}}\sum_{j=1}^{n-1} f_n f_i f_j \theta_j = \sum_{j=1}^{i-1}\Big(\sum_{n=i+1}^{\bar{n}} f_n f_i f_j\Big)\theta_j + \sum_{j=i}^{\bar{n}-1}\Big(\sum_{n=j+1}^{\bar{n}} f_n f_i f_j\Big)\theta_j, \tag{A.6}$$

$$\sum_{m=\bar{m}}^{i-1}\sum_{j=m+1}^{-1} f_m f_i f_j \theta_j = \sum_{j=i+1}^{-1}\Big(\sum_{m=\bar{m}}^{i-1} f_m f_i f_j\Big)\theta_j + \sum_{j=\bar{m}+1}^{i}\Big(\sum_{m=\bar{m}}^{j-1} f_m f_i f_j\Big)\theta_j, \tag{A.7}$$

where f_n, f_m, f_i and f_j are generic functions of the displacements and electric potential differences with the n, m, i and j subscripts, the variational terms are transformed to a more convenient representation where the variations become decoupled from the sums. For the sake of brevity only some changes in the terms are shown in the following equations. However, similar transformations are obtained for the stiffness terms and for the bottom layers.

$$\sum_{n=1}^{\bar{n}}\rho_n\sum_{i=1}^{n-1} 2h_i A_n\ddot{\theta}_i = \sum_{i=1}^{\bar{n}}\sum_{n=i+1}^{\bar{n}}\rho_n 2h_i A_n\ddot{\theta}_i = \sum_{n=1}^{\bar{n}}\sum_{i=n+1}^{\bar{n}}\rho_i 2h_n A_i\ddot{\theta}_n, \tag{A.8}$$

$$\sum_{n=1}^{\bar{n}}\rho_n h_0\sum_{i=1}^{n-1} 2h_i A_n\ddot{\theta}_i = \sum_{i=1}^{\bar{n}}\sum_{n=i+1}^{\bar{n}}\rho_n h_0 2h_i A_n\ddot{\theta}_i = \sum_{n=1}^{\bar{n}}\sum_{i=n+1}^{\bar{n}}\rho_i h_0 2h_n A_i\ddot{\theta}_n, \tag{A.9}$$

$$\begin{aligned}
&\sum_{n=1}^{\bar{n}}\sum_{i=1}^{n-1}\delta\theta_i\Big(\rho_n 2h_i A_n\ddot{u}_0 + \rho_n 2h_i h_0 A_n\ddot{\theta}_0 + \rho_n 4h_i\sum_{j=1}^{n-1} h_j A_n\ddot{\theta}_j + \rho_n 2h_i\bar{I}_n\ddot{\theta}_n\Big)\\
&= \sum_{i=1}^{\bar{n}}\sum_{n=i+1}^{\bar{n}}\delta\theta_i\Big(\rho_n 2h_i A_n\ddot{u}_0 + \rho_n 2h_i h_0 A_n\ddot{\theta}_0 + \rho_n 2h_i\bar{I}_n\ddot{\theta}_n\Big) + \sum_{i=1}^{\bar{n}}\sum_{n=i+1}^{\bar{n}}\delta\theta_i\rho_n 4h_i\sum_{j=1}^{n-1} h_j A_n\ddot{\theta}_j\\
&= \sum_{n=1}^{\bar{n}}\sum_{i=n+1}^{\bar{n}}\delta\theta_n\Big(\rho_i 2h_n A_i\ddot{u}_0 + \rho_i 2h_n h_0 A_i\ddot{\theta}_0 + \rho_i 2h_n\bar{I}_i\ddot{\theta}_i\Big) + \sum_{i=1}^{\bar{n}}\delta\theta_i\Big(\sum_{n=i+1}^{\bar{n}}\rho_n 4h_i\sum_{j=1}^{n-1} h_j A_n\ddot{\theta}_j\Big),
\end{aligned} \tag{A.10}$$

$$\begin{aligned}
&\sum_{i=1}^{\bar{n}}\delta\theta_i\Big(\sum_{n=i+1}^{\bar{n}}\sum_{j=1}^{n-1}\rho_n 4h_i h_j A_n\ddot{\theta}_j\Big) = \sum_{i=1}^{\bar{n}}\delta\theta_i\Big(\sum_{j=1}^{i-1}\sum_{n=i+1}^{\bar{n}}\rho_n 4h_i h_j A_n\ddot{\theta}_j\Big)\\
&+\sum_{i=1}^{\bar{n}}\delta\theta_i\Big(\sum_{j=i}^{\bar{n}-1}\sum_{n=j+1}^{\bar{n}}\rho_n 4h_i h_j A_n\ddot{\theta}_j\Big) = \sum_{n=1}^{\bar{n}}\delta\theta_n\Big(\sum_{i=1}^{n-1}\sum_{j=n+1}^{\bar{n}}\rho_j 4h_n h_i A_j\ddot{\theta}_i\Big)\\
&\qquad+\sum_{n=1}^{\bar{n}}\delta\theta_n\Big(\sum_{j=n}^{\bar{n}-1}\sum_{i=j+1}^{\bar{n}}\rho_i 4h_n h_j A_i\ddot{\theta}_j\Big),
\end{aligned} \tag{A.11}$$

$$\sum_{n=1}^{\bar{n}}\sum_{i=1}^{n-1}\delta\theta_i 2h_i X_n = \sum_{i=1}^{\bar{n}}\sum_{n=i+1}^{\bar{n}}\delta\theta_i 2h_i X_n = \sum_{n=1}^{\bar{n}}\delta\theta_n\sum_{i=n+1}^{\bar{n}} 2h_n X_i, \tag{A.12}$$

$$\sum_{n=1}^{\bar{n}}\sum_{i=1}^{n-1}\delta\theta_i' 2h_i A_n\frac{e_{31}^{*n}}{2h_n}\phi_n = \sum_{i=1}^{\bar{n}}\sum_{n=i+1}^{\bar{n}}\delta\theta_i' 2h_i A_n\frac{e_{31}^{*n}}{2h_n}\phi_n = \sum_{n=1}^{\bar{n}}\sum_{i=n+1}^{\bar{n}}\delta\theta_n' 2h_n A_i\frac{e_{31}^{*i}}{2h_i}\phi_i. \tag{A.13}$$

Thus, considering the transformations, after some algebra Equation (A.3) becomes

$$
\begin{aligned}
&\int_{t_0}^{t_1}\int_L\Bigg\{\sum_{n=1}^{\bar{n}}\Bigg[\delta u_0\Big(\rho_n A_n\ddot{u}_0+\rho_n h_0 A_n\ddot{\theta}_0+\Big\{\sum_{i=n+1}^{\bar{n}}\rho_i 2h_n A_i+\rho_n\bar{I}_n\Big\}\ddot{\theta}_n\Big)+\delta w_0\rho_n A_n\ddot{w}_0\\
&+\delta\theta_0\Big(\rho_n h_0 A_n\ddot{u}_0+\rho_n {h_0}^2 A_n\ddot{\theta}_0+\Big\{\sum_{i=n+1}^{\bar{n}}\rho_i h_0 2h_n A_i+\rho_n h_0\bar{I}_n\Big\}\ddot{\theta}_n\Big)+\delta\theta_n\Big(\Big\{\sum_{i=n+1}^{\bar{n}}\rho_i 2h_n A_i\\
&+\rho_n\bar{I}_n\Big\}\ddot{u}_0+\Big\{\sum_{i=n+1}^{\bar{n}}\rho_i 2h_n h_0 A_i+\rho_n h_0\bar{I}_n\Big\}\ddot{\theta}_0+\sum_{i=1}^{n-1}\Big\{\sum_{j=n+1}^{\bar{n}}\rho_j 4h_n h_i A_j+\rho_n 2h_i\bar{I}_n\Big\}\ddot{\theta}_i\\
&+\Big\{\sum_{i=n+1}^{\bar{n}}\rho_i 4h_n h_n A_i+\rho_n I_n\Big\}\ddot{\theta}_n+\sum_{j=n+1}^{\bar{n}}\Big\{\sum_{i=j+1}^{\bar{n}}\rho_i 4h_n h_j A_i+\rho_j 2h_n\bar{I}_j\Big\}\ddot{\theta}_j\Big)\\
&+\delta u_0'\Big(c_{11}^{*n}A_n u_0'+c_{11}^{*n}h_0 A_n\theta_0'+\Big\{\sum_{i=n+1}^{\bar{n}}c_{11}^{*i}2h_n A_i+c_{11}^{*n}\bar{I}_n\Big\}\theta_n'+A_n\frac{e_{31}^{*n}}{2h_n}\phi_n\Big)\\
&+\delta w_0'\Big(\bar{c}_{55}^{n(\phi)}A_n w_0'-\bar{c}_{55}^{n(\phi)}A_n\theta_n\Big)+\delta\theta_0'\Big(c_{11}^{*n}h_0 A_n u_0'+c_{11}^{*n}{h_0}^2 A_n\theta_0'+\Big\{\sum_{i=n+1}^{\bar{n}}c_{11}^{*i}h_0 2h_n A_i\\
&+c_{11}^{*n}h_0\bar{I}_n\Big\}\theta_n'+h_0 A_n\frac{e_{31}^{*n}}{2h_n}\phi_n\Big)+\delta\theta_n'\Big(\Big\{\sum_{i=n+1}^{\bar{n}}c_{11}^{*i}2h_n A_i+c_{11}^{*n}\bar{I}_n\Big\}u_0'+\Big\{\sum_{i=n+1}^{\bar{n}}c_{11}^{*i}2h_n h_0 A_i\\
&+c_{11}^{*n}h_0\bar{I}_n\Big\}\theta_0'+\sum_{i=1}^{n-1}\Big\{\sum_{j=n+1}^{\bar{n}}c_{11}^{*j}4h_n h_i A_j+c_{11}^{*n}2h_i\bar{I}_n\Big\}\theta_i'+\Big\{\sum_{i=n+1}^{\bar{n}}c_{11}^{*i}4h_n h_n A_i+\bar{c}_{11}^{n(\phi)}I_n\Big\}\theta_n'\\
&+\sum_{j=n+1}^{\bar{n}-1}\Big\{\sum_{i=j+1}^{\bar{n}}c_{11}^{*i}4h_n h_j A_i+c_{11}^{*j}2h_n\bar{I}_j\Big\}\theta_j'+c_{11}^{*\bar{n}}2h_n\bar{I}_{\bar{n}}\theta_{\bar{n}}'+\bar{I}_n\frac{e_{31}^{*n}}{2h_n}\phi_n+\sum_{i=n+1}^{\bar{n}}2h_n A_i\frac{e_{31}^{*i}}{2h_i}\phi_i\Big)\\
&+\delta\theta_n\Big(c_{55}^{n}A_n\theta_n-c_{55}^{n}A_n w_0'\Big)-\delta u_0 X_n-\delta\theta_0 h_0 X_n-\delta\theta_n\Big\{\sum_{i=n+1}^{\bar{n}}2h_n X_i+h_n X_n+M_n\Big\}\\
&-\delta w_0 Z_n\Bigg]+\delta\phi_n\Big(\frac{e_{31}^{*n}}{2h_n}A_n u_0'+\frac{e_{31}^{*n}}{2h_n}h_0 A_n\theta_0'+\sum_{i=1}^{n-1}\frac{e_{31}^{*n}}{2h_n}2h_i A_n\theta_i'+\frac{e_{31}^{*n}}{2h_n}\bar{I}_n\theta_n'\Big)-\delta\phi_n\frac{\varepsilon_{33}^{*n}A_n}{4{h_n}^2}\phi_n\\
&+\delta\phi_n b\tau_n+\delta u_0\rho_c A_c\ddot{u}_0+\delta w_0\rho_c A_c\ddot{w}_0+\delta\theta_0\rho_c I_c\ddot{\theta}_0+\delta u_0' c_{11}^{*c}A_c u_0'+\delta w_0'\Big(c_{55}^{c}A_c w_0'-c_{55}^{c}A_c\theta_0\Big)\\
&+\delta\theta_0' c_{11}^{*c}I_c\theta_0'+\delta\theta_0\Big(c_{55}^{c}A_c\theta_0-c_{55}^{c}A_c w_0'\Big)-\delta u_0 X_c-\delta\theta_0 M_c-\delta w_0 Z_c+\sum_{m=\bar{m}}^{-1}\Bigg[\delta u_0\Big(\rho_m A_m\ddot{u}_0\\
&-\rho_m h_0 A_m\ddot{\theta}_0+\Big\{-\sum_{i=\bar{m}}^{m-1}\rho_i 2h_m A_i+\rho_m\bar{I}_m\Big\}\ddot{\theta}_m\Big)+\delta w_0\rho_m A_m\ddot{w}_0+\delta\theta_0\Big(-\rho_m h_0 A_m\ddot{u}_0\\
&+\rho_m {h_0}^2 A_m\ddot{\theta}_0+\Big\{\sum_{i=\bar{m}}^{m-1}\rho_i h_0 2h_m A_i-\rho_m h_0\bar{I}_m\Big\}\ddot{\theta}_m\Big)+\delta\theta_m\Big(\Big\{-\sum_{i=\bar{m}}^{m-1}\rho_i 2h_m A_i+\rho_m\bar{I}_m\Big\}\ddot{u}_0\\
&+\Big\{\sum_{i=\bar{m}}^{m-1}\rho_i 2h_m h_0 A_i-\rho_m h_0\bar{I}_m\Big\}\ddot{\theta}_0+\sum_{i=m+1}^{-1}\Big\{\sum_{j=\bar{m}}^{m-1}\rho_j 4h_m h_i A_j-\rho_m 2h_i\bar{I}_m\Big\}\ddot{\theta}_i\\
&+\Big\{\sum_{i=\bar{m}}^{m-1}\rho_i 4h_m h_m A_i+\rho_m I_m\Big\}\ddot{\theta}_m+\sum_{j=\bar{m}+1}^{m-1}\Big\{\sum_{i=\bar{m}}^{j-1}\rho_i 4h_m h_j A_i-\rho_j 2h_m\bar{I}_j\Big\}\ddot{\theta}_j-\rho_{\bar{m}}2h_m\bar{I}_{\bar{m}}\ddot{\theta}_{\bar{m}}\Big)\\
&+\delta u_0'\Big(c_{11}^{*m}A_m u_0'-c_{11}^{*m}h_0 A_m\theta_0'+\Big\{\sum_{i=\bar{m}}^{m-1}-c_{11}^{*i}2h_m A_i+c_{11}^{*m}\bar{I}_m\Big\}\theta_m'+A_m\frac{e_{31}^{*m}}{2h_m}\phi_m\Big)\\
&+\delta w_0'\Big(\bar{c}_{55}^{m(\phi)}A_m w_0'-\bar{c}_{55}^{m(\phi)}A_m\theta_m\Big)+\delta\theta_0'\Big(-c_{11}^{*m}h_0 A_m u_0'+c_{11}^{*m}{h_0}^2 A_m\theta_0'+\Big\{\sum_{i=\bar{m}}^{m-1}c_{11}^{*i}h_0 2h_m A_i
\end{aligned}
$$

$$
\begin{aligned}
&-c_{11}^{*m} h_0 \bar{I}_m\Big\}\theta_m' - h_0 A_m \frac{e_{31}^{*m}}{2h_m}\phi_m\Big) + \delta\theta_m'\Big(\Big\{\sum_{i=\bar{m}}^{m-1} -c_{11}^{*i} 2h_m A_i + c_{11}^{*m}\bar{I}_m\Big\}u_0' + \Big\{\sum_{i=\bar{m}}^{m-1} c_{11}^{*i} 2h_m h_0 A_i \\
&-c_{11}^{*m} h_0 \bar{I}_m\Big\}\theta_0' + \sum_{i=m+1}^{-1}\Big\{\sum_{j=\bar{m}}^{m-1} c_{11}^{*j} 4h_m h_i A_j - c_{11}^{*m} 2h_i \bar{I}_m\Big\}\theta_i' + \Big\{\sum_{i=\bar{m}}^{m-1} c_{11}^{*i} 4h_m h_m A_i + \bar{c}_{11}^{m(\phi)} I_m\Big\}\theta_m' \\
&\quad + \sum_{j=\bar{m}}^{m-1}\Big\{\sum_{i=\bar{m}}^{j-1} c_{11}^{*i} 4h_m h_j A_i - c_{11}^{*j} 2h_m \bar{I}_j\Big\}\theta_j' + \bar{I}_m \frac{e_{31}^{*m}}{2h_m}\phi_m - \sum_{i=\bar{m}}^{m-1} 2h_m A_i \frac{e_{31}^{*i}}{2h_i}\phi_i\Big) \\
&+\delta\theta_m\Big(c_{55}^{m} A_m \theta_m - c_{55}^{m} A_m w_0'\Big) - \delta u_0 X_m + \delta\theta_0 h_0 X_m - \delta\theta_m\Big\{\sum_{i=\bar{m}}^{m-1} -2h_m X_i - h_m X_m + M_m\Big\} \\
&\quad -\delta w_0 Z_m + \delta\phi_m\Big(\frac{e_{31}^{*m}}{2h_m} A_m u_0' - \frac{e_{31}^{*m}}{2h_m} h_0 A_m \theta_0' - \sum_{i=m+1}^{-1}\frac{e_{31}^{*m}}{2h_m} 2h_i A_m \theta_i' + \frac{e_{31}^{*m}}{2h_m}\bar{I}_m \theta_m'\Big) \\
&\qquad -\delta\phi_m \frac{\varepsilon_{33}^{*m} A_m}{4{h_m}^2}\phi_m + \delta\phi_m b\tau_m\Big]\Big\}\mathrm{d}L\mathrm{d}t = 0. \qquad \text{(A.14)}
\end{aligned}
$$

Considering the generalized mechanical displacements and electric potential differences grouped in the generalized vectors of displacement and potential difference

$$
\mathbf{u}(x,t) = \{u_0(x,t), w_0(x,t), \theta_0(x,t), \theta_1(x,t), \dots, \theta_{\bar{n}}(x,t), \theta_{\bar{m}}(x,t), \dots, \theta_{-1}(x,t)\}^{\mathrm{T}}, \quad \text{(A.15)}
$$

$$
\boldsymbol{\phi}(x,t) = \left\{\phi_1(x,t), \dots, \phi_{\bar{n}}(x,t), \phi_{\bar{m}}(x,t), \dots, \phi_{-1}(x,t)\right\}^{\mathrm{T}}, \quad \text{(A.16)}
$$

and since Equation (A.14) can only be satisfied if the integral term relative to L is zero, the weak form of the analytical model can be expressed in matrix form as

$$
\begin{aligned}
\int_L \Big[&\delta\mathbf{u}^{\mathrm{T}}\mathbf{J}\ddot{\mathbf{u}} + (\mathbf{L}_{xx}\delta\mathbf{u})^{\mathrm{T}}\mathbf{Y}\mathbf{L}_{xx}\mathbf{u} + (\mathbf{L}_{zx}\delta\mathbf{u})^{\mathrm{T}}\mathbf{G}\mathbf{L}_{zx}\mathbf{u} + (\mathbf{L}_{xx}\delta\mathbf{u})^{\mathrm{T}}\mathbf{P}^{\mathrm{T}}\boldsymbol{\phi} - \delta\mathbf{u}^{\mathrm{T}}\mathbf{f} \\
&+\delta\boldsymbol{\phi}^{\mathrm{T}}\mathbf{P}\mathbf{L}_{xx}\mathbf{u} + \delta\boldsymbol{\phi}^{\mathrm{T}}\mathbf{C}\boldsymbol{\phi} - \delta\boldsymbol{\phi}^{\mathrm{T}}\boldsymbol{\tau}\Big]\mathrm{d}L = 0. \qquad \text{(A.17)}
\end{aligned}
$$

The differential operators

$$
\mathbf{L}_{xx} = diag\left(\frac{\partial}{\partial x}, 0, \frac{\partial}{\partial x}, \dots, \frac{\partial}{\partial x}\right), \mathbf{L}_{zx} = diag\left(0, \frac{\partial}{\partial x}, 1, \dots, 1\right), \quad \text{(A.18a,b)}
$$

are used for the definition of the generalized extensional and shear strains and the non-zero terms of the symmetric positive definite inertia matrix $\mathbf{J}$ and of the symmetric semi-positive definite extensional and shear stiffness matrices $\mathbf{Y}$ and $\mathbf{G}$, of size $[(\bar{k}-1)\times(\bar{k}-1)]$, piezoelectric equivalent stiffness and capacitance matrices $\mathbf{P}$ and $\mathbf{C}$, of size $[\bar{p}\times(\bar{k}-1)]$ and $(\bar{p}\times\bar{p})$, and applied mechanical forces and electric charge density vectors $\mathbf{f}$ and $\boldsymbol{\tau}$, of size $[(\bar{k}-1)\times 1]$ and $(\bar{p}\times 1)$, have elements defined in (A.14). Here, $\bar{p} = \bar{n} - \bar{m}$ is the total number of piezoelectric layers and $\bar{k}-1$, with $\bar{k} = \bar{p}+4$, is the total number of generalized displacements. The non-zero symmetric inertial terms $J_{(i,j)} = J_{(j,i)}$, extensional stiffness terms $Y_{(i,j)} = Y_{(j,i)}$ and shear stiffness terms $G_{(i,j)} = G_{(j,i)}$, and the piezoelectric equivalent stiffness terms $P_{(l,i)}$ and capacitance terms $C_{(l,l)}$, with $i, j = 1, \ldots, \bar{k}-1$ and $l = 1, \ldots, \bar{p}$, of the matrices utilized in (A.17), are given by

$$\begin{gathered}
J_{(1,1)} = \sum_{k=\bar{m}}^{\bar{n}} \rho_k A_k,\ J_{(1,3)} = \sum_{n=1}^{\bar{n}} \rho_n h_0 A_n - \sum_{m=\bar{m}}^{-1} \rho_m h_0 A_m,\ J_{(1,\hat{n}+3)} = \sum_{i=\hat{n}+1}^{\bar{n}} \rho_i 2h_{\hat{n}} A_i \\
+\rho_{\hat{n}} \bar{I}_{\hat{n}},\ J_{(1,\bar{n}+3)} = \rho_{\bar{n}} \bar{I}_{\bar{n}},\ J_{(1,\bar{n}+4)} = \rho_{\bar{m}} \bar{I}_{\bar{m}},\ J_{(1,\bar{k}+\hat{m})} = -\sum_{i=\bar{m}}^{\hat{m}-1} \rho_i 2h_{\hat{m}} A_i + \rho_{\hat{m}} \bar{I}_{\hat{m}}, \\
J_{(2,2)} = \sum_{k=\bar{m}}^{\bar{n}} \rho_k A_k,\ J_{(3,3)} = \sum_{n=1}^{\bar{n}} \rho_n h_0^2 A_n + \sum_{m=\bar{m}}^{-1} \rho_m h_0^2 A_m + \rho_0 I_0, \\
J_{(3,\hat{n}+3)} = 2h_0 h_{\hat{n}} \sum_{i=\hat{n}+1}^{\bar{n}} \rho_i A_i + \rho_{\hat{n}} h_0 \bar{I}_{\hat{n}},\ J_{(3,\bar{n}+3)} = \rho_{\bar{n}} h_0 \bar{I}_{\bar{n}},\ J_{(3,\bar{n}+4)} = -\rho_{\bar{m}} h_0 \bar{I}_{\bar{m}}, \\
J_{(3,\bar{k}+\hat{m})} = 2h_0 h_{\hat{m}} \sum_{i=\bar{m}}^{\hat{m}-1} \rho_i A_i - \rho_{\hat{m}} h_0 \bar{I}_{\hat{m}},\ J_{(\hat{n}+3,\hat{n}+3)} = \sum_{i=\hat{n}+1}^{\bar{n}} \rho_i 4{h_{\hat{n}}}^2 A_i + \rho_{\hat{n}} I_{\hat{n}}, \\
J_{(\hat{n}+3,j+3)} = \sum_{i=j+1}^{\bar{n}} \rho_i 4h_{\hat{n}} h_j A_i + \rho_j 2h_{\hat{n}} \bar{I}_j,\ J_{(\hat{n}+3,\bar{n}+3)} = \rho_{\bar{n}} 2h_{\hat{n}} \bar{I}_{\bar{n}},\ J_{(\bar{n}+3,\bar{n}+3)} = \rho_{\bar{n}} I_{\bar{n}}, \\
J_{(\bar{n}+4,\bar{n}+4)} = \rho_{\bar{m}} I_{\bar{m}},\ J_{(\bar{n}+4,\bar{k}+\hat{m})} = -\rho_{\bar{m}} 2h_{\hat{m}} \bar{I}_{\bar{m}},\ J_{(\bar{k}+\hat{m},\bar{k}+\hat{m})} = \sum_{i=\bar{m}}^{\hat{m}-1} \rho_i 4{h_{\hat{m}}}^2 A_i + \rho_{\hat{m}} I_{\hat{m}}, \\
J_{(\bar{k}+\hat{m},\bar{k}+i)} = \sum_{j=\bar{m}}^{\hat{m}-1} \rho_j 4h_{\hat{m}} h_i A_j - \rho_{\hat{m}} 2h_i \bar{I}_{\hat{m}}, \qquad \text{(A.19)}
\end{gathered}$$

$$\begin{gathered}
Y_{(1,1)} = \sum_{k=\bar{m}}^{\bar{n}} c_{11}^{*k} A_k,\ Y_{(1,3)} = \sum_{n=1}^{\bar{n}} c_{11}^{*n} h_0 A_n - \sum_{m=\bar{m}}^{-1} c_{11}^{*m} h_0 A_m,\ Y_{(1,\hat{n}+3)} = \sum_{i=\hat{n}+1}^{\bar{n}} c_{11}^{*i} 2h_{\hat{n}} A_i \\
+c_{11}^{*\hat{n}} \bar{I}_{\hat{n}},\ Y_{(1,\bar{n}+3)} = c_{11}^{*\bar{n}} \bar{I}_{\bar{n}},\ Y_{(1,\bar{n}+4)} = c_{11}^{*\bar{m}} \bar{I}_{\bar{m}},\ Y_{(1,\bar{k}+\hat{m})} = -\sum_{i=\bar{m}}^{\hat{m}-1} c_{11}^{*i} 2h_{\hat{m}} A_i + c_{11}^{*\hat{m}} \bar{I}_{\hat{m}}, \\
Y_{(3,3)} = \sum_{n=1}^{\bar{n}} c_{11}^{*n} {h_0}^2 A_n + \sum_{m=\bar{m}}^{-1} c_{11}^{*m} {h_0}^2 A_m + c_{11}^{*0} I_0,\ Y_{(3,\hat{n}+3)} = 2h_0 h_{\hat{n}} \sum_{i=\hat{n}+1}^{\bar{n}} c_{11}^{*i} A_i \\
+c_{11}^{*\hat{n}} h_0 \bar{I}_{\hat{n}},\ Y_{(3,\bar{n}+3)} = c_{11}^{*\bar{n}} h_0 \bar{I}_{\bar{n}},\ Y_{(3,\bar{n}+4)} = -c_{11}^{*\bar{m}} h_0 \bar{I}_{\bar{m}},\ Y_{(3,\bar{k}+\hat{m})} = 2h_0 h_{\hat{m}} \sum_{i=\bar{m}}^{\hat{m}-1} c_{11}^{*i} A_i \\
-c_{11}^{*\hat{m}} h_0 \bar{I}_{\hat{m}},\ Y_{(\hat{n}+3,\hat{n}+3)} = \sum_{i=\hat{n}+1}^{\bar{n}} c_{11}^{*i} 4{h_{\hat{n}}}^2 A_i + \bar{c}_{11}^{\hat{n}(\phi)} I_{\hat{n}},\ Y_{(\hat{n}+3,j+3)} = \sum_{i=j+1}^{\bar{n}} c_{11}^{*i} 4h_{\hat{n}} h_j A_i \\
+c_{11}^{*j} 2h_{\hat{n}} \bar{I}_j,\ Y_{(\hat{n}+3,\bar{n}+3)} = c_{11}^{*\bar{n}} 2h_{\hat{n}} \bar{I}_{\bar{n}},\ Y_{(\bar{n}+3,\bar{n}+3)} = \bar{c}_{11}^{\bar{n}(\phi)} I_{\bar{n}},\ Y_{(\bar{n}+4,\bar{n}+4)} = \bar{c}_{11}^{\bar{m}(\phi)} I_{\bar{m}}, \\
Y_{(\bar{n}+4,\bar{k}+\hat{m})} = -c_{11}^{*\bar{m}} 2h_{\hat{m}} \bar{I}_{\bar{m}},\ Y_{\left(\bar{k}+\hat{m},\bar{k}+\hat{m}\right)} = \sum_{i=\bar{m}}^{\hat{m}-1} c_{11}^{*i} 4{h_{\hat{m}}}^2 A_i + \bar{c}_{11}^{\hat{m}(\phi)} I_{\hat{m}}, \\
Y_{\left(\bar{k}+\hat{m},\bar{k}+i\right)} = \sum_{j=\bar{m}}^{\hat{m}-1} c_{11}^{*j} 4h_{\hat{m}} h_i A_j - c_{11}^{*\hat{m}} 2h_i \bar{I}_{\hat{m}}, \qquad \text{(A.20)}
\end{gathered}$$

$$\begin{gathered}
G_{(2,2)} = \sum_{n=1}^{\bar{n}} \bar{c}_{55}^{n(\phi)} A_n + c_{55}^{0} A_0 + \sum_{m=\bar{m}}^{-1} \bar{c}_{55}^{m(\phi)} A_m,\ G_{(2,3)} = -c_{55}^{0} A_0,\ G_{(2,\hat{n}+3)} = -\bar{c}_{55}^{\hat{n}(\phi)} A_{\hat{n}}, \\
G_{(2,\bar{n}+3)} = -\bar{c}_{55}^{\bar{n}(\phi)} A_{\bar{n}},\ G_{(2,\bar{n}+4)} = -\bar{c}_{55}^{\bar{m}(\phi)} A_{\bar{m}},\ G_{(2,\bar{k}+\hat{m})} = -\bar{c}_{55}^{\hat{m}(\phi)} A_{\hat{m}},\ G_{(3,3)} = c_{55}^{0} A_0, \\
G_{(\hat{n}+3,\hat{n}+3)} = \bar{c}_{55}^{\hat{n}(\phi)} A_{\hat{n}},\ G_{(\bar{n}+3,\bar{n}+3)} = \bar{c}_{55}^{\bar{n}(\phi)} A_{\bar{n}},\ G_{(\bar{n}+4,\bar{n}+4)} = \bar{c}_{55}^{\bar{m}(\phi)} A_{\bar{m}}, \\
G_{\left(\bar{k}+\hat{m},\bar{k}+\hat{m}\right)} = \bar{c}_{55}^{\hat{m}(\phi)} A_{\hat{m}}, \qquad \text{(A.21)}
\end{gathered}$$

$$P_{(n,1)} = \frac{e_{31}^{*n}}{2h_n} A_n,\ P_{(n,3)} = \frac{e_{31}^{*n}}{2h_n} h_0 A_n,\ P_{(n,i+3)} = \frac{e_{31}^{*n}}{2h_n} 2h_i A_n,\ P_{(n,n+3)} = \frac{e_{31}^{*n}}{2h_n} \bar{I}_n,$$
$$P_{(\bar{p}+1+m,1)} = \frac{e_{31}^{*m}}{2h_m} A_m,\ P_{(\bar{p}+1+m,3)} = -\frac{e_{31}^{*m}}{2h_m} h_0 A_m,\ P_{(\bar{p}+1+m,\bar{k}+m)} = \frac{e_{31}^{*m}}{2h_m} \bar{I}_m,$$
$$P_{(\bar{p}+1+m,\bar{k}+i)} = -\frac{e_{31}^{*m}}{2h_m} 2h_i A_m, \quad \text{(A.22)}$$

$$C_{(n,n)} = -\frac{\varepsilon_{33}^{*n} A_n}{4{h_n}^2},\ C_{(\bar{p}+1+m,\bar{p}+1+m)} = -\frac{\varepsilon_{33}^{*m} A_m}{4{h_m}^2}, \quad \text{(A.23)}$$

where $\hat{n} = 1, \ldots, \bar{n} - 1$ and $\hat{m} = \bar{m} + 1, \ldots, -1$. Furthermore, the applied mechanical forces and electric charge densities terms $f_{(i)}$ and $\tau_{(l)}$ are defined as

$$f_{(1)} = \sum_{k=\bar{m}}^{\bar{n}} X_k,\ f_{(2)} = \sum_{k=\bar{m}}^{\bar{n}} Z_k,\ f_{(3)} = \sum_{n=1}^{\bar{n}} h_0 X_n + M_0 - \sum_{m=\bar{m}}^{-1} h_0 X_m,$$
$$f_{(\hat{n}+3)} = h_{\hat{n}} X_{\hat{n}} + \sum_{i=\hat{n}+1}^{\bar{n}} 2h_{\hat{n}} X_i + M_{\hat{n}},\ f_{(\bar{n}+3)} = h_{\bar{n}} X_{\bar{n}} + M_{\bar{n}},$$
$$f_{(\bar{n}+4)} = -h_{\bar{m}} X_{\bar{m}} + M_{\bar{m}},\ f_{(\bar{k}+\hat{m})} = -h_{\hat{m}} X_{\hat{m}} - \sum_{i=\bar{m}}^{\hat{m}-1} 2h_{\hat{m}} X_i + M_{\hat{m}}, \quad \text{(A.24)}$$

$$\tau_{(n)} = -b\tau_n,\ \tau_{(\bar{p}+1+m)} = -b\tau_m. \quad \text{(A.25)}$$

Splitting Equation (A.17) into two matrix equations in terms of the variations of the generalized displacements and electric potential differences, $\delta\mathbf{u}$ and $\delta\boldsymbol{\phi}$, and rearranging the terms, yields

$$\int_L \left[\delta\mathbf{u}^{\mathrm{T}}\mathbf{J}\ddot{\mathbf{u}} + \delta\mathbf{u}^{\mathrm{T}}(\mathbf{L}_{xx}^{\mathrm{T}}\mathbf{Y}\mathbf{L}_{xx} + \mathbf{L}_{zx}^{\mathrm{T}}\mathbf{G}\mathbf{L}_{zx})\mathbf{u} + \delta\mathbf{u}^{\mathrm{T}}\mathbf{L}_{xx}^{\mathrm{T}}\mathbf{P}^{\mathrm{T}}\boldsymbol{\phi}\right]\mathrm{d}L = \int_L \delta\mathbf{u}^{\mathrm{T}}\mathbf{f}\,\mathrm{d}L, \quad \text{(A.26)}$$
$$\int_L (\delta\boldsymbol{\phi}^{\mathrm{T}}\mathbf{P}\mathbf{L}_{xx}\mathbf{u} + \delta\boldsymbol{\phi}^{\mathrm{T}}\mathbf{C}\boldsymbol{\phi})\mathrm{d}L = \int_L \delta\boldsymbol{\phi}^{\mathrm{T}}\boldsymbol{\tau}\,\mathrm{d}L. \quad \text{(A.27)}$$

Equations (A.26) and (A.27) are the weak forms, governing the motion and electric charge equilibrium, of the layered beam with arbitrary ACLD treatments, and the generalized displacements and electrical potential differences vectors are the unknown independent variables.

A.3 Strong Forms

In order to get rid of the differentiation in the $\mathbf{L}_{xx}\delta\mathbf{u}$ and $\mathbf{L}_{zx}\delta\mathbf{u}$ terms, Equation (A.17) is integrated by parts, yielding

$$\left[\delta\mathbf{u}^{\mathrm{T}}\mathbf{Y}\mathbf{L}_{xx}\mathbf{u} + (\mathbf{L}_{zx}^{1}\delta\mathbf{u})^{\mathrm{T}}\mathbf{G}\mathbf{L}_{zx}\mathbf{u} + \delta\mathbf{u}^{\mathrm{T}}\mathbf{P}^{\mathrm{T}}\boldsymbol{\phi}\right]_0^L$$
$$+ \int_L \Big[\delta\mathbf{u}^{\mathrm{T}}\mathbf{J}\ddot{\mathbf{u}} - \delta\mathbf{u}^{\mathrm{T}}\mathbf{Y}\mathbf{L}_{xx}\mathbf{L}_{xx}\mathbf{u} - \delta\mathbf{u}^{\mathrm{T}}\mathbf{G}\mathbf{L}_{zx}^{2}\mathbf{L}_{zx}^{2}\mathbf{u} + \delta\mathbf{u}^{\mathrm{T}}\mathbf{L}_{zx}^{3\mathrm{T}}\mathbf{G}\mathbf{L}_{zx}^{3}\mathbf{u}$$
$$- \delta\mathbf{u}^{\mathrm{T}}\mathbf{P}^{\mathrm{T}}\mathbf{L}_{\phi\phi}\boldsymbol{\phi} - \delta\mathbf{u}^{\mathrm{T}}\mathbf{f} + \delta\boldsymbol{\phi}^{\mathrm{T}}\mathbf{P}\mathbf{L}_{xx}\mathbf{u} + \delta\boldsymbol{\phi}^{\mathrm{T}}\mathbf{C}\boldsymbol{\phi} - \delta\boldsymbol{\phi}^{\mathrm{T}}\boldsymbol{\tau}\Big]\mathrm{d}L = 0, \quad \text{(A.28)}$$

where

$$\mathbf{L}_{zx}^{1} = diag\,(0, 1, 0, \ldots, 0)\,,\ \mathbf{L}_{zx}^{2} = diag\left(0, \frac{\partial}{\partial x}, 0, \ldots, 0\right), \quad \text{(A.29a,b)}$$

$$\mathbf{L}_{zx}^{3} = diag\,(0,0,1,\ldots,1)\,,\ \mathbf{L}_{\phi\phi} = diag\left(\frac{\partial}{\partial x},\ldots,\frac{\partial}{\partial x}\right). \qquad \text{(A.30a,b)}$$

Rearranging Equation (A.28) and collecting the terms involving the variations yields

$$\left[\delta\mathbf{u}^{\mathrm{T}}\left(\mathbf{Y}\mathbf{L}_{xx}\mathbf{u}+\mathbf{L}_{zx}^{1\mathrm{T}}\mathbf{G}\mathbf{L}_{zx}\mathbf{u}+\mathbf{P}^{\mathrm{T}}\boldsymbol{\phi}\right)\right]_{0}^{L}+\int_{L}\delta\mathbf{u}^{\mathrm{T}}\left(\mathbf{J}\ddot{\mathbf{u}}-\mathbf{Y}\mathbf{L}_{xx}\mathbf{L}_{xx}\mathbf{u}-\mathbf{G}\mathbf{L}_{zx}^{2}\mathbf{L}_{zx}^{2}\mathbf{u}\right.$$
$$\left.+\mathbf{G}\mathbf{L}_{zx}^{3}\mathbf{u}-\mathbf{P}^{\mathrm{T}}\mathbf{L}_{\phi\phi}\boldsymbol{\phi}-\mathbf{f}\right)\mathrm{d}L+\int_{L}\delta\boldsymbol{\phi}^{\mathrm{T}}\left(\mathbf{P}\mathbf{L}_{xx}\mathbf{u}+\mathbf{C}\boldsymbol{\phi}-\boldsymbol{\tau}\right)\mathrm{d}L=0. \qquad \text{(A.31)}$$

Since the variational generalized displacements and electric potential differences in Equation (A.31) are independent and arbitrary in the interval $[0, L]$, the equation can only be satisfied if the coefficients of the variational displacements and electric potential differences are zero. Thus, the electro-mechanical equations of motion, electric charge equilibrium equations and electro-mechanical boundary conditions can be derived accordingly.

A.3.1 Electro-Mechanical Equations of Motion

The electro-mechanical equations of motion are derived from Equation (A.31) by considering the integral term involving $\delta\mathbf{u}$,

$$\int_{L}\delta\mathbf{u}^{\mathrm{T}}\left(\mathbf{J}\ddot{\mathbf{u}}-\mathbf{Y}\mathbf{L}_{xx}\mathbf{L}_{xx}\mathbf{u}-\mathbf{G}\mathbf{L}_{zx}^{2}\mathbf{L}_{zx}^{2}\mathbf{u}+\mathbf{G}\mathbf{L}_{zx}^{3}\mathbf{u}-\mathbf{P}^{\mathrm{T}}\mathbf{L}_{\phi\phi}\boldsymbol{\phi}-\mathbf{f}\right)\,\mathrm{d}L=0, \qquad \text{(A.32)}$$

where the non-trivial solution is given by

$$\mathbf{Y}\mathbf{L}_{xx}\mathbf{L}_{xx}\mathbf{u}+\mathbf{G}\mathbf{L}_{zx}^{2}\mathbf{L}_{zx}^{2}\mathbf{u}-\mathbf{G}\mathbf{L}_{zx}^{3}\mathbf{u}+\mathbf{P}^{\mathrm{T}}\mathbf{L}_{\phi\phi}\boldsymbol{\phi}+\mathbf{f}=\mathbf{J}\ddot{\mathbf{u}}. \qquad \text{(A.33)}$$

Thus, rewriting the previous equation in non-matrix form, the system of partial differential equations involving the variations δu_0, δw_0, $\delta\theta_0$, $\delta\theta_{\hat{n}}$ ($\hat{n}=1,\ldots,\bar{n}-1$), $\delta\theta_{\bar{n}}$, $\delta\theta_{\bar{m}}$ and $\delta\theta_{\hat{m}}$ ($\hat{m}=\bar{m}+1,\ldots,-1$), is given by

δu_0 :

$$\sum_{k=\bar{m}}^{\bar{n}}c_{11}^{*k}A_k u_0''+\Big(\sum_{n=1}^{\bar{n}}c_{11}^{*n}h_0A_n-\sum_{m=\bar{m}}^{-1}c_{11}^{*m}h_0A_m\Big)\theta_0''+\sum_{\hat{n}=1}^{\bar{n}-1}\Big(\sum_{i=\hat{n}+1}^{\bar{n}}\rho_i 2h_{\hat{n}}A_i+\rho_{\hat{n}}\bar{I}_{\hat{n}}\Big)\theta_{\hat{n}}''$$
$$+c_{11}^{*\bar{n}}\bar{I}_{\bar{n}}\theta_{\bar{n}}''+c_{11}^{*\bar{m}}\bar{I}_{\bar{m}}\theta_{\bar{m}}''+\sum_{\hat{m}=\bar{m}+1}^{-1}\Big(-\sum_{i=\bar{m}}^{\hat{m}-1}\rho_i 2h_{\hat{m}}A_i+\rho_{\hat{m}}\bar{I}_{\hat{m}}\Big)\theta_{\hat{m}}''+\sum_{n=1}^{\bar{n}}A_n\frac{e_{31}^{*n}}{2h_n}\phi_n'$$
$$+\sum_{m=\bar{m}}^{-1}A_m\frac{e_{31}^{*m}}{2h_m}\phi_m'+\sum_{k=\bar{m}}^{\bar{n}}X_k=\sum_{k=\bar{m}}^{\bar{n}}\rho_kA_k\ddot{u}_0+\Big(\sum_{n=1}^{\bar{n}}\rho_nh_0A_n-\sum_{m=\bar{m}}^{-1}\rho_mh_0A_m\Big)\ddot{\theta}_{0i}$$
$$+\sum_{\hat{n}=1}^{\bar{n}-1}\Big(\sum_{i=\hat{n}+1}^{\bar{n}}c_{11}^{*i}2h_{\hat{n}}A+c_{11}^{*\hat{n}}\bar{I}_{\hat{n}}\Big)\ddot{\theta}_{\hat{n}}+\rho_{\bar{n}}\bar{I}_{\bar{n}}\ddot{\theta}_{\bar{n}}+\rho_{\bar{m}}\bar{I}_{\bar{m}}\ddot{\theta}_{\bar{m}}$$
$$+\sum_{\hat{m}=\bar{m}+1}^{-1}\Big(-\sum_{i=\bar{m}}^{\hat{m}-1}c_{11}^{*i}2h_{\hat{m}}A_i+c_{11}^{*\hat{m}}\bar{I}_{\hat{m}}\Big)\ddot{\theta}_{\hat{m}} \qquad \text{(A.34)}$$

δw_0 :

$$\Big(\sum_{n=1}^{\bar{n}}\bar{c}_{55}^{n(\phi)}A_n+c_{55}^{0}A_0+\sum_{m=\bar{m}}^{-1}\bar{c}_{55}^{m(\phi)}A_m\Big)w_0''-c_{55}^{c}A_c\theta_0'-\sum_{\hat{n}=1}^{\bar{n}-1}\bar{c}_{55}^{\hat{n}(\phi)}A_{\hat{n}}\theta_{\hat{n}}'-\bar{c}_{55}^{\bar{n}(\phi)}A_{\bar{n}}\theta_{\bar{n}}'$$
$$-\bar{c}_{55}^{\bar{m}(\phi)}A_{\bar{m}}\theta_{\bar{m}}'-\sum_{\hat{m}=\bar{m}+1}^{-1}\bar{c}_{55}^{\hat{m}(\phi)}A_{\hat{m}}\theta_{\hat{m}}'+\sum_{k=\bar{m}}^{\bar{n}}Z_k=\sum_{k=\bar{m}}^{\bar{n}}\rho_kA_k\ddot{w}_0 \qquad \text{(A.35)}$$

$\delta\theta_0$:

$$\begin{aligned}
&\Big(\sum_{n=1}^{\bar{n}} c_{11}^{*n} h_0 A_n - \sum_{m=\bar{m}}^{-1} c_{11}^{*m} h_0 A_m\Big) u_0'' + \Big(\sum_{n=1}^{\bar{n}} c_{11}^{*n} {h_0}^2 A_n + c_{11}^{*0} I_0 + \sum_{m=\bar{m}}^{-1} c_{11}^{*m} {h_0}^2 A_m\Big)\theta_0'' \\
&\quad + \sum_{\hat{n}=1}^{\bar{n}-1}\Big(2h_0 h_{\hat{n}} \sum_{i=\hat{n}+1}^{\bar{n}} c_{11}^{*i} A_i + c_{11}^{*\hat{n}} h_0 \bar{I}_{\hat{n}}\Big)\theta_{\hat{n}}'' + c_{11}^{*\bar{n}} h_0 \bar{I}_{\bar{n}} \theta_{\bar{n}}'' - \rho_{\bar{m}} h_0 \bar{I}_{\bar{m}} \theta_{\bar{m}}'' \\
&+ \sum_{\hat{m}=\bar{m}+1}^{-1}\Big(2h_0 h_{\hat{m}} \sum_{i=\bar{m}}^{\hat{m}-1} c_{11}^{*i} A_i - c_{11}^{*\hat{m}} h_0 \bar{I}_{\hat{m}}\Big)\theta_{\hat{m}}'' + c_{55}^0 A_0 w_0' - c_{55}^0 A_0 \theta_0 + \sum_{n=1}^{\bar{n}} \frac{e_{31}^{*n}}{2h_n} h_0 A_n \phi_n' \\
&- \sum_{m=\bar{m}}^{-1} \frac{e_{31}^{*m}}{2h_m} h_0 A_m \phi_m' + \sum_{n=1}^{\bar{n}} h_0 X_n + M_0 - \sum_{m=\bar{m}}^{-1} h_0 X_m = \Big(\sum_{n=1}^{\bar{n}} \rho_n h_0 A_n - \sum_{m=\bar{m}}^{-1} \rho_m h_0 A_m\Big)\ddot{u}_0 \\
&\quad + \ddot{\theta}_0\Big(\sum_{n=1}^{\bar{n}} \rho_n h_0^2 A_n + \rho_0 I_0 + \sum_{m=\bar{m}}^{-1} \rho_m h_0^2 A_m\Big) + \sum_{\hat{n}=1}^{\bar{n}-1}\Big(2h_0 h_{\hat{n}} \sum_{i=\hat{n}+1}^{\bar{n}} \rho_i A_i + \rho_{\hat{n}} h_0 \bar{I}_{\hat{n}}\Big)\ddot{\theta}_{\hat{n}} \\
&\quad + \rho_{\bar{n}} h_0 \bar{I}_{\bar{n}} \ddot{\theta}_{\bar{n}} - c_{11}^{*\bar{m}} h_0 \bar{I}_{\bar{m}} \ddot{\theta}_{\bar{m}} + \sum_{\hat{m}=\bar{m}+1}^{-1}\Big(2h_0 h_{\hat{m}} \sum_{i=\bar{m}}^{\hat{m}-1} \rho_i A_i - \rho_{\hat{m}} h_0 \bar{I}_{\hat{m}}\Big)\ddot{\theta}_{\hat{m}} \qquad \text{(A.36)}
\end{aligned}$$

$\delta\theta_{\hat{n}}$:

$$\begin{aligned}
&\Big(\sum_{i=\hat{n}+1}^{\bar{n}} c_{11}^{*i} 2h_{\hat{n}} A_i + c_{11}^{*\hat{n}} \bar{I}_{\hat{n}}\Big) u_0'' + \Big(2h_0 h_{\hat{n}} \sum_{i=\hat{n}+1}^{\bar{n}} c_{11}^{*i} A_i + c_{11}^{*\hat{n}} h_0 \bar{I}_{\hat{n}}\Big)\theta_0'' + \sum_{i=1}^{\hat{n}-1}\Big(\sum_{j=\hat{n}+1}^{\bar{n}} \rho_j 4h_{\hat{n}} h_i A_j \\
&+ \rho_{\hat{n}} 2h_i \bar{I}_{\hat{n}}\Big)\theta_i'' + \Big(\sum_{i=\hat{n}+1}^{\bar{n}} c_{11}^{*i} 4{h_{\hat{n}}}^2 A_i + \bar{c}_{11}^{\hat{n}(\phi)} I_{\hat{n}}\Big)\theta_{\hat{n}}'' + \sum_{j=\hat{n}+1}^{\bar{n}-1}\Big(\sum_{i=j+1}^{\bar{n}} c_{11}^{*i} 4h_{\hat{n}} h_j A_i + c_{11}^{*j} 2h_{\hat{n}} \bar{I}_j\Big)\theta_j'' \\
&\quad + c_{11}^{*\bar{n}} 2h_{\hat{n}} \bar{I}_{\bar{n}} \theta_{\bar{n}}'' + \bar{c}_{55}^{\hat{n}(\phi)} A_{\hat{n}} w_0' - \bar{c}_{55}^{\hat{n}(\phi)} A_{\hat{n}} \theta_{\hat{n}} + \frac{e_{31}^{*\hat{n}}}{2h_{\hat{n}}} \bar{I}_{\hat{n}} \phi_{\hat{n}}' + \sum_{i=\hat{n}+1}^{\bar{n}} 2h_{\hat{n}} A_i \frac{e_{31}^{*i}}{2h_i} \phi_i' + h_{\hat{n}} X_{\hat{n}} \\
&+ \sum_{i=\hat{n}+1}^{\bar{n}} 2h_{\hat{n}} X_i + M_{\hat{n}} = \Big(\sum_{i=\hat{n}+1}^{\bar{n}} \rho_i 2h_{\hat{n}} A_i + \rho_{\hat{n}} \bar{I}_{\hat{n}}\Big)\ddot{u}_0 + \Big(2h_0 h_{\hat{n}} \sum_{i=\hat{n}+1}^{\bar{n}} \rho_i A_i + \rho_{\hat{n}} h_0 \bar{I}_{\hat{n}}\Big)\ddot{\theta}_0 \\
&\quad + \sum_{i=1}^{\hat{n}-1}\Big(\sum_{j=\hat{n}+1}^{\bar{n}} \rho_j 4h_{\hat{n}} h_i A_j + \rho_{\hat{n}} 2h_i \bar{I}_{\hat{n}}\Big)\ddot{\theta}_i + \Big(\sum_{i=\hat{n}+1}^{\bar{n}} \rho_i 4{h_{\hat{n}}}^2 A_i + \rho_{\hat{n}} I_{\hat{n}}\Big)\ddot{\theta}_{\hat{n}} \\
&\quad + \sum_{j=\hat{n}+1}^{\bar{n}-1}\Big(\sum_{i=j+1}^{\bar{n}} \rho_i 4h_{\hat{n}} h_j A_i + \rho_j 2h_{\hat{n}} \bar{I}_j\Big)\ddot{\theta}_j + \rho_{\bar{n}} 2h_{\hat{n}} \bar{I}_{\bar{n}} \ddot{\theta}_{\bar{n}}, \qquad \text{(A.37)}
\end{aligned}$$

$\delta\theta_{\bar{n}}$:

$$\begin{aligned}
&c_{11}^{*\bar{n}} \bar{I}_{\bar{n}} u_0'' + c_{11}^{*\bar{n}} h_0 \bar{I}_{\bar{n}} \theta_0'' + \sum_{\hat{n}=1}^{\bar{n}-1} c_{11}^{*\bar{n}} 2h_{\hat{n}} \bar{I}_{\bar{n}} \theta_{\hat{n}}'' + \bar{c}_{11}^{\bar{n}(\phi)} I_{\bar{n}} \theta_{\bar{n}}'' + \bar{c}_{55}^{\bar{n}(\phi)} A_{\bar{n}} w_0' - \bar{c}_{55}^{\bar{n}(\phi)} A_{\bar{n}} \theta_{\bar{n}} \\
&+ \frac{e_{31}^{*\bar{n}}}{2h_{\bar{n}}} \bar{I}_{\bar{n}} \phi_{\bar{n}}' + h_{\bar{n}} X_{\bar{n}} + M_{\bar{n}} = \rho_{\bar{n}} \bar{I}_{\bar{n}} \ddot{u}_0 + \rho_{\bar{n}} h_0 \bar{I}_{\bar{n}} \ddot{\theta}_0 + \sum_{\hat{n}=1}^{\bar{n}-1} \rho_{\bar{n}} 2h_{\hat{n}} \bar{I}_{\bar{n}} \ddot{\theta}_{\hat{n}} + \rho_{\bar{n}} I_{\bar{n}} \ddot{\theta}_{\bar{n}}, \qquad \text{(A.38)}
\end{aligned}$$

$\delta\theta_{\bar{m}}$:

$$\begin{aligned}
&c_{11}^{*\bar{m}} \bar{I}_{\bar{m}} u_0'' - c_{11}^{*\bar{m}} h_0 \bar{I}_{\bar{m}} \theta_0'' + \bar{c}_{11}^{\bar{m}(\phi)} I_{\bar{m}} \theta_{\bar{m}}'' - \sum_{\hat{m}=\bar{m}+1}^{-1} c_{11}^{*\bar{m}} 2h_{\bar{m}} \bar{I}_{\bar{m}} \theta_{\hat{m}}'' + \bar{c}_{55}^{\bar{m}(\phi)} A_{\bar{m}} w_0' - \bar{c}_{55}^{\bar{m}(\phi)} A_{\bar{m}} \theta_{\bar{m}} \\
&+ \frac{e_{31}^{*\bar{m}}}{2h_{\bar{m}}} \bar{I}_{\bar{m}} \phi_{\bar{m}}' - h_{\bar{m}} X_{\bar{m}} + M_{\bar{m}} = \rho_{\bar{m}} \bar{I}_{\bar{m}} \ddot{u}_0 - \rho_{\bar{m}} h_0 \bar{I}_{\bar{m}} \ddot{\theta}_0 - \sum_{\hat{m}=\bar{m}+1}^{-1} \rho_{\bar{m}} 2h_{\bar{m}} \bar{I}_{\bar{m}} \ddot{\theta}_{\hat{m}} + \rho_{\bar{m}} I_{\bar{m}} \ddot{\theta}_{\bar{m}}, \\
&\qquad \text{(A.39)}
\end{aligned}$$

$\delta\theta_{\bar{m}}$:

$$\Big(-\sum_{i=\bar{m}}^{\hat{m}-1} c_{11}^{*i} 2h_{\hat{m}} A_i + c_{11}^{*\hat{m}} \bar{I}_{\hat{m}} \Big) u_0'' + \Big(2h_0 h_{\hat{m}} \sum_{i=\bar{m}}^{\hat{m}-1} c_{11}^{*i} A_i - c_{11}^{*\hat{m}} h_0 \bar{I}_{\hat{m}} \Big) \theta_0'' + \sum_{j=\hat{m}+1}^{\hat{m}-1} \Big(\sum_{i=\bar{m}}^{j-1} c_{11}^{*i} 4h_{\hat{m}} h_j A_i$$
$$- c_{11}^{*j} 2h_{\hat{m}} \bar{I}_j \Big) \theta_j'' + \Big(\sum_{i=\bar{m}}^{\hat{m}-1} c_{11}^{*i} 4h_{\hat{m}}{}^2 A_i + \bar{c}_{11}^{\hat{m}(\phi)} I_{\hat{m}} \Big) \theta_{\hat{m}}'' + \sum_{i=\hat{m}+1}^{-1} \Big(\sum_{j=\bar{m}}^{\hat{m}-1} \rho_j 4h_{\hat{m}} h_i A_j - \rho_{\hat{m}} 2h_i \bar{I}_{\hat{m}} \Big) \theta_i''$$
$$- c_{11}^{*\bar{m}} 2h_{\hat{m}} \bar{I}_{\bar{m}} \theta_{\bar{m}}'' + \bar{c}_{55}^{\hat{m}(\phi)} A_{\hat{m}} w_0' - \bar{c}_{55}^{\hat{m}(\phi)} A_{\hat{m}} \theta_{\hat{m}} + \frac{e_{31}^{*\hat{m}}}{2h_{\hat{m}}} \bar{I}_{\hat{m}} \phi_{\hat{m}}' - \sum_{i=\bar{m}}^{\hat{m}-1} 2h_{\hat{m}} A_i \frac{e_{31}^{*i}}{2h_i} \phi_i' - h_{\hat{m}} X_{\hat{m}}$$
$$- \sum_{i=\bar{m}}^{\hat{m}-1} 2h_{\hat{m}} X_i + M_{\hat{m}} = \Big(-\sum_{i=\bar{m}}^{\hat{m}-1} \rho_i 2h_{\hat{m}} A_i + \rho_{\hat{m}} \bar{I}_{\hat{m}} \Big) \ddot{u}_0 + \Big(2h_0 h_{\hat{m}} \sum_{i=\bar{m}}^{\hat{m}-1} \rho_i A_i - \rho_{\hat{m}} h_0 \bar{I}_{\hat{m}} \Big) \ddot{\theta}_0$$
$$\sum_{j=\bar{m}+1}^{\hat{m}-1} \Big(\sum_{i=\bar{m}}^{j-1} \rho_i 4h_{\hat{m}} h_j A_i - \rho_j 2h_{\hat{m}} \bar{I}_j \Big) \ddot{\theta}_j + \Big(\sum_{i=\bar{m}}^{\hat{m}-1} \rho_i 4h_{\hat{m}}{}^2 A_i + \rho_{\hat{m}} I_{\hat{m}} \Big) \ddot{\theta}_{\hat{m}}$$
$$+ \sum_{i=\hat{m}+1}^{-1} \Big(\sum_{j=\bar{m}}^{\hat{m}-1} \rho_j 4h_{\hat{m}} h_i A_j - \rho_{\hat{m}} 2h_i \bar{I}_{\hat{m}} \Big) \ddot{\theta}_i + \rho_{\bar{n}} 2h_{\hat{n}} \bar{I}_{\hat{n}} \ddot{\theta}_{\bar{n}}. \tag{A.40}$$

A.3.2 Electric Charge Equilibrium Equations

Similarly, the electric charge equilibrium equations are derived from Equation (A.31) by considering the integral term involving $\delta\phi$,

$$\int_L \delta\boldsymbol{\phi}^{\mathrm{T}} \big(\mathbf{P}\mathbf{L}_{xx}\mathbf{u} + \mathbf{C}\boldsymbol{\phi} - \boldsymbol{\tau} \big)\, \mathrm{d}L = 0, \tag{A.41}$$

where the non-trivial solution is given by

$$\mathbf{P}\mathbf{L}_{xx}\mathbf{u} + \mathbf{C}\boldsymbol{\phi} = \boldsymbol{\tau}. \tag{A.42}$$

Thus, rewriting the previous equation in non-matrix form, the system of partial differential equations involving the variations of the electric potential differences of the generic top and bottom piezoelectric layers, $\delta\phi_n$ $(n = 1, \ldots, \bar{n})$ and $\delta\phi_m$ $(m = \bar{m}, \ldots, -1)$, is given by

$\delta\phi_n$:

$$\frac{e_{31}^{*n}}{2h_n} A_n u_0' + \frac{e_{31}^{*n}}{2h_n} h_0 A_n \theta_0' + \sum_{i=1}^{n-1} \frac{e_{31}^{*n}}{2h_n} 2h_i A_n \theta_i' + \frac{e_{31}^{*n}}{2h_n} \bar{I}_n \theta_n' - \frac{\varepsilon_{33}^{*n} A_n}{4h_n{}^2} \phi_n = -b\tau_n, \tag{A.43}$$

$\delta\phi_m$:

$$\frac{e_{31}^{*m}}{2h_m} A_m u_0' - \frac{e_{31}^{*m}}{2h_m} h_0 A_m \theta_0' + \frac{e_{31}^{*m}}{2h_m} \bar{I}_m \theta_m' - \sum_{i=m+1}^{-1} \frac{e_{31}^{*m}}{2h_m} 2h_i A_m \theta_i' + -\frac{\varepsilon_{33}^{*m} A_m}{4h_m{}^2} \phi_m = -b\tau_m. \tag{A.44}$$

A.3.3 Electro-Mechanical Boundary Conditions

The electro-mechanical boundary conditions are obtained from the boundary terms at $x = 0, L$ in Equation (A.31),

$$\delta\mathbf{u}^{\mathrm{T}} \Big[\mathbf{Y}\mathbf{L}_{xx}\mathbf{u} + \mathbf{L}_{zx}^{1\mathrm{T}} \mathbf{G}\mathbf{L}_{zx}\mathbf{u} + \delta\mathbf{u}^{\mathrm{T}}\mathbf{P}^{\mathrm{T}}\boldsymbol{\phi} \Big]_0^L = 0, \tag{A.45}$$

which can be expressed in non matrix form as

$$\delta u_0\Big[\sum_{k=\bar m}^{\bar n} c_{11}^{*k}A_k u_0' + \Big(\sum_{n=1}^{\bar n} c_{11}^{*n}h_0A_n - \sum_{m=\bar m}^{-1} c_{11}^{*m}h_0A_m\Big)\theta_0' + \sum_{\hat n=1}^{\bar n-1}\Big(\sum_{i=\hat n+1}^{\bar n}\rho_i 2h_{\hat n}A_i + \rho_{\hat n}\bar I_{\hat n}\Big)\theta_{\hat n}'$$
$$+c_{11}^{*\bar n}\bar I_{\bar n}\theta_{\bar n}' + c_{11}^{*\bar m}\bar I_{\bar m}\theta_{\bar m}' + \sum_{\hat m=\bar m+1}^{-1}\Big(-\sum_{i=\bar m}^{\hat m-1}\rho_i 2h_{\hat m}A_i + \rho_{\hat m}\bar I_{\hat m}\Big)\theta_{\hat m}'$$
$$+\sum_{n=1}^{\bar n} A_n\frac{e_{31}^{*n}}{2h_n}\phi_n + \sum_{m=\bar m}^{-1} A_m\frac{e_{31}^{*m}}{2h_m}\phi_m\Big] = 0, \qquad (A.46)$$

$$\delta w_0\Big[\Big(\sum_{n=1}^{\bar n}\bar c_{55}^{n(\phi)}A_n + c_{55}^0A_0 + \sum_{m=\bar m}^{-1}\bar c_{55}^{m(\phi)}A_m\Big)w_0' + c_{55}^cA_c\theta_0 + \sum_{\hat n=1}^{\bar n-1}\bar c_{55}^{\hat n(\phi)}A_{\hat n}\theta_{\hat n} + \bar c_{55}^{\bar n(\phi)}A_{\bar n}\theta_{\bar n}$$
$$+\bar c_{55}^{\bar m(\phi)}A_{\bar m}\theta_{\bar m} + \sum_{\hat m=\bar m+1}^{-1}\bar c_{55}^{\hat m(\phi)}A_{\hat m}\theta_{\hat m}\Big] = 0, \qquad (A.47)$$

$$\delta\theta_0\Big[\Big(\sum_{n=1}^{\bar n} c_{11}^{*n}h_0A_n - \sum_{m=\bar m}^{-1} c_{11}^{*m}h_0A_m\Big)u_0' + \Big(\sum_{n=1}^{\bar n} c_{11}^{*n}h_0{}^2A_n + c_{11}^{*0}I_0 + \sum_{m=\bar m}^{-1} c_{11}^{*m}h_0{}^2A_m\Big)\theta_0'$$
$$+\sum_{\hat n=1}^{\bar n-1}\Big(2h_0h_{\hat n}\sum_{i=\hat n+1}^{\bar n} c_{11}^{*i}A_i + c_{11}^{*\hat n}h_0\bar I_{\hat n}\Big)\theta_{\hat n}' + c_{11}^{*\bar n}h_0\bar I_{\bar n}\theta_{\bar n}' - \rho_{\bar m}h_0\bar I_{\bar m}\theta_{\bar m}' + \sum_{\hat m=\bar m+1}^{-1}\Big(2h_0h_{\hat m}\sum_{i=\bar m}^{\hat m-1} c_{11}^{*i}A_i$$
$$-c_{11}^{*\hat m}h_0\bar I_{\hat m}\Big)\theta_{\hat m}' + \sum_{n=1}^{\bar n}\frac{e_{31}^{*n}}{2h_n}h_0A_n\phi_n - \sum_{m=\bar m}^{-1}\frac{e_{31}^{*m}}{2h_m}h_0A_m\phi_m\Big] = 0, \qquad (A.48)$$

$$\delta\theta_{\hat n}\Big[\Big(\sum_{i=\hat n+1}^{\bar n} c_{11}^{*i}2h_{\hat n}A_i + c_{11}^{*\hat n}\bar I_{\hat n}\Big)u_0' + \Big(2h_0h_{\hat n}\sum_{i=\hat n+1}^{\bar n} c_{11}^{*i}A_i + c_{11}^{*\hat n}h_0\bar I_{\hat n}\Big)\theta_0'$$
$$+\sum_{i=1}^{\hat n-1}\Big(\sum_{j=\hat n+1}^{\bar n}\rho_j 4h_{\hat n}h_iA_j + \rho_{\hat n}2h_i\bar I_{\hat n}\Big)\theta_i' + \Big(\sum_{i=\hat n+1}^{\bar n} c_{11}^{*i}4h_{\hat n}{}^2A_i + \bar c_{11}^{\hat n(\phi)}I_{\hat n}\Big)\theta_{\hat n}'$$
$$+\sum_{j=\hat n+1}^{\bar n-1}\Big(\sum_{i=j+1}^{\bar n} c_{11}^{*i}4h_{\hat n}h_jA_i + c_{11}^{*j}2h_{\hat n}\bar I_j\Big)\theta_j' + c_{11}^{*\bar n}2h_{\hat n}\bar I_{\bar n}\theta_{\bar n}' + \frac{e_{31}^{*\hat n}}{2h_{\hat n}}\bar I_{\hat n}\phi_{\hat n} + \sum_{i=\hat n+1}^{\bar n} 2h_{\hat n}A_i\frac{e_{31}^{*i}}{2h_i}\phi_i\Big] = 0, \qquad (A.49)$$

$$\delta\theta_{\bar n}\Big(c_{11}^{*\bar n}\bar I_{\bar n}u_0' + c_{11}^{*\bar n}h_0\bar I_{\bar n}\theta_0' + \sum_{\hat n=1}^{\bar n-1} c_{11}^{*\bar n}2h_{\hat n}\bar I_{\bar n}\theta_{\hat n}' + \bar c_{11}^{\bar n(\phi)}I_{\bar n}\theta_{\bar n}' + \frac{e_{31}^{*\bar n}}{2h_{\bar n}}\bar I_{\bar n}\phi_{\bar n}\Big) = 0, \qquad (A.50)$$

$$\delta\theta_{\bar m}\Big(c_{11}^{*\bar m}\bar I_{\bar m}u_0' - c_{11}^{*\bar m}h_0\bar I_{\bar m}\theta_0' + \bar c_{11}^{\bar m(\phi)}I_{\bar m}\theta_{\bar m}' - \sum_{\hat m=\bar m+1}^{-1} c_{11}^{*\bar m}2h_{\hat m}\bar I_{\bar m}\theta_{\hat m}' + \frac{e_{31}^{*\bar m}}{2h_{\bar m}}\bar I_{\bar m}\phi_{\bar m}\Big) = 0, \qquad (A.51)$$

$$\delta\theta_{\hat m}\Big(-\sum_{i=\bar m}^{\hat m-1} c_{11}^{*i}2h_{\hat m}A_i + c_{11}^{*\hat m}\bar I_{\hat m}\Big)u_0' + \sum_{j=\hat m+1}^{\hat m-1}\Big(2h_0h_{\hat m}\sum_{i=\bar m}^{\hat m-1} c_{11}^{*i}A_i - c_{11}^{*\hat m}h_0\bar I_{\hat m}\Big)\theta_0'$$
$$-c_{11}^{*\bar m}2h_{\hat m}\bar I_{\bar m}\theta_{\bar m}' + \sum_{j=\bar m+1}^{\hat m-1}\Big(\sum_{i=\bar m}^{j-1} c_{11}^{*i}4h_{\hat m}h_jA_i - c_{11}^{*j}2h_{\hat m}\bar I_j\Big)\theta_j' + \Big(\sum_{i=\bar m}^{\hat m-1} c_{11}^{*i}4h_{\hat m}{}^2A_i + \bar c_{11}^{\hat m(\phi)}I_{\hat m}\Big)\theta_{\hat m}'$$
$$+\sum_{i=\hat m+1}^{-1}\Big(\sum_{j=\bar m}^{\hat m-1}\rho_j 4h_{\hat m}h_iA_j - \rho_{\hat m}2h_i\bar I_{\hat m}\Big)\theta_i' + \frac{e_{31}^{*\hat m}}{2h_{\hat m}}\bar I_{\hat m}\phi_{\hat m} - \sum_{i=\bar m}^{\hat m-1} 2h_{\hat m}A_i\frac{e_{31}^{*i}}{2h_i}\phi_i\Big] = 0. \qquad (A.52)$$